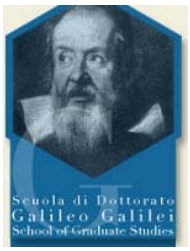

Università di Pisa - Dipartimento di Scienze della Terra

Scuola di Dottorato di Ricerca in Scienze di Base Galileo Galilei
Programma di Scienze della Terra
XXIV Ciclo 2009 – 2011

Settore scientifico-disciplinare: GEO/05

Dissertazione Finale

Yuri Galanti

Rainfall-induced shallow landslides in Northern Tuscany (Italy): geotechnical characterization and rainfall thresholds

Tutore:
Prof. Alberto Puccinelli

Referees:
Prof. Carlo Alberto Garzonio

Co-tutori:
Dott. Giacomo D'Amato Avanzi

Dott. Leonardo Disperati

Dott. Roberto Giannecchini

Direttore della Scuola
Prof. Fabrizio Broglia

Presidente del Programma
Prof. Roberto Santacroce

Contents

Preface

In this preface we introduce the PhD Thesis on rainfall-induced landslides entitled "*Rainfall-induced shallow landslides in Northern Tuscany (Italy): geotechnical characterization and rainfall thresholds*". Rainfall-induced landslides deserved a large interest in international literature in the last decades. The literature on this matter shows a markedly interdisciplinary approach, with contributions from different fields, such as engineering geology, soil mechanics, hydrology and geomorphology. The subject is of high interest for many practical and scientific reasons. In fact, rainfall is the most relevant factor for triggering shallow landslides, and rainfall analysis is the most frequently adopted approach in forecasting the occurrence of such phenomena. Moreover, the estimation of the properties of materials mainly involved by shallow landslides is fundamental in understanding their triggering mechanism.

With the aim of contributing in studying the rainfall-induced shallow landslides in Northern Tuscany, different topics were considered: the analysis of the rainstorms of 2009-2010 period and of their consequences, the geotechnical characterization of the source areas of shallow landslides, and the determination of critical rainfall thresholds for triggering such phenomena. For these reasons, the manuscript was structured in three different but complementary papers.

The papers are briefly introduced, examining their contribution in understanding of the rainfall-induced shallow landslides, as follows.

The first paper "*The 2009 and 2010 meteorological events in Northern Tuscany (Italy): Characteristics and effects on slope stability*" describes characteristics and main effects on slope stability of the rainstorms which hit the Northern Tuscany in December 2009 (north-western Tuscany), June 2010 (Serchio River Valley) and October 2010 (Massa-Carrara province). The rainfall events were analyzed in terms of rainfall amount, intensity and duration. Moreover, the antecedent rainfall related to such events was analyzed, focusing on its role in causing instability conditions of slopes.

The paper highlights again that the shallow landslides commonly occurred in peculiar geologic and geomorphologic environments: colluvium/debris thin slope cover, semi-permeable or impermeable bedrock, hollow shaped slope, high slope gradient. Moreover, it

highlights that the shallow landslides in Northern Tuscany mainly involve the soils covering the arenaceous formations, such as the Macigno Fm.

In this context, the second paper "*Geotechnical characterization of source areas of shallow landslides by dynamic penetration tests in Northern Tuscany (Italy): first results and perspectives*" aims at contributing to the characterization of the typical source areas of the shallow landslides in the Serchio River Valley, by means of dynamic penetration tests (Dynamic Probing, DP). In fact, these tools are particularly suitable to obtain geotechnical properties of the soils in difficult access slopes. Original data, coming from inspections of existing databases or expressly performed tests, are presented and discussed. Relative density and friction angle were determined processing the results of DP tests by means of empirical methods. Moreover, the soil properties obtained by DP tests were compared with those obtained by Standard Penetration Tests (SPT) and direct shear tests. The comparison suggests that the DP tests can be an effective tools in geotechnical characterization of potentially unstable soil slope covers.

Finally, the last paper "*Critical rainfall thresholds for triggering shallow landslides in the Serchio River Valley (Tuscany, Italy)*" proposes the critical rainfall thresholds for triggering shallow landslides in Middle Serchio River Valley. The rainfall data recorded by three rain gauges in the 1935-2010 period were analyzed and compared with the occurrence of shallow landslides. The rainfall thresholds were defined in terms of mean intensity, rainfall duration and normalized using the mean annual precipitation. Some attempts were also carried out to analyze the role of rainfall prior to the damaging events. Moreover, the rainfall thresholds obtained for the study area were compared with the local, regional and global thresholds proposed by various authors. The results of these analysis suggest that in the Middle Serchio River Valley, and in general in Northern Tuscany, landslides activity initiation requires a higher amount of rainfall and greater intensity than elsewhere.

At present, further research is necessary in order to reach a zonation of the shallow landslide hazard in the study area. The methodological approach used for the characterization of the source areas of the shallow landslides may be improved in several aspects (e.g. performing of direct shear tests on undisturbed soils, calibration of DP tests results and performing of empirical relations specifically calibrated on the considered soils). Other important parameters, such as slope gradient and soil thickness, may be considered. The

critical rainfall thresholds obtained in this work may be tested and compared with those obtained by statistical or deterministic approaches.

The evolution of this research is towards performing of susceptibility maps and comparison with rainfall thresholds for triggering shallow landslides. This is crucial for the preparation of landslide hazard maps and scenarios for different rainfall amounts in an area particularly prone to shallow landslides.

List of figures

List of tables

1 The 2009 and 2010 meteorological events in Northern Tuscany (Italy): Characteristics and effects on slope stability

Abstract

Owing to its geographical, geomorphologic and climatic features, the Northern Tuscany is frequently hit by rainstorms. In many cases such meteorological events trigger rapid, shallow landslides. They are generally first time movements, mainly referable to complex, translational debris slide-flows or soil slip-debris flows, typically triggered by intense rainfall. In Northern Tuscany they occurred in peculiar geologic and geomorphologic environments: colluvium/debris thin slope cover, semi-permeable or impermeable bedrock, hollow shaped slope, high slope gradient. Despite their little size, they caused heavy damage and also causalities, due to their high speed and erosion power.

The source areas of shallow landslides are often located along the road network, generally for lack or deficiency of surficial water draining systems. In fact, the concentration and of uncontrolled running water on the roads and its subsequent flowing downslope may produce an "unnatural" increase in pore pressure that the only rainfall, hitting the same slope in natural conditions, should not have produced. Actually, this phenomenon generates the reaching and exceeding of the local critical rainfall threshold, making landslide prevision and hazard assessment difficult.

This paper summarises characteristics and main effects of the meteorological events, that hit the Northern Tuscany in December 2009, June 2010 and October 2010, focusing on their consequences on the slopes.

Keywords: Shallow landslides, rainstorm, territory, infrastructure, Tuscany.

1.1 Introduction

Landslides induced by rainfall are significantly increasing in Italy (Guzzetti, 2000) as well as worldwide (Munich Re, 2009). Consequently, they are responsible for considerably greater socioeconomic losses (Schuster, 1996). Changing climate is often used to explain the proliferation and escalation of extreme rainfall events. In many cases, the climate changes, though significant, do not indicate a defined trend but may fit the normal climate cycles. On this controversial topic the scientific discussion is still open. Medium and long-term case studies suggest a change in rainfall trends. Some Authors individuate an apparent increase of rainstorms frequency in time (Guzzetti, 2000; Guzzetti et al., 2005; Giannecchini and D'Amato Avanzi, 2012). Such events have often caused landslides and floods with serious damages to territory and community.

Rising in landslide risk may be however related to the progressive development of urban zones and infrastructures on or close to hill/mountain areas, with little or no regard to proper construction, precautionary works and land use planning. Consequently, also not exceptional rainfall events often generate landsliding problems.

During the last decades, the Northern Tuscany (north-western Apennines, Apuan Alps, Serchio River Valley, Versilia) has been hit by several meteorological events. They caused huge damages and casualties mainly in Lucca, Massa-Carrara and Pistoia provinces, as happened on 19 June 1996 in Versilia and Garfagnana (14 deaths) (ANPA-ARPAT, 1998; D'Amato Avanzi and Giannecchini, 2003; D'Amato Avanzi et al., 2004), on 20 November 2000 in the Serchio River Valley (5 deaths) (D'Amato Avanzi et al., 2002; Banducci et al., 2005) and in the Pistoia province (Casagli et al., 2006; Giannecchini and Verani, 2006) and on 23 September 2003 in the Carrara Marble Basin (Apuan Alps) (Cortopassi et al., 2008).

Recent intense rainfall events also occurred in December 2009 (north-western Tuscany), June 2010 (Serchio River Valley) and October 2010 (Massa-Carrara province, 3 casualties). These events caused hundreds of shallow landslides mainly referable to complex, translational debris slide-flows (Cruden and Varnes, 1996) or soil slip-debris flows (Campbell 1974, 1975; Crosta et al., 1990; Crosta, 1998). These phenomena were usually superficial (0.5-2 m thick), linear (width/length ratio 0.03-0.5), and involved soil and sometimes portions of fractured bedrock. They mainly triggered in the hollows of the slopes underlain by sandstone, metamorphic sandstone and phyllitic-schist, at the top of the zero-order basins. The concave morphology of the hollows favoured runoff and/or infiltration, while the concave soil-bedrock

interface induced the concentration of subsurface downflow, saturation and build-up of pore pressures. These landslides are usually associated with intense rainfalls (Campbell, 1974, 1975; Wieczorek, 1987, 1996). This association has been highlighted in Hong Kong (Fuchu et al., 1999; Dai and Lee, 2001), Japan (Fukuoka, 1980), New Zealand (Selby, 1976; Pierson, 1980), USA (Ellen and Wieczorek, 1988), and in many other places worldwide (Caine, 1980; Crozier, 1986; Jibson, 1989; Chien-Yuan et al., 2005).

The triggering mechanism is generally characterised by rainwater infiltration into the soil, which may cause the increase in pore water pressure and consequently deterioration of slope stability. It may be facilitated by the presence of a road network characterized by lack or deficiency of surficial water draining systems. This implies an unnatural concentration of the flow, which may contribute to the increase in pore water pressure. Moreover, the sliding surface usually corresponds to the soil–bedrock interface or to a textural–granulometric discontinuity within the soil, which drastically changes the infiltration rate (Wieczorek, 1987).

This work summarises characteristics and main effects of the meteorological events which hit the Lucca and Pistoia provinces in December 2009, focusing especially on their consequences on slopes and human environment. Moreover, it also describes the main characteristics of the heavy rainstorms which hit the Lucca and Massa-Carrara provinces in June 2010 and October 2011, respectively.

1.2 The December 2009 events

1.2.1 Main features

From 18 to 21 December 2009 heavy rainfalls and snowfalls occurred in Northern Tuscany. They caused floods and several landslides in the Serchio River Valley and Apuan Alps (Lucca province) and in the Pistoia Apennines (Pistoia province) (Fig. 1.1). The Serchio R. discharge reached almost 2000 m^3/s (Nardi, 2010), causing the breaking of the embankments (Fig. 1.2) and floods in some areas (about 30 km^2 wide, Fig. 1.1) of the Lucca and Pisa plains.

Throughout the considered area (Serchio River Valley - SRV, Apuan Alps - AA and Pistoia Apennines - PA), the cumulative rainfall of December 2009 corresponds to about 30% of the mean annual precipitation (MAP), as shown in Table 1.1. The monthly precipitation was particularly abundant at Campagrina (997.8 mm), Cardoso (664.6 mm) and Fabbriche di

Vallico (648.8 mm) in Lucca province (Fig. 1.3a; Table 1.1) and at Pracchia (676.8 mm) and Acquerino (613.0 mm) in Pistoia province (Fig. 1.3b; Table 1.1).

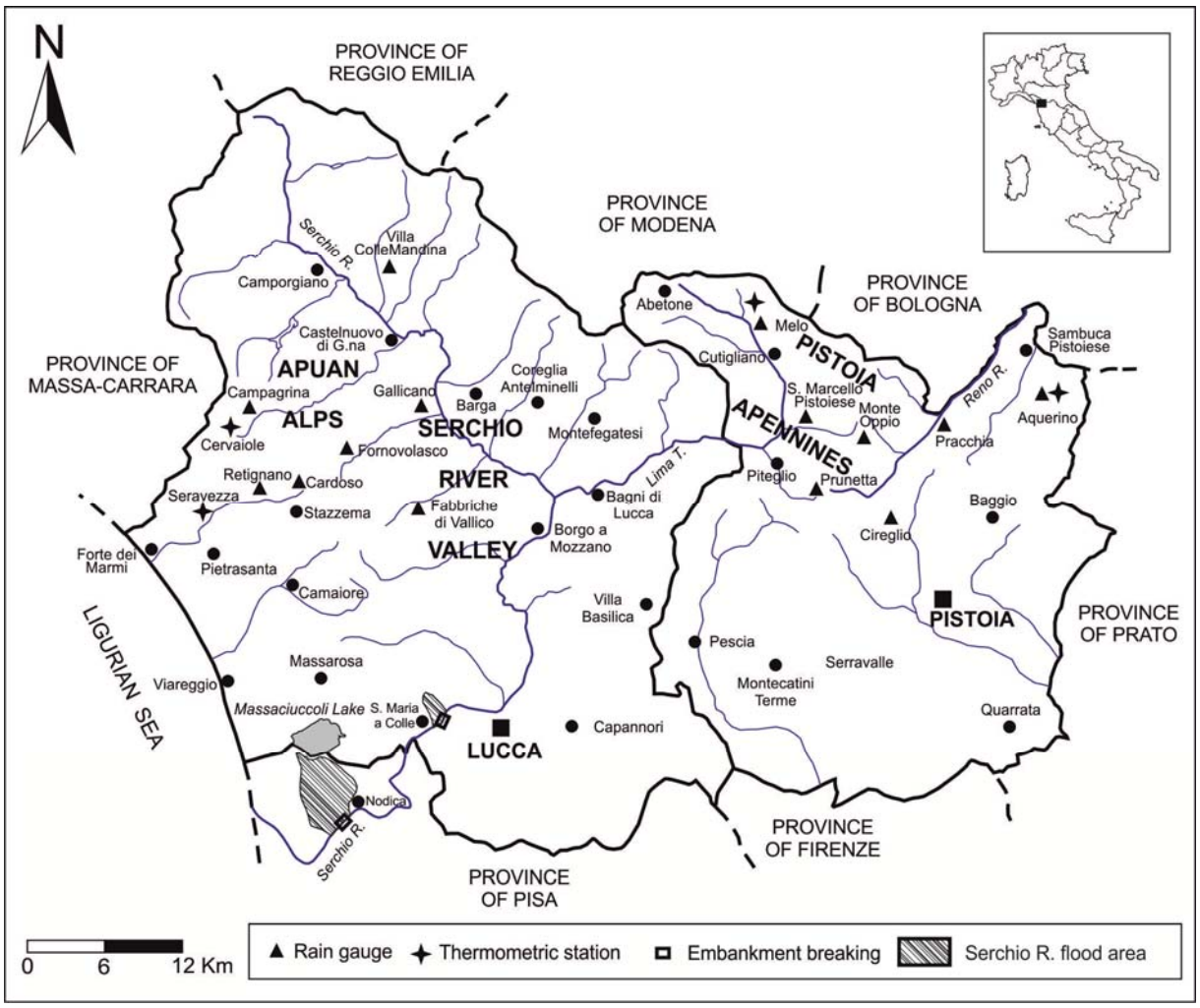

Fig. 1.1. Location map of Lucca and Pistoia provinces. Rain gauges and thermometric stations are also shown.

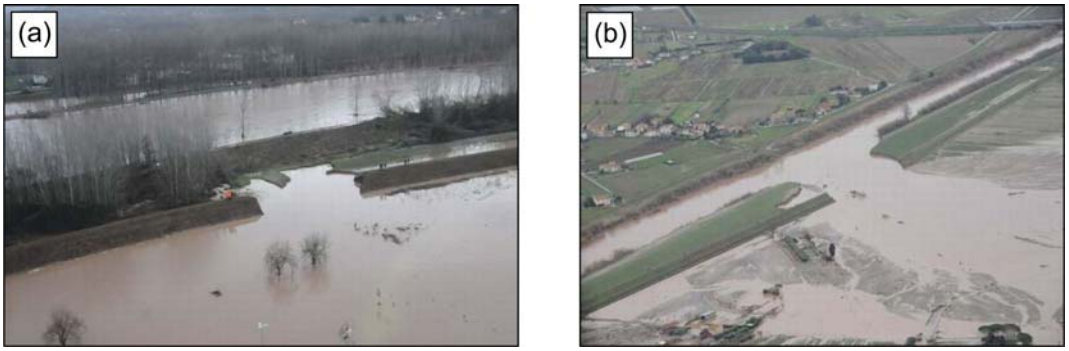

Fig. 1.2. Breaking of embankment of the Serchio R. in the Lucca **(a)** and Pisa **(b)** plains (Tuscany Region Hydrologic Service and Authority of the Serchio River Basin, 2010, modified).

Table 1.1. Rainfall data of December 2009. Rainy day: day characterized by at least 1 mm of rainfall. The rain gauges are located in Fig. 1.1. MAP: mean annual precipitation; AA: Apuan Alps; SRV: Serchio River valley; PA: Pistoia Apennines; -: undetermined data.

Rain gauge	Elevation (m)	Area	Rain amount (mm)	Rainy days*	Average rainy days (mm)	MAP (mm)	Period	%
Campagrina	807	AA	997.8	14	62.3	2922.4	1975-2005	34.1
Cardoso	398	AA	664.6	15	41.4	2041.2	1998-2005	32.6
Retignano	440	AA	501.0	15	33.3	1757.8	1975-2005	28.5
Villa Collemandina	524	SRV	402.8	12	30.8	1415.8	1975-2005	28.4
Fabbriche di Vallico	417	SRV	648.8	13	49.8	2033.3	1996-2005	31.9
Fornovolasco	470	SRV	579.6	12	44.6	2346.9	1965-1985	24.7
Gallicano	186	SRV	524.6	15	34.9	1626.8	1975-2005	32.2
S. Marcello Pistoiese	1019	PA	456.4	15	30.3	-	-	-
Monte Oppio	816	PA	457.2	15	30.5	1914	1966-1986	24.0
Acquerino	900	PA	613.0	17	36.1	-	-	-
Cireglio	630	PA	572.4	16	35.7	1594.8	1975-2005	35.9
Melo	992	PA	589.2	16	36.8	-	-	-
Pracchia	635	PA	675.8	16	42.2	-	-	-
Prunetta	951	PA	530.4	16	33.2	1763.5	1975-2005	30.1
Baggio	434	PA	393.6	16	24.5	1105.4	1996-2005	35.6

Abundant rainfalls together with rapid snow melting determined limit equilibrium conditions in many slopes in the study area. In fact, many slopes were collapsed during the subsequent heavy rainfalls on 22-23 (Figs. 1.3c and 1.3d) December and especially on 24-25 December (Figs. 1.3e and 1.3f).

Unfortunately, the lack of automatic snow gauges in the regional monitoring network prevented an accurate estimation of snowfalls. However, the Abetone station (1340 m a.s.l., Fig. 1.1) recorded 70, 30 and 7 cm of snow on 22, 24 and 27 December respectively, highlighting a rapid snow melting. This might have had a significant role, actually difficult to quantify, in causing the instability conditions of slopes. This instability was also caused by a rapid increase of the minimum temperature recorded in few days and by the concomitant heavy rainfalls. Figure 1.4 shows the comparison between the daily rainfall and the minimum temperature recorded at Melo (Cutigliano, Fig. 1.4a) and Acquerino (Sambuca Pistoiese, Fig. 1.4b) stations in the Pistoia Apennines. The most abundant rainfall was recorded from 21 to 25 December, together with an increase of 16-17°C of the minimum temperature. This

phenomenon also occurred in Lucca province, as shown in Figs. 1.4c and 1.4d for the Apuan Alps area.

Landslides were activated during the 22-23 and 24-25 December events. Rainfall fell to a nearly saturated soil, which was probably in limit equilibrium conditions, because of antecedent rainfalls and snowfalls occurred between 18 and 21 December. For example, during the previous 30 days, the Campagrina, Cardoso, Fabbriche di Vallico and Gallicano rain gauges recorded 553.8, 343.4 , 327.2 and 269.6 mm, respectively.

Figures 1.3c and 1.3d show the cumulative rainfall recorded during the first event (22-23 December) in some rain gauges of Lucca (Fig. 1.3c) and Pistoia (Fig. 1.3d) provinces. This event affected mainly the SRV and the AA. The event started on 21 December with a light rain. In the Lucca province, rainfalls ranging between 60 and 130 mm were measured from 06:00 on 21 December to 17:00 on 22 December. Rainfall intensity increased rapidly since 17:00. The first rainfall burst lasted 11 h, from 17:00 of 22 December to 04:00 of 23 December. During this period the Campagrina, Cardoso, Fabbriche di Vallico, and Fornovolasco rain gauges recorded 131.2 (11.9 mm h^{-1}) ,116.4 (10.6 mm h^{-1}), 126.2 (11.5 mm h^{-1}), and 112.8 mm (10.3 mm h^{-1}), respectively (Fig. 1.3c). The first event ended at approximately 09:00 on 23 December with average intensity of 1.5 mm h^{-1}.

The most damaging rainfall event hit from 21:00 on 23 to 11:00 on 25 December the Lucca province (Fig. 1.3e) and from 21:00 on 23 to 13:00 on 25 December the Pistoia province (Fig. 1.3f). In Lucca province, the rainfall reached the highest intensity from 12:00 on 24 to 3:00 on 25 December. During this period (15 h) the Campagrina, Cardoso, Retignano, Fabbriche di Vallico, Fornovolasco, and Gallicano rain gauges measured 263.8, 167.2, 139.6, 164.6, 147.8, 121.6 mm, respectively (Fig. 1.3e). Rainfall intensity of 17.6, 11.1, 11.0 and 9.8 mm h^{-1} in 15 h were recorded at Campagrina, Cardoso, Fabbriche di Vallico, and Fornovolasco, respectively (Fig. 1.3e).

Likewise, in the Pistoia Apennines the Pracchia, Prunetta, Melo, Cireglio and Monte Oppio rain gauges recorded 168.8 (11.3 mm h^{-1}), 168.4 mm (11.2 mm h^{-1}) and 153.8 mm (10,3 mm h^{-1}), 141.6 (9.44 mm h^{-1}), 135.0 mm (9.0 mm h^{-1}) respectively, from 13:00 on 24 to 4:00 on 25 December (Fig. 1.3f).

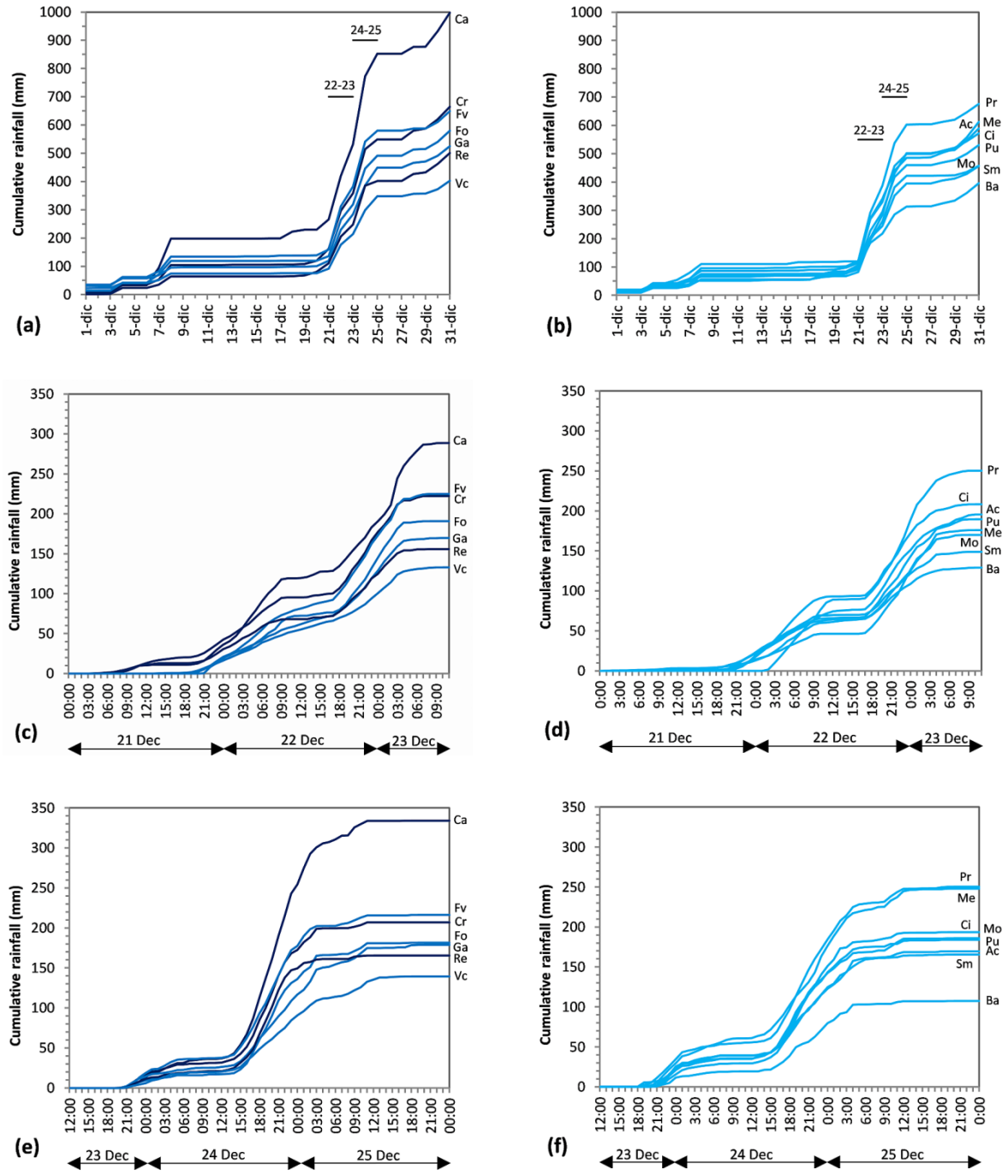

Fig. 1.3. Rainfall condition that resulted in landslides in Northern Tuscany in December 2009. **(a)** and **(b)** daily rainfall recorded in Lucca and Pistoia provinces, respectively. The 22-23 and 24-25 rainfall events are indicate. **(c)** and **(d)** hourly rainfall recorded in the period between 21 December, at 00:00, and 23 December, at 11:00, in Lucca and Pistoia provinces, respectively. **(e)** and **(f)** hourly rainfall recorded in the period between 23 December, at 12:00, and 26 December, at 00:00, in Lucca and Pistoia provinces, respectively. The rain gauges arrange geographically in three groups. Group 1, dark blue lines: Ca, Campagrina; Cr, Cardoso; Re, Retignano. Group 2, blue lines: Fv, Fabbriche di Vallico; Fo, Fornovolasco; Ga, Gallicano; Vc, Villa Collemandina. Group 3, sky-blue lines: Pr, Pracchia; Ac, Acquerino; Me, Melo; Ci, Cireglio; Pu, Prunetta; Mo, Monte Modino; Sm, San Marcello Pistoiese; Ba, Baggio. The rain gauges are located in Fig. 1.1.

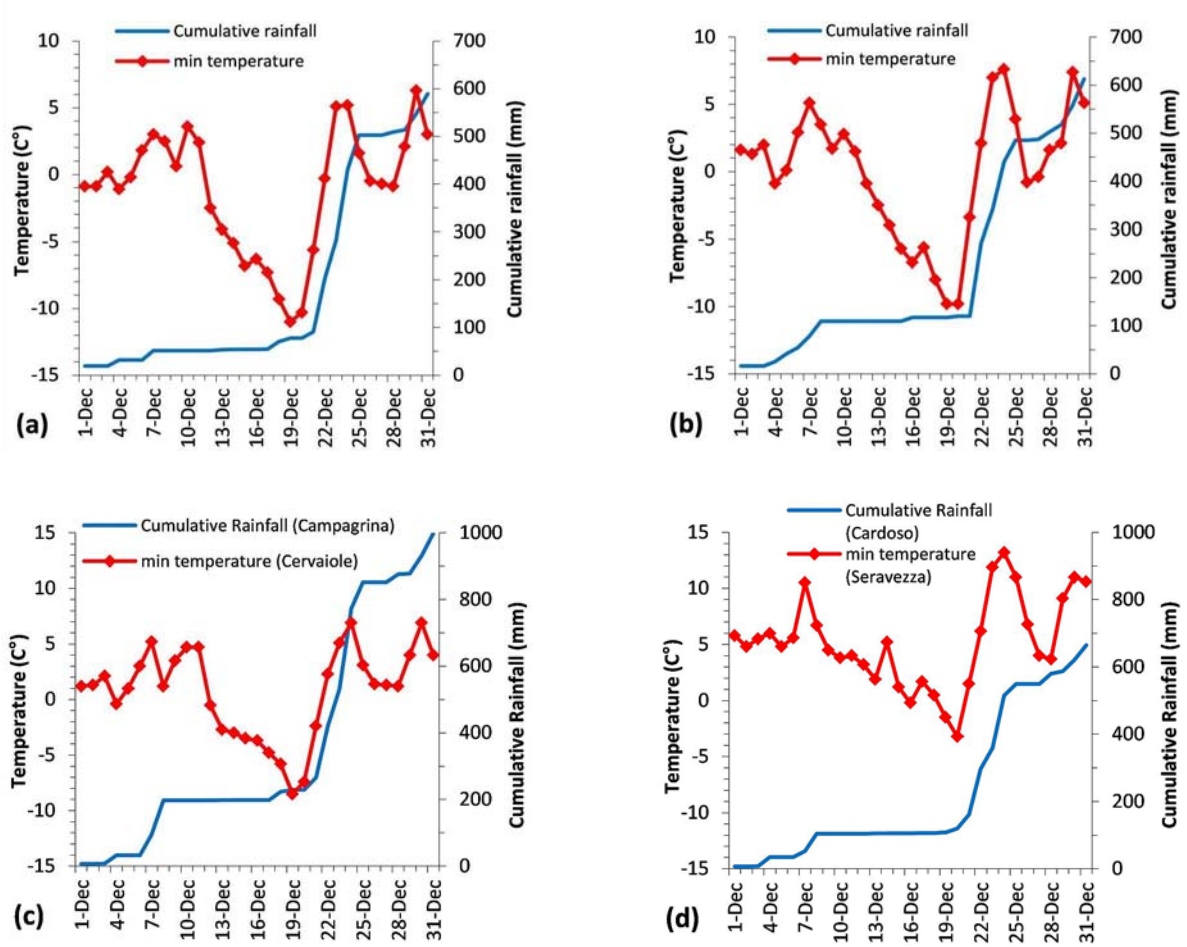

Fig. 1.4. Daily rainfall and minimum temperature of December 2009. Data recorded at Melo **(a)**, Acquerino **(b)**, Campagrina and Cervaiole (1009 m a.s.l.) **(c)**, and Cardoso and Seravezza (35 m a.s.l.) **(d)**. Rain gauges and thermometric stations are located in Fig. 1.1.

In order to highlight the importance of the December 2009 events, Fig. 1.5 shows the duration *D* (h) and intensity *I* (mm h^{-1}) values recorded by the Cardoso rain gauge (AA) on 22-23 and 24-25 December (11 h and 10.6 mm h^{-1}, 15 h and 11.1 mm h^{-1}, respectively). They are compared with the intensity-duration (ID) thresholds for triggering shallow landslides, obtained by Giannecchini (2006) for this area. Basing on several landslide-triggering rainstorms, the Author individuated the rainfall duration and intensity of the rainstorms able to trigger shallow landslides in Southern Apuan Alps. He individuated two threshold curves (lower and upper curves), which identify three fields with different degrees of stability. Below the lower threshold (blue dashed line) stability generally prevails. Above the upper curve (blue continuous line) instability prevails, while the field between the two curves includes intermediate or uncertain stability (Fig. 1.5). The December 2009 events are placed in the

field between the lower and the upper thresholds, where the rainfall may cause, locally or diffusely, instability phenomena.

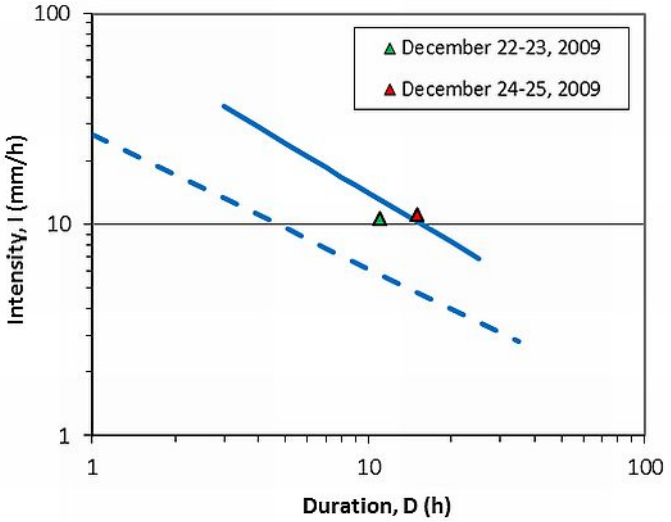

Fig. 1.5. Comparison between the December 2009 rainstorms and the critical threshold curves in terms of duration and intensity obtained by Giannecchini (2006) for the Southern Apuan Alps.

1.2.2 Effects of December 2009 events

The December 2009 rainfall events triggered more than 600 landslides in Northern Tuscany. Landslides often affected the road network, generally for lack or deficiency of surficial water draining systems. In Lucca province 132 landslides affected the roads: 22 occurred along the main roads, the other 110 along the secondary ones. This is a recurrent case in many regions of the world (Anderson, 1983; Haigh et al., 1993; Larsen and Parks, 1997).

In relation to the study area and considering the numerous 2009 failures, a position of the 2009 events above the upper curve of Giannecchini (2006) should be expected (Fig. 1.5). Really, the I-D features place the 2009 rainfall events just below the upper curve, where only some failures should occur. Therefore, the unnatural concentration of the running waters probably contributed in slope instability, even during rainfall events placed below the upper threshold (D'Amato Avanzi et al., 2012).

The road network in several places of the study area is rather old and the maintenance is often deficient (Fig. 1.6a). This implies uncorrect control and draining of the runoff, which may be directed towards critical slopes (e.g. debris/colluvium deposits, high slope gradient,

hollows, dormant landslides, etc., Fig. 1.6b). The unnatural and concentrated flow determines an increase in pore water pressure, destabilizing the slope cover (Kuriakose et al., 2008).

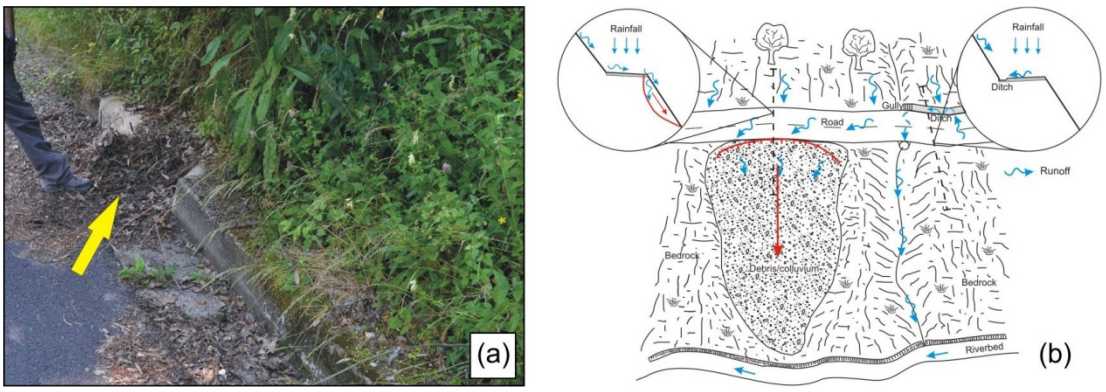

Fig. 1.6. (a) Examples of a gully grating completely occluded. **(b)** Block diagram of the triggering mechanism of landsliding along the road network (after D'Amato Avanzi et al., 2012).

For example, this occurred along the regional road n. 445 next to Camporgiano (Fig. 1.7a) and Piazza al Serchio (SRV), along the national road n. 12 next to Popiglio (Piteglio, PA) and along many other roads of the Lucca (Figs. 1.7b and 1.7c) and Pistoia provinces. Moreover, some landslides cut off 13 villages for several days, while other mass movements involved a few houses, as happened at Castelnuovo di Garfagnana and Campolemisi (SRV, Lucca province).

Many December 2009 landslides were first time movements, mainly referable to complex, translational debris slide-flows (Fig. 1.7d), typically triggered by intense rainfall. In the study area they occurred in peculiar geologic and geomorphologic environments: (i) colluvium/debris thin slope cover (from few decimetres to some metres thick), (ii) semi-permeable or impermeable bedrock, (iii) hollow shaped slope, and (iv) high slope gradient, as already highlighted by D'Amato Avanzi et al. (2002, 2004) for some Apuan Alps areas.

Some mass movements also involved the uppermost, weathered and fractured portion of the bedrock. This bedrock was mainly formed of by sandstone (Macigno Fm., Tuscan *Nappe*), metamorphic sandstone, siltstone or phyllite (Pseudomacigno Fm., Apuan Metamorphic Complex). However, in some cases different types of movements occurred, as rock and debris rotational slides (Pracchia, PA, Fig. 1.8) and debris flows (close to Montefegatesi village, SRV, Fig. 1.9).

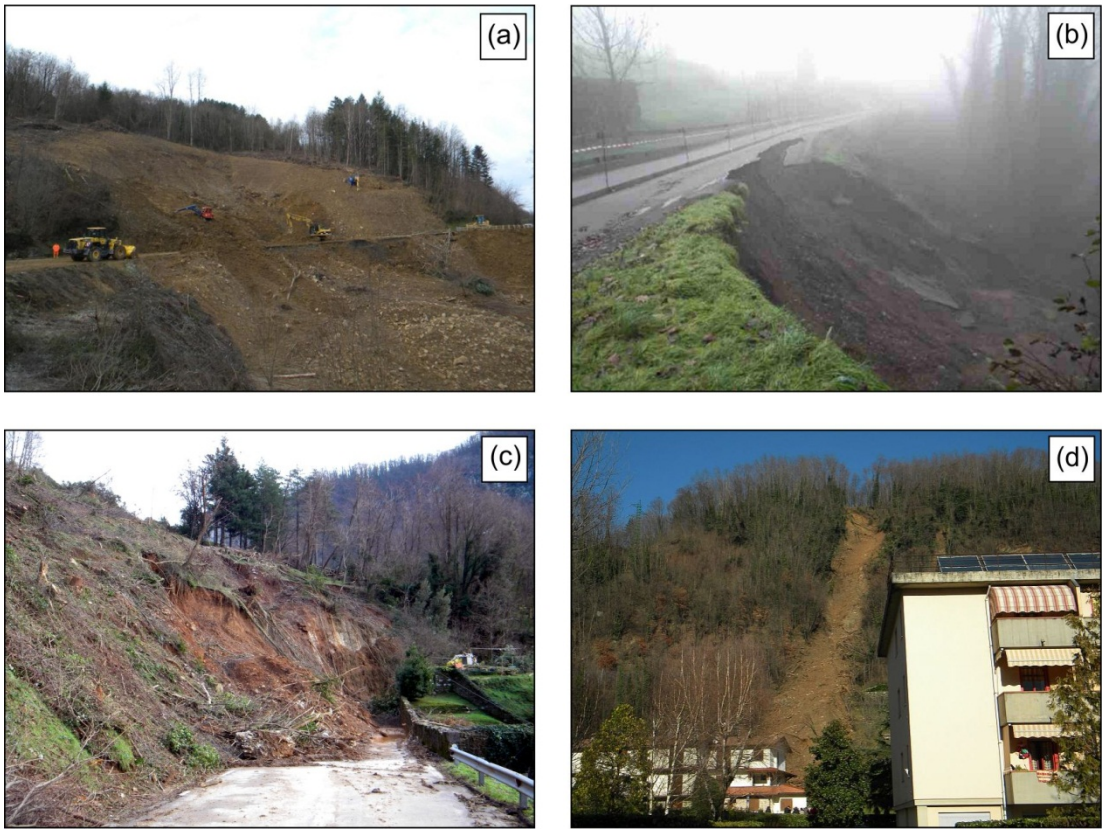

Fig. 1.7. Landslide triggered by intense rainfall in December 2009 in Lucca Province. **(a)** Debris slide triggered along the SR 445 road near Camporgiano (SRV). **(b)** Source area of soil slip-debris flow near Coreglia Antelminelli (SRV). **(c)** Debris slide triggered along the SP 10 road near Stazzema (AA). **(d)** Complex, translational debris slide-flow near Castelnuovo Garfagnana (SRV).

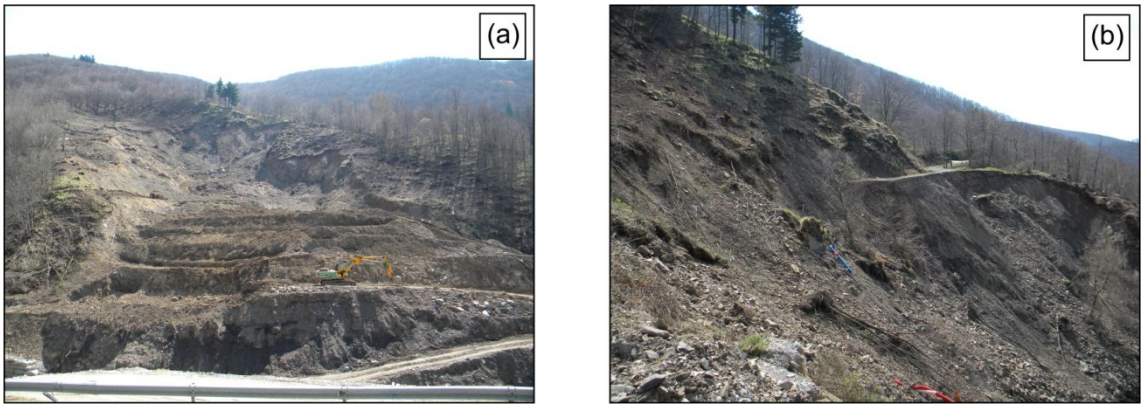

Fig. 1.8. Rotational slide involving debris and fractured rock (sandstone and siltstone) near Pracchia (Reno River valley, PA). **(b)** Particular of the main scarp.

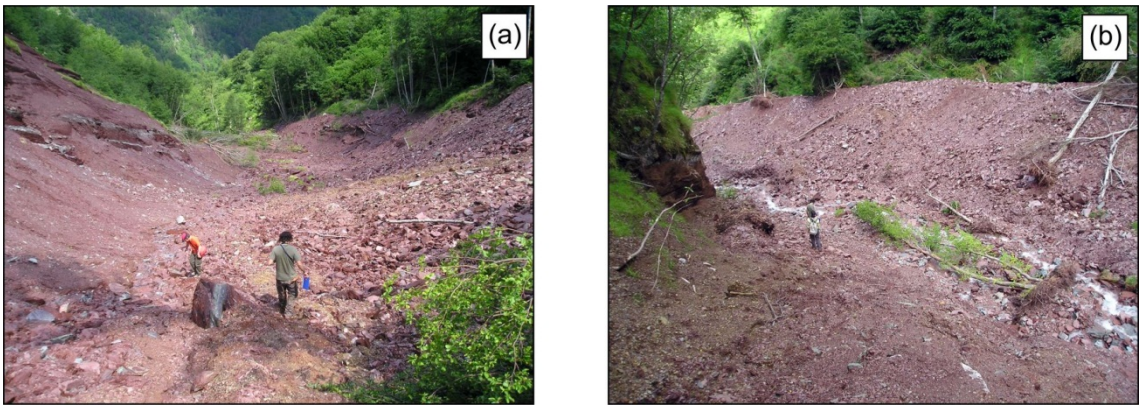

Fig. 1.9. (a) Channelized debris flow involving the pelitic lithofacies of the Scaglia Toscana Fm. (SRV). **(b)** Particular of lateral levee on the right side.

1.3 The June 2010 event

The Tramonte area in the Serchio River Valley (Fig. 1.10) was hit by heavy rainstorm on 19 June 2010, causing tens of shallow landslides mainly referable to soil slip-debris flows (Crosta et al., 1990). The Piaggione rain gauge (45 m a.s.l., Fig. 1.10) recorded 150.0 mm from 00.00 to 13.00 (13 h and 11.5 mm h^{-1}) on 19 June 2010. Maximum rainfall intensity of 40.0 and 45.0 mm h^{-1} were recorded in 2 h (from 5.00 to 7.00) and 1 h (from 6.00 to 7.00), respectively (Fig. 1.11a).

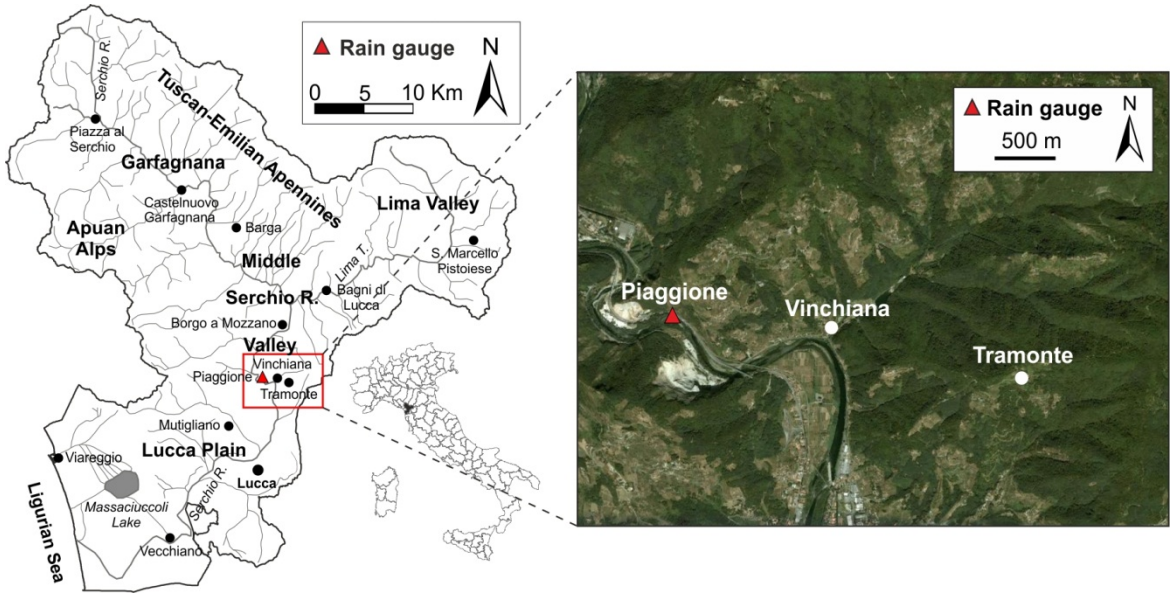

Fig. 1.10. Map of the Serchio River Valley and location of the Piaggione rain gauge (base map by Google Earth, 2011). Red rectangle and satellite image show the area hit by 19 June 2010 rainstorm.

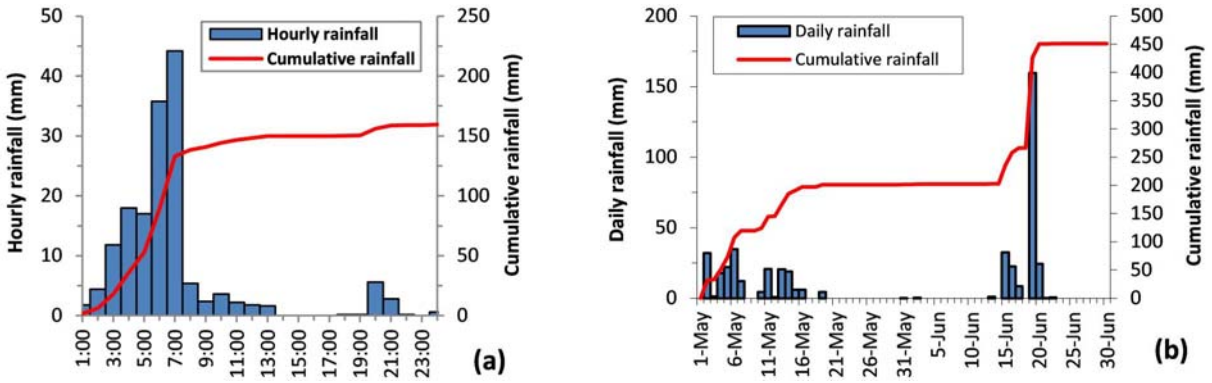

Fig. 1.11. Hourly rainfall of 19 June 2010 **(a)** and daily rainfall of May-June 2010 **(b)** at Piaggione.

Formerly heavy rainfall hit this area on 20 November 2000, inducing around 150 landslides (D'Amato Avanzi et al., 2002). Considering that cumulative rainfall and rainfall intensity of two events are similar, the difference number of landslides is probably due to the antecedent rainfall amount. In fact, the Piaggione rain gauge recorded 317.2 and 65.0 mm (Fig. 1.11b) in the 30-days prior to the 20 November 2000 and the 19 June 2010 events, respectively. This highlights the significant role of the antecedent rainfall in the initiation of landslides.

As on December 2009, landslides especially affected the road network (1.12b), blocking some secondary roads and the national road n. 12 in Vinchiana. These landslides involved chiefly colluvium and debris deposits of the Macigno Fm. (Tuscan *Nappe)*. The latter consists of siliciclastic turbidites made of grey-brown sandstone and normally shows a high sandstone/shale ratio and thick to very thick, coarse-grained strata.

The source areas of the shallow landslides triggered on June 2010 were typically located in the zero-order basins. This location is also typical of other regions of Italy frequently prone to intense rainstorms, mainly some areas of Campania (Guida, 2003; Cascini et al., 2008) and Calabria (Calcaterra and Parise, 2005). The term "zero-order basins", coined by Tsukamoto (1973), indicates unchannellized convergent slope located above ephemeral, intermittent or perennial first-order streams and n+1-order streams (Guida, 2003).

In the Tramonte area, two types of source area were mainly identified: the top part of the first-order tributary with open channel flow (e.g. Solco dell'Angelo basin, Figs. 1.12a and

1.13a), and the upper portion of the zero-order basins alongside the first-order or n+1-order streams (e.g. Solco del Miglino basin, Figs. 1.12c and 1.13b).

Fig. 1.12. Landslides triggered during the 19 June 2010 rainstorm in Tramonte area. **(a)** and **(b)** source and travel areas of a soil slip-debris flow in the top part of the Solco dell'Angelo stream. **(c)** Soil slips triggered in the zero order basins and flowed in the Solco del Miglino stream, as debris flow. **(d)** and **(e)** track and deposition areas of a soil slip-debris flow into the Solco del Miglino stream.

The landslides originated mostly as shallow, translational or rotational slides on slope ranging from 30° to 45°, and involved soil (especially silty sand with gravel) and the weathered and fractured portion of the bedrock. In the source area, thickness of the failed material ranged between 30 cm and 1 m, with an estimated average of 50 cm. Scars left by soil slip-debris flows had width *W* ranging from 5 to 10 m, length *L* ranging from 50 to 150 m, and a *W/L* ratio <<1 (0.03-0.5). Scars seems to be more abundant on reverse dip slopes, where the layers of the sandstone rocks dips into the slope.

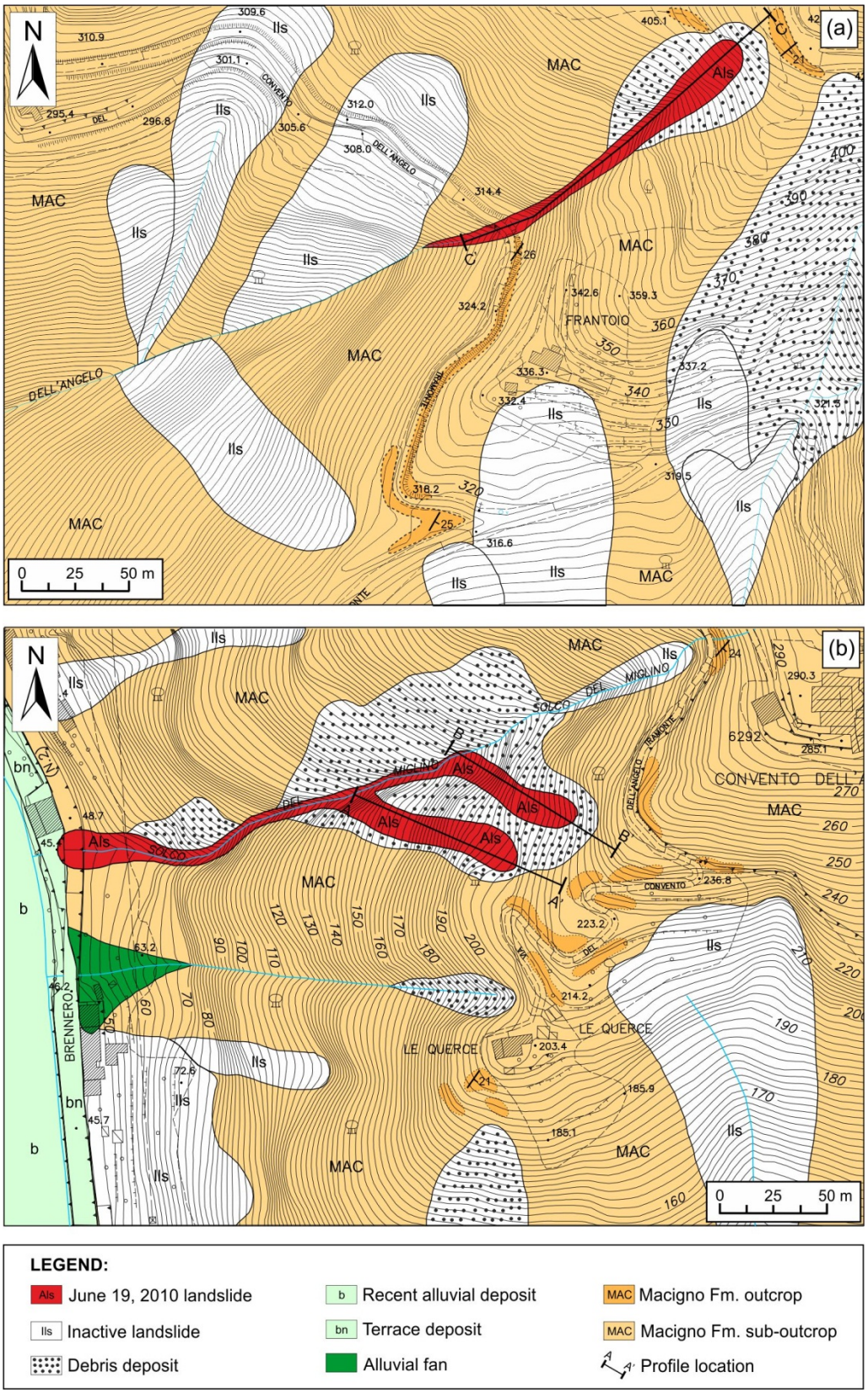

Fig. 1.13 Geologic map of the S. dell'Angelo **(a)** and S. del Miglino **(b)** basins. **(a)** Soil slip-debris flow triggered in the upslope of the S. dell'Angelo stream. **(b)** Debris flow originated as soil slip in the zero order basins along the S. del Miglino stream.

1.4 The October 2010 event

Northern Tuscany was further hit by heavy and nearly continuous rainfall in autumn 2010, causing damage in particular in the Massa-Carrara province (Fig. 1.14) on 31 October. Here, the rainstorm triggered hundreds of landslides, mostly of first generation, mainly referable to soil slip-debris flows.

Fig. 1.14. The area of Massa-Carrara province most affected by the 31 October 2010 rainstorm (base map by Google Earth, 2011). Yellow triangles show location of the four considered rain gauges.

On 31 October 2010 the Canevara (Massa, 109 m a.s.l.), Cerreto (Montignoso, 480 m a.s.l.), Candia Scurtarola (Massa, 150 m a.s.l.), and Carrara (39 m a.s.l.) rain gauges recorded 179.0, 198.8, 177.0 and 145.0 mm, in 24 hours respectively (Fig. 1.15). The highest intensity was recorded from 3.00 to 4.00 at Canevara and Cerreto (42.8 and 46.0 mm h^{-1}, respectively) and from 2.00 to 3.00 at Candia and Carrara (30.2 and 21.4 mm h^{-1}, respectively).

However, the extended rainfall period already began during the 30 preceding days and continued in November (Fig. 1.16). In fact, from 1 to 30 October, the Canevara, Cerreto, Candia Scurtarola, and Carrara rain gauges recorded 251.8, 248.8, 245.4, and 161.0 mm, respectively. In particular, rainfall concentrated in three main periods (4-5, 16-17 and 24-25 October). Such events did not trigger landslides, but probably played a significant role in

preparing the slopes instability, which collapsed during the subsequent heavy rainfall on 31 October. In November rainfall became almost continuous but less intense (344.8 in 23 rainy days and 344.0 mm in 22 rainy days at Canevara and Cerreto respectively, Fig. 1.16).

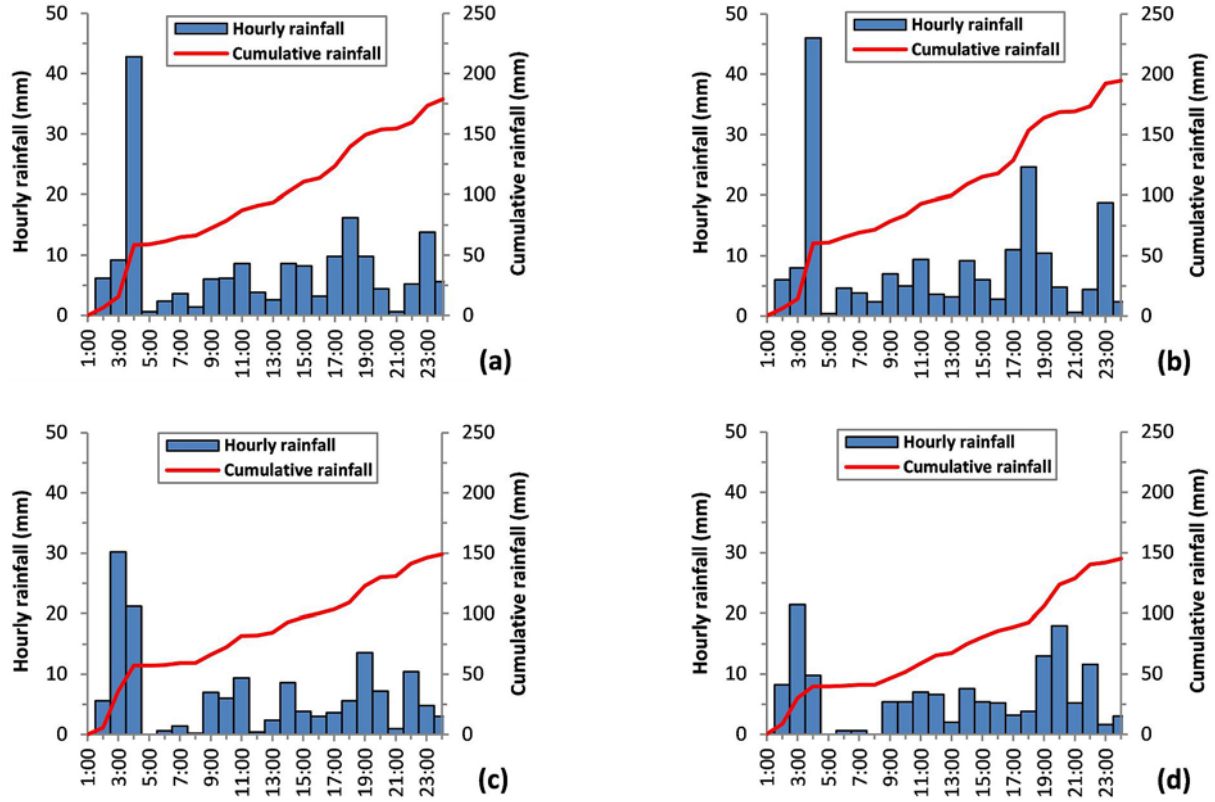

Fig. 1.15. Hourly and cumulative rainfall of 31 October 2010 at Canevara **(a)**, Cerreto **(b)**, Candia Scurtarola **(c)**, and Carrara **(d)**.

As for the events previously described, the mass movements especially affected the road network (Fig. 1.17), according to the triggering mechanism shown in Fig. 1.6. Consequently, many roads were blocked isolating some villages for days. Some landslides also involved houses, causing serious damage and three victims, like at Lavacchio (2 deaths – Fig. 1.17a) and Mirteto villages (1 death) in the Massa hinterland. Tens of people were evacuated in various villages of the study area.

Approximately, the landslides source area was located along the road network in almost the 60% of the examined landslides, while 22% of landslides involved buildings, showing the fragility of this territory once more (D'Amato Avanzi et al., 2012).

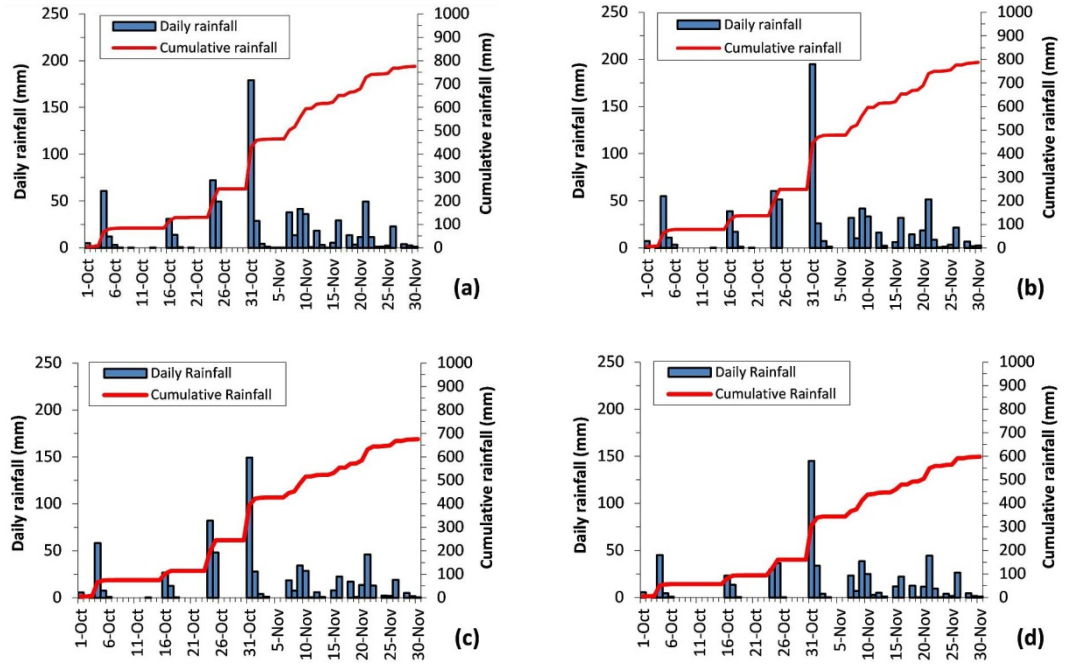

Fig. 1.16. Daily and cumulative rainfall of October and November 2010 at Canevara **(a)**, Cerreto **(b)**, Candia Scurtarola **(c)**, and Carrara **(d)**.

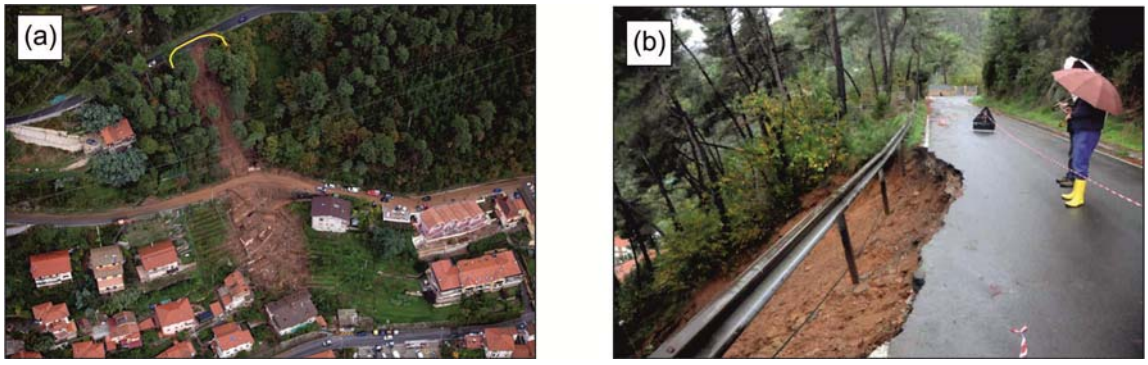

Fig. 1.17. (a) Soil slip-debris flow triggered at Lavacchio (Massa), burying a house and killed two people. Yellow line shows the source area. **(b)** Particular of source area at the road.

1.5 Final remarks

The rainfall events of December 2009, June 2010 and October 2010 again highlighted the fragility of wide areas of the Northern Tuscany. The landslides triggered during these events were typical of intense rainstorms, i.e., shallow landslides (chiefly soil slip-debris flows) which mainly involved the surface soil materials. In the cases of the December 2009 and

October 2010 events, the 30-days antecedent cumulative rainfall was also important for the initiation of landslides in the study areas.

The landslides were triggered in geological and geomorphological typical environments: (i) colluvium/debris thin slope cover, (ii) semi-permeable or impermeable bedrock, (iii) hollow shaped slope, and (iv) high slope gradient.

Many landslides occurred along the road network and involved buildings and infrastructures. Despite their little size, they caused heavy damage and also casualties (three deaths in October 2010 in the Massa hinterland). This often caused by the lack of a correct maintenance of the road drainage systems in hill/mountains areas, but a short-sighted territorial planning might have contributed by underestimating hazard and risk.

Landslide risk maps can identify unstable areas, but also potential first time landslide prone areas. At present geologists have the knowledge to identify the main landslides risk factors, but their job and importance are often neglected or denied.

Social and economic losses due to landslides can be reduced by means of effective planning and management which involved landslide hazard assessment, slope assessment for landslide prediction, mitigation measures and warning systems (Schuster, 1995; Dai et al., 2002).

At present, further research is necessary in order to reach a zonation of the shallow landslide hazard in the areas under consideration. The parameters to be considered regard the slope gradient, the system governing the surface water regime, the thickness of the soil materials, the local geotechnical characteristics and the degree of saturation of the soil slope cover. The influence of factors of anthropic origin on landslide occurrence also must be considered.

Further data should be collected by means of penetration tests, permeability tests and undisturbed sampling of the cover materials, in order to better define their geotechnical features. Furthermore, the critical rainfall thresholds for triggering shallow landslides should be determined.

References

Anderson, M. G.: Road-cut slope topography and stability relationships in St. Lucia, West Indies, Applied Geography., 3, 104–114, 1983.

ANPA-ARPAT: 19 giugno 1996: Alluvione in Versilia e Garfagnana. Un caso di studio, Graf. Il Fiorino, Firenze, 315 pp., 1998.

Banducci, E., Giorgi, R., Giacomelli, L., and Palazzetti, M (Eds.): Novembre 2000, Pacini Editore, Ospedaletto (Pisa), Italy, 158 pp., 2005.

Caine, N.: The rainfall intensity-duration control of shallow landslides and debris flows, Geogr. Ann. A., 62, 23–27, 1980.

Calcaterra, D. and Parise, M.: Landslide types and their relationships with weathering in a Calabrian basin, southern Italy, Bull. Eng. Geol. Environ., 64, 193–207, 2005.

Campbell, R. H.: Debris flows originating from soil slips during rainstorms in Southern California, Q. J. Eng. Geol. Hydroge., 7, 339–349, 1974.

Campbell, R. H.: Soil slips, debris flows, and rainstorms in the Santa Monica mountains and vicinity, southern California, U.S. Geological Survey Professional Paper, 851, 51 pp., 1975.

Casagli, N., Dapporto, S., Ibsen, M. L., Tofani, V., and Vannocci, P.: Analysis of the landslide triggering mechanism during the storm of 20th-21st November 2000, in Northern Tuscan, Landslides, 3, 1321, 2006.

Cascini, L., Cuomo, S., and Guida, D.: Typical source areas of May 1998 flow-like mass movements in the Campania region, Southern Italy, Eng. Geol., 96, 107–125, 2008.

Chien-Yuan, C., Tien-Chien, C., Fan-Chieh, Y. and Chun-Chieh, T.: Rainfall duration and debris-flow initiated studies for real-time monitoring, Environmental Geology, 47, 715–724, 2005.

Corominas, J., Remondo, R., Farias, P., Estevao, M., Zezere, J., Diaz De Teran, J., Dikau, R., Schrott, L., Moya, J., Gonzalez, A.: Debris flow, in: Dikau, R., Brunsden, D., Schrott, L., Ibsen, M.-L. (Eds.), Landslide Recognition: Identification, Movement and Causes, Wiley, Chichester, 161–180, 1996.

Cortopassi, P. F., Daddi, M., D'Amato Avanzi, G., Giannecchini, R., Lattanzi, G., Merlini, A., and Milano, P. F.: Quarry waste and slope instability: preliminary assessment of some controlling factors in the Carrara marble basin (Italy), Italian Journal of Engineering Geology and Environment, Special Issue 1, 99–118, 2008.

Crosta, G.: Regionalization of rainfall thresholds: an aid to landslide hazard evaluation, Environ. Geol., 35(2–3), 131–145, 1998.

Crosta, G., Guzzetti, F., Marchetti, M., and Reichenbach, P.: Morphological classification of debris-flow processes in South-Central Alps (Italy), in: Proceeding of 6th International IAEG Congress, 1990, Balkema, Rotterdam, 1565–1572, 1990.

Crozier, M. J.: Landslides: Causes, Consequences and Environment, Routledge, London–New York, 252pp., 1986.

Cruden, D. M. and Varnes, D. J.: Landslide type and processes, in: Landslides investigation and mitigation, Turner, A. K. and Schuster, R. L. (Eds.), Transportation Research Board Special Report 247, National Research Council, National Academy Press, Washington D.C., 36–75, 1996.

D'Amato Avanzi, G., Galanti, Y., Giannecchini, R., and Puccinelli, A.: Fragility of territory and infrastructures resulting from rainstorms in Northern Tuscany (Italy), in: Proceedings of the 2nd World Landslide Forum, Roma, 3–9 October 2011, Springer-Verlag, in press, 2012.

D'Amato Avanzi, G. and Giannecchini, R.: Eventi alluvionali e fenomeni franosi nelle Alpi Apuane (Toscana): primi risultati di un'indagine retrospettiva nel bacino del Fiume Versilia, Rivista Geografica Italiana, 110, 527–559, 2003.

D'Amato Avanzi, G., Giannecchini, R., and Puccinelli, A.: I movimenti franosi del novembre 2000 nella provincia di Lucca: osservazioni preliminari, Atti Conv. "Il dissesto idrogeologico: inventario e prospettive", Roma, 5/6/2001, Atti Conv. Lincei, 181, 365–377, 2002.

D'Amato Avanzi, G., Giannecchini, R., and Puccinelli, A.: The influence of the geological and geomorphological settings on shallow landslides. An example in a temperate climate environment: the June 19, 1996 event in the north western Tuscany (Italy), Eng. Geol., 73, 215–228, 2004.

Dai, F. C. and Lee, C. F.: Frequency–volume relation and prediction of rainfall-induced landslides, Eng. Geol., 59, 253–266, 2001.

Dai, F. C., Lee, C. F., and Ngai, Y. Y.: Landslide risk assessment and management: an overview, Eng. Geol., 64, 65–87, 2002.

Ellen, S. D. and Wieczorek, G. F.: Landslides, floods, and marine effects of the storm of January 3-5, 1982, in the San Francisco Bay region, California, U.S. Geological Survey Professional paper 1434, 310 pp., 1988.

Fuchu, D., Lee, C. F. and Sijing, W.: Analysis of rainstorm-induced slide-debris flows on natural terrain of Lantau Island, Hong Kong, Eng. Geol., 51, 279–290, 1999.

Fukuoka, M.: Landslides associated with rainfall, Geotechnical Engineering, 11(1), 1–29, 1980.

Giannecchini, R.: Relationship between rainfall and shallow landslides in the southern Apuan Alps, Nat. Hazards Earth Syst. Sci., 6, 375–364, 2006.

Giannecchini, R. and D'Amato Avanzi, G.: Historical research as a tool in estimating hydrogeological hazard in a typical small alpine-like area: The example of the Versilia River basin (Apuan Alps, Italy), J. Phys. Chem. Earth, doi:10.1016/j.pce.2011.12.005, 2012.

Giannecchini, R. and Verani, M.: The November 2000 intense rainfall in the Pescia area (north Tuscany, Italy): characteristics and effects of the pluviometric event, Italian Journal of Engineering Geology and Environment, 1, 19–34, 2006.

Guida, D.: The role of the zero-order basins in flowslide-debris flow occurrence and recurrence in Campania (Italy), Proc. Int. Conf. on fast slope movements – prediction and prevention for risk mitigation (IC-FSM 2003), Naples, Italy, 11–13 May 2003, 255–262, 2003.

Guzzetti, F.: Landslide fatalities and evaluation of landslide risk in Italy, Eng. Geol., 58, 89–107, 2000.

Guzzetti, F., Stark, C. P., and Salvati, P.: Evaluation of flood and landslide risk to the population of Italy, Environ. Manage., 36(1), 15–36, 2005.

Haigh, M. J., Rawat, J. S., and Bartarya, S. K.: Environmental correlations of landslide frequency along new highways in the Hymalaya - preliminary results, Catena, 15, 539–553, 1988.

Jibson, R. W.: Debris flow in southern Porto Rico, Geological Society of America, 236, 29–55, 1989.

Kuriakose, S. L., Jetten, V. G., van Westen, C. J., Sankar G., and van Beek, L. P. H.: Pore water pressure as a trigger of shallow landslides in the Western Ghats of Kerala, India: some preliminary observations from an experimental catchment, Phys. Geogr., 29, 374–386, 2009.

Larsen, M. C. and Parks, J. E.: How wide is a road? The association of roads and mass-wasting in a forested montane environment, Earth Surf. Proc. Land., 22, 835–848, 1997.

Munich Re: Topics Geo - Natural catastrophes 2008, Analyses, assessments, positions. Knowledge Series, No. 302-06022, Münchener Rück Munich Re Group., 50pp., 2009.

Nardi R.: Le rotture arginali del fiume Serchio durante la piena del 25 dicembre 2009, Geoitalia, 30, 34–37, 2010.

Pierson, T. C.: Piezometric response to rainstorms in forested hillslope drainage depressions, Journal of Hydrology, New Zealand 19(1), 1–10, 1980.

Schuster, R. L.: Reducing landslide risk in urban areas – experience in the united states, in: Urban Disaster Mitigation: The Role of Engineering and Technology, edited by: Cheng, F. Y. and Sheu, M.-S., Elsevier, 217–230, 1995.

Schuster, R. L.: Socioeconomics significance of landslides, in: Landslides investigation and mitigation, edited by: Turner, A. K. and Schuster, R. L., Transportation Research Board Special Report 247, National Research Council, National Academy Press, Washington D.C., 12–35, 1996.

Selby, M. J.: Slope erosion due to extreme rainfall: a case study from New Zealand, Geogr. Ann. A., 58(2), 131–138, 1976.

Tsukamoto, Y.: Study on the growth of stream channel, (I) Relation between stream channel growth and landslides occurring during heavy storm, Shin sabo, 25(4), 4–13, 1973.

Tuscany Region Hydrologic Service and Authority of the Serchio River Basin: Report sull'evento alluvionale registrato nei giorni 24-25 dic. 2009 nel Bacino del Fiume Serchio, 59 pp., 2010.

Wieczorek, G. F.: Effect of rainfall intensity and duration on debris flows in central Santa Cruz Mountains, California, in: Debris Flows/Avalanches: Processes, Recognition and Mitigation, edited by: Costa, J. E. and Wieczorek, G. F., Reviews in Engineering Geology, Geological Society of America, 7, 23–104, 1987.

Wieczorek, G.F.: Landslide triggering mechanisms, in: Landslides investigation and mitigation, edited by: Turner, A. K. and Schuster, R. L., Transportation Research Board Special Report 247, National Research Council, National Academy Press, Washington D.C., 76–90, 1996.

2 Geotechnical characterization of source areas of shallow landslides by dynamic penetration tests in Northern Tuscany (Italy): first results and perspectives

Abstract

In Northern Tuscany (Italy) shallow landslides often cause victims and severe damages. Aiming at contributing to the characterization of the source areas of shallow landslides, this study deals with the geotechnical parameterization of the involved material by means of dynamic penetration tests (Dynamic Probing, DP). The study considered the soils covering the Macigno Fm. (Tuscan *Nappe*), which mainly consist of debris and/or colluvium, granular deposits. The Macigno Fm., formed of siliciclastic turbidite, constitutes the main Apennines ridge and underlies hundreds of square kilometres of Tuscany. Most of the shallow landslides in Northern Tuscany really involve the soils covering the Macigno Fm. The source areas are usually located in difficult areas, where boring and undisturbed sampling are very complicated and onerous. Therefore, in order to determine the typical soil properties, the results of 210 geotechnical tests were analysed, including Medium (DPM) and Super Heavy Dynamic Probing (DPSH) tests, Standard Penetration Tests (SPT) and laboratory tests. The results of DP tests were related to Relative density D_R and friction angle φ' of the soil by means of empirical methods considering the most typical soil categories (sand-silt mixtures, sands and sand-gravel mixtures). Distribution and variability of these parameters were analysed and related to soil type, test type and probing depth.

The D_R and φ' values coming from different test types resulted comparable. The φ' values coming from DP tests and direct shear tests showed an acceptable correlation, confirming utility of the DP tests. Therefore, the DP can be an effective tool for the geotechnical characterization of potentially unstable soil slope covers. Landslide susceptibility assessment is among the most relevant uses.

Keywords: Penetration test, shallow landslides, coarse-grained soils, shear strength, relative density, Tuscany.

2.1 Introduction

In Italy and all over the world intense and persistent rainfalls trigger shallow landslides, mostly soil slip-debris flows, which cause victims and damages (Campbell, 1975; Ellen and Wieczorek, 1988). When rainfalls exceed the critical value, these rapid landslides quickly spread over the region and reach very high concentration (Jibson, 1989; Wieczorek, 1996), while destructive torrential debris flows often run the hydrographical net (Pierson and Costa, 1987; Corominas et al., 1996).

Many meaningful examples of disasters caused by rapid, shallow landslides and debris flows could be mentioned in the world: for example, in USA (Ellen and Wieczorek, 1988), Japan (Wang et al., 2002), or New Zealand (Ekanayake and Philipps, 2002). In Italy, examples come from Campania (Del Prete et al., 1998; Guadagno and Revellino, 2005), Northern Tuscany (D'Amato Avanzi et al., 2004; Delmonaco et al., 2003; Casagli et al., 2006) and Ischia Island (De Vita et al., 2007). Once more, in October 2010 shallow, rapid landslides caused huge damages and deaths in the Massa hinterland (north-western Tuscany) and in October 2011 in the Magra River valley (north-western Tuscany) and in Eastern Liguria (Vara River valley and Cinque Terre area).

In Northern Tuscany, rainstorms triggering shallow landslides commonly involve soil deposits lying on impermeable or semi-permeable rock formations (D'Amato Avanzi et al., 2004; Giannecchini, 2005, 2006). Really the Macigno Fm., which largely crops out in the hilly-mountain areas of the Tuscany, underlies most of the soil deposits involved in landsliding. The physical-mechanical properties of the involved material play a key role in determining the landsliding, as evidenced by Giannecchini and Pochini (2003).

In this context, this research aims at contributing to the characterization of the source areas of the shallow landslides, by means of Dynamic Probing tests (DP). These tools are particularly suitable to obtain the soil properties (e.g. relative density D_R and friction angle φ') in difficult access slopes, as in the study area. Original data, coming from inspections of existing databases or expressly performed tests, are presented and discussed here. They refer to several areas of the Lucca province in Northern Tuscany (Fig. 2.1) and the related experiences and considerations can be of general interest.

The research focused on soil deposits mainly consisting of debris and/or colluvium, underlain by peculiar arenaceous formations, well represented in Tuscany. Among them the

Macigno Fm. (Tuscan *Nappe*) was firstly considered. It forms the main Apennine ridge and crops out for hundreds of square kilometres. Other arenaceous formations crop out in Northern Tuscany, such as the Monte Modino Fm. and the Pseudomacigno Fm. Their features are substantially similar to those of the Macigno Fm. Therefore, many considerations and results here exposed may be extended to them and can contribute in assessing the landslide hazard of a high risk area.

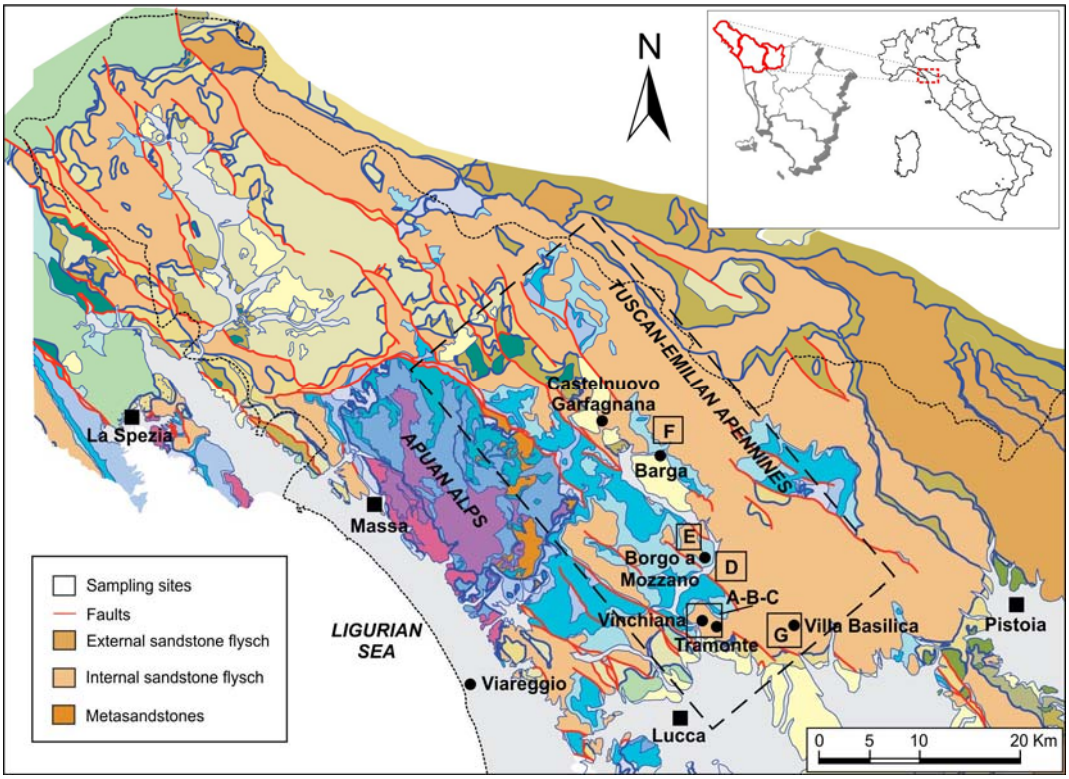

Fig. 2.1. Geologic sketch of Northern Tuscany (after Carmignani and Lazzarotto, 2004, modified) and outcrop areas of the main arenaceous formations. Dashed rectangle shows the study area. The boxes show the sampling sites.

2.2 Study area

Northern Tuscany falls within the Northern Apennines (Fig. 2.1), a fold-and-thrust belt. The chain resulted from the consumption of the Liguria-Piedmont oceanic basin (western Tethys) and the consequent collision between the Adria and the European plates, which started in the Upper Cretaceous (Carmignani et al, 2004; Conti and Lazzarotto, 2004). The upper Miocene tensional tectonics gave origin to tectonic depressions bounded by NW-SE trending normal faults, where either marine or continental successions deposited. On the northern Tuscan side of the Apennines several tectonic units took place, coming from

different paleogeographic domains (from west to east: Ligurian Domain, Sub-Ligurian Domain, Tuscan Domain). Afterwards, continental sequences sedimented.

The Macigno Fm. (Tuscan *Nappe* unit, Tuscan Domain) consists of siliciclastic turbidites, made of grey-brown sandstone and thin siltstone or mudstone intervals. It normally shows high to very high sandstone/shale ratio and thick to very thick (0.5-3 m), coarse-grained strata. Quartz, feldspar, mica, minor lithics and a high fraction of carbonate cement mainly form this sandstone. The depositional environment is mainly referable to channelled submarine fans (Pandeli et al., 1994).

Rock mass classification and laboratory tests on this formation were performed in the area of Castelnuovo Garfagnana (Serchio River Valley) in order to create a middle scale landslide hazard map (Federici et al. 2011). Based on the ISRM's (1978, 1981) suggestions and the Bieniawski's (1989) Rock Mass Rating, the typical Macigno Fm. can be described as a stratified, medium strong rock (uniaxial compressive strength of 40-50 MPa), intersected by 2-3 joint sets. Discontinuities are close spaced, very persistent, open, smooth or slightly rough, from moderate to high weathered and dry to damp. Infilling is not very significant. The rock mass may be considered as a poor rock (Rock Mass Rating of about 35).

Intense fracturing, geotechnical features, climate and rainfall regime (referable to the Apennine-Mediterranean type with transition to the sub-coastal type, D'Amato Avanzi et al., 2004; Giannecchini and D'Amato Avanzi, 2012) favour the sandstone weathering and the debris/colluvium production. Therefore, large soil slope deposits mantle most of the slopes underlain by the Macigno Fm., hiding the bedrock. These deposits mainly consist of sand and gravel with a minor part of finer materials (silt and clay).

As mentioned above, intense and persistent rainfalls frequently trigger shallow, rapid landslides in Northern Tuscany. According to the Cruden and Varnes' (1996) classification, they can be classified as complex, rapid to extremely rapid debris slide-debris flows, but are also known as soil slip-debris flows, or simply debris flows (Campbell, 1975). In Northern Tuscany the shallow, rapid landslides involving slopes underlain by the Macigno Fm. are generally referable to soil slip-debris flows and exhibit some typical features (D'Amato Avanzi et al., 2004): hollow-shaped or zero-order basin, 30-45° steep slope, small thickness of the sliding material (0.5 to 3 m). Sliding and subsequent flowing take a very short time and velocity is extremely high. Afterwards, the material usually flows into the riverbeds and quickly reaches the main valley bottom, where the reduced slope gradient induces deposition.

Due to the relative little length of hilly slope and streams, the travel distance is not so high and rarely is more than one hundred metres. Channelized debris flows prevail, while open-slope debris flows are a minority. These features allow us to define most of the above mentioned shallow, rapid landslides as extremely rapid, saturated debris flows following established channels over a large part of their path (Hungr et al., 2001).

2.3 Materials and methods

The methodological approach included different phases, summarized as follows. During the first phase, many technical reports were collected from public administrations, professional geologists and companies. The reports were analysed and categorized, in order to obtain physical and mechanical data on the soil covering the Macigno Fm. The reports provided results of 195 tests, including: (i) Dynamic Probing (DP) tests, (ii) Standard Penetration Tests (SPT), and (iii) laboratory tests.

In the second phase, some source areas of shallow landslides were selected, where existing DP data were available (boxes in Figs. 2.1 and 2.2). In these areas the soils were expressly sampled, in order to perform grain-size analyses and Atterberg limits and to support the collected data with additional information. Finally, all data were processed.

2.3.1 Data collection

Measured mechanical properties of coarse-grained soils (sands and gravels) are rarely published (e.g. Blijenberg, 1995; Kokusho et al., 1995). Great difficulties and high costs often limit and make it difficult to obtain undisturbed samples from these materials, to perform direct shear tests. Consequently, their mechanical properties are mostly based on indirect tests, such as penetration tests. Very little reliable mechanical data of the Macigno Fm. soil cover are available for the study area. On the contrary, dynamic penetration tests are commonly used and can be a base for an areal characterization of this particular material. Actually, the dynamic penetrometer is a practical, simple and quick tool for testing soil properties, also in difficult areas.

Therefore, the data collection was focused in searching for data in technical reports available at archives of local authority, professional geological offices and companies. The database of the Tuscany Region, Seismic Risk Division (Il Rischio sismico in Toscana, 2012),

available online and including much geognostic information, was also inspected. Thus, 133 reports and some individual data were collected, analysed and categorized. This data collection provided the results of 177 field investigations (131 DP tests and 46 SPT tests) and 18 laboratory tests, including 12 direct shear (DS) test. These investigations come from several areas of the Lucca province (Northern Tuscany, Figs. 2.1 and 2.2).

Furthermore, 15 laboratory investigations were performed during this work, in order to support the collected data with additional information on grain-size distribution and Atterberg limits of the soil covering of the Macigno Fm. On site, the soils were sampled in selected source areas of shallow landslides (Fig. 2.2), where data coming from existing DP tests were available (boxes in Figs. 2.1 and 2.2).

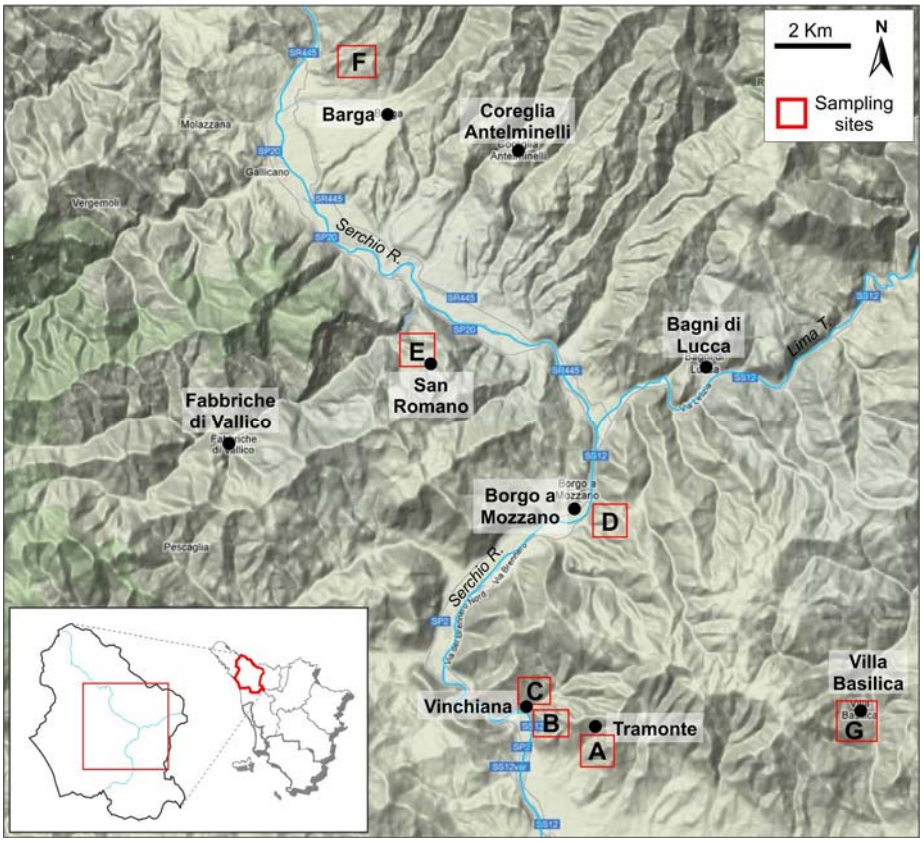

Fig. 2.2. Sampling sites in the Province of Lucca, Northern Tuscany (base map by Google Maps, 2012).

2.3.2 Laboratory analysis

Laboratory tests were performed on 33 soil samples coming from selected source areas of shallow landslides, where DP data were already available (boxes in Figs. 2.1 and 2.2). During this research 6 and 9 disturbed soil samples were taken in the sites A and B (Tramonte area),

respectively. These samples were taken on the scarps of shallow landslides (Fig. 2.3) at a depth of around 0.5 m. Moreover, the results of laboratory tests performed on 18 soil samples were collected in technical reports. These samples come from the Vinchiana area (site C), the Borgo a Mozzano area (sites D and E), the Barga area (site F), and the Villa Basilica area (site G).

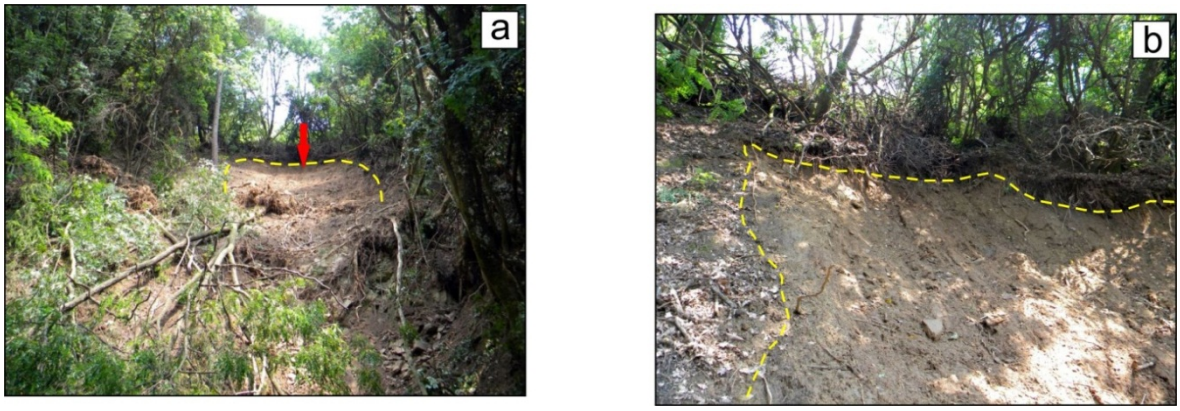

Fig. 2.3. Example of shallow landslide scarp **(a)** and particular of it **(b)**, where samples were collected. Dashed yellow line shows the scarp. Red arrow indicates the sampling point.

The laboratory tests were performed according to the ASTM (1996) specifications, in order to determine grain-size distribution and Atterberg limits of the soil. The grain-size distribution was measured using sieve and hydrometer methods as described in ASTM D-422. Atterberg limits were measured using the procedure described in ASTM D-4318.

Generally, the variables tested include: (i) various grain-size distribution parameters (D_{10}, D_{30}, D_{50}, D_{60}, and gravel, sand, and fine-grained percentage – *Fc*), (ii) coefficient of uniformity C_U, (iii) coefficient of curvature C_C, and (iv) Atterberg limits (liquid limit – *LL*, plastic limit – *PL*, Plasticity Index – *PI*). The grain-size distribution parameter *D* refers to the apparent grain-size diameter (mm) and the subscripts (10, 30, 50, 60) refer to the percent of the soil mass that is finer than that diameter. The variable F_C consists of the percentage of the total dry soil mass passing the #200 (0.075 mm) sieve (silt + clay). The variable C_U (D_{60}/D_{10}) is an indicator of the particle range of the soil, whereas C_C ($(D_{30})^2/(D_{10}\cdot D_{60})$) is a measure of the shape of the grain-size distribution curve.

The results of the laboratory tests were used to classify the soil, according to the Unified Soil Classification System (USCS, ASTM D-2487), and to apply the proper parameters in the equation (2.5) and in the equations showed in Fig. 2.5, mentioned afterwards.

In addition, the results of 12 direct shear (DS) tests were collected in technical reports. The DS tests were performed on undisturbed soil samples, coming from the Vinchiana (site C) and Villa Basilica (site G) areas, frequently involved in landslides (Figs. 2.1 and 2.2). The shear strength parameters (cohesion c' and friction angle φ') were useful in calibrating the φ' values obtained by Dynamic Probing tests.

2.3.3 Dynamic Probing tests

As mentioned above, the dynamic penetrometer is a practical and simple tool for testing soil properties. Its first use in soil science can probably be ascribed to Parker and Jenny (1945), which estimated the soil strength by measuring the energy required to drive a soil-sampling tube into the soil. The penetration test is based on the number of blows the penetrometer hammer needs to insert a probe for a predetermined length. The probe may consist of a steel cone (Dynamic Probing – DP) or a sampler (Standard Penetration Test – SPT).

DP test may be directly executed on the natural ground surface, while SPT usually need a borehole. Moreover, ease of transport and of use makes DP test suitable and cheaper than SPT. Nowadays DP is commonly used to estimate some soil properties, such as thickness, relative density D_R and friction angle φ' (Eurocode 7, 2004; Cestari, 2005; Odebrecht et al. 2005; Lo Presti et al., 2007; Lo Presti and Squeglia, 2008; Schnaid, 2009). Nevertheless, in Italy and all over the world DP instruments have different features and different methods of investigation may be used. This causes problems of standardization and comparability of results (Cestari, 2005).

Stefanoff et al. (1988) proposed a classification of the dynamic penetrometers based on the mass of their hammer, which is commonly used worldwide: DP penetrometers are subdivided into Light (DPL), Medium (DPM), Heavy (DPH), and Super Heavy Dynamic Probing (DPSH) penetrometers (Table 2.1).

The standard EN ISO 22476-2:2005 (Geotechnical investigation and testing. Field testing. Dynamic probing) specifies technical features and requirements of the DP equipment for geotechnical investigations and subdivides the DPSH penetrometers into the classes DPSH-A and DPSH-B. The main difference between these classes concerns the fall height of the hammer; this directly influences the specific work per blow (194 KJ/m^2 and 238 KJ/m^2 for

DPSH-A and DPSH-B, respectively) and, therefore, the efficiency of the DP apparatus. In Italy the DPSH penetrometers, similar at DPSH-B type, are frequently used (Cestari, 2005), while the DPM penetrometers (Fig. 2.4), more easy to transport, are mainly used in difficult areas, such as slopes, woodlands, etc.

Table 2.1. Classification of the dynamic penetrometers (after Stefanoff et al., 1988).

Type of penetrometer	Acronym	Hammer mass, *M* (Kg)
Light	DPL	$M \leq 10$
Medium	DPM	$10 < M < 40$
Heavy	DPH	$40 \leq M < 60$
Super Heavy	DPSH	$M \geq 60$

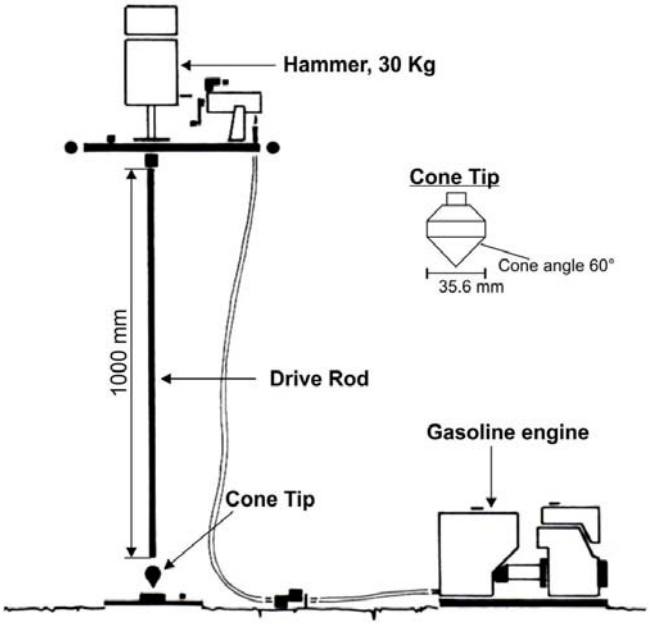

Fig. 2.4. Sketch of medium Dynamic Probing (DPM). The dimensions of cone tip are also highlighted.

As mentioned above, dynamic penetrometers are often used to estimate important geotechnical properties of soil (Sivrikaya and Toğrol, 2006; Squeglia et al., 2006; Lo Presti and Squeglia, 2008; Mohammadi et al., 2008 Hettiarachchi and Brown 2009; Schnaid et al. 2009), such as D_R and φ'. This implies the use of empirical correlations that may not be particularly accurate. This due to of a lack of a complete standardization of the DP

equipments commonly used (Cestari, 2005; Lo Presti et al., 2007; Lo Presti and Squeglia, 2008).

In order to compare data of different penetrometers, normalization to SPT is required by determining the number of blows N_{SPT} referred to the SPT. It uses a correlation factor *CF*, namely the ratio between the specific energy per blow of DP (Q_{DP}) and SPT (Q_{SPT}). *CF* is calculated as follows, obtaining values of 1.48 for DPSH and 0.76 for DPM penetrometers.

$$CF = \frac{Q_{DP}}{Q_{SPT}} = \frac{(M_{DP}H_{DP}/(A_{DP}\delta_{DP})}{(M_{SPT}H_{SPT})/(A_{SPT}\delta_{SPT})} \tag{2.1}$$

where $M_{DP\text{-}SPT}$: hammer mass (kg); $H_{DP\text{-}SPT}$: hammer falling height (cm); $A_{DP\text{-}SPT}$: steel cone area (cm^2); $\delta_{DP\text{-}SPT}$: cone penetration depth (cm).

N_{SPT} is then calculated by the following equation:

$$N_{SPT} = CF \cdot N_{DP} \tag{2.2}$$

where N_{DP} is the number of blows of the DP test and *CF* is calculated by equation (2.1).

N_{SPT} is usually normalized according to a standard penetrometer efficiency *ER* of 60% (Skempton, 1986) and an atmospheric pressure of 98.1 kPa (Liao and Whitman, 1986). *ER* depends on the hammer system of the instrument and on the interaction between hammer and anvil. Most of the penetrometers used in Italy for SPTs have an *ER* of 60% (Cestari, 2005), the same as the standard. For DPSH and DPM tests an *ER* of 73% (Pagani Geotechnical Equipment, 2012) and 80%, respectively, may be considered. Moreover, the N_{SPT} value should be corrected for a number of site-specific factors, to improve its comparability and repeatability (Rogers, 2006), obtaining the final $(N_1)_{60}$ value. Therefore, the corrected $(N_1)_{60}$ represents the normalized value of N_{SPT} (calculated by the equation 2.2) and can be obtained using the following equation (Robertson and Wride, 1997):

$$(N_1)_{60} = N_{SPT}(C_N C_E C_B C_R C_S) \tag{2.3}$$

where N_{SPT}: number of blows of SPT; $C_N=(Pa/\sigma'_{V0})^{0.5}$: correction factor for effective overburden stress that consider the degree of saturation of soil (Liao and Whitman, 1986), where Pa is the reference pressure (98.1 kPa) and σ'_{V0} is the vertical effective stress; $C_E = ER/60\%$: correction factor for the hammer efficiency, where ER (%) is the efficiency of the penetrometer (C_E = 1.33 for DPM; C_E = 1.22 for DPSH; C_E = 1.00 for SPT); C_B: correction factor for the borehole diameter; C_R: correction factor for the drill rod length; C_S: correction factor for the sampler type. Table 2.2 shows the correction values commonly used for SPT and DP test blow-count values.

Table 2.2. Correction factors for SPT and DP blow-count values, taken from Robertson and Wride (1997) and Yound and Idriss (2001), as modified by Skempton (1986).

Factor	**Equipment Variable**	**Term**	**Correction factor**
Overburden pressure		C_N	$(98.1/\sigma'_{V0})^{0.5}$
Borehole diameter	65-115 mm	C_B	1.0
	150 mm		1.05
	200 mm		1.15
Rod length	10-30 m	C_R	1.0
	6-10 m		0.95
	4-6 m		0.85
	3-4 m		0.80
	< 3 m		0.75
Sampling method	Standard sampler	C_S	1.0
	Raymond sampler without liners		1.1-1.3

Since 1986, published correlations have increasingly used $(N_1)_{60}$ values with other parameters, such as relative density D_R and friction angle φ' (Rogers, 2006). For example, the knowledge of $(N_1)_{60}$ allows to estimate D_R by the parameters of Table 2.3 (Clayton, 1995) or by empirical equations, as that of Skempton (1986).

Table 2.3. Estimation of relative density according to $(N_1)_{60}$ value (Clayton, 1995).

$(N_1)_{60}$	Classification	Relative density, D_R (%)
0−3	Very loose	0−15
3−8	Loose	15−35
8−25	Medium	35−65
25−42	Dense	65−85
42−58	Very dense	85−100

In this study D_R was calculated by the Skempton's (1986) equation, because allows to obtain more accurate values of it. This equation is expressed in the form:

$$\frac{(N_1)_{60}}{D_R^{\,2}} = a + b \tag{2.4}$$

The equation (2.4) can also be written as:

$$D_R = \sqrt{\frac{(N_1)_{60}}{(a+b)}} \tag{2.5}$$

Skempton (1986) considered the ratio $(N_1)_{60}/D_R^{\,2}$ as a parameter affected by overburden pressures, ageing and grain size (Cubrinovski and Ishihara, 1999). The parameter $(a+b)$ for sandy soils assumes values of 55, 60 or 65 for fine, medium and coarse sand, respectively (Skempton, 1986). These assumptions were checked by means of the Cubrinowski and Ishihara (1999) approach which gives the possibility of assessing the $(a+b)$ parameter as a function of the mean grain size D_{50} or the coefficient of uniformity C_U.

In this study, such values were assigned to three soil type, namely: sand-silt mixtures (silty sand to sandy silt), sands (clean sands to sands with gravel), and sand-gravel mixtures (gravelly sand to sandy gravel), respectively. They normally constitute the soils involved in landsliding in the study areas and analyzed in this research. These soil types come from laboratory tests and site observations on the considered soils.

The friction angle φ' can be estimated by empirical methods, using: the N_{SPT} value (e.g. Peck et al., 1953; Dunham, 1954; De Mello, 1971; Japan Road Association, 1990), the N_{SPT} and the effective overburden stress σ'_{V0} values (Hatanaka and Uchida, 1996), and the linear relationships between φ' and D_R, as proposed by Schmertmann (1978). Also the Bolton (1986) approach, which takes into account the stress level at failure, could be used. But for the case under consideration it is not worthwhile to refer to it. Because, the knowledge of the sand mineralogy is necessary to define the constant volume friction angle φ'_{cv} and the stress crushability parameter Q (Bolton, 1986). Considering that the soil under consideration results from the degradation of Macigno Fm., values of Q = 10 and of φ'_{cv} = 30–32° could be assumed, as for Siliceous sands. Moreover, as for a plane strain conditions, a value of the coefficient m = 5 should be considered. Anyway, the debris thickness is usually of few meters and the effect of the overburden stress from 1 kPa to 100 kPa is of only 1° for medium dense and dense sands (Bellotti et al., 1986). This effect seems less relevant than the uncertainties introduced by the assumption of the Q and φ'_{cv} values.

Considering the foregoing, the Schmertmann (1978) approach (Fig. 2.5) was chosen for determine the friction angle φ'. This considers the grain-size distribution of the soil and, as noted by Squeglia et al. (2006), allows to obtain φ' values characterized by lower variability.

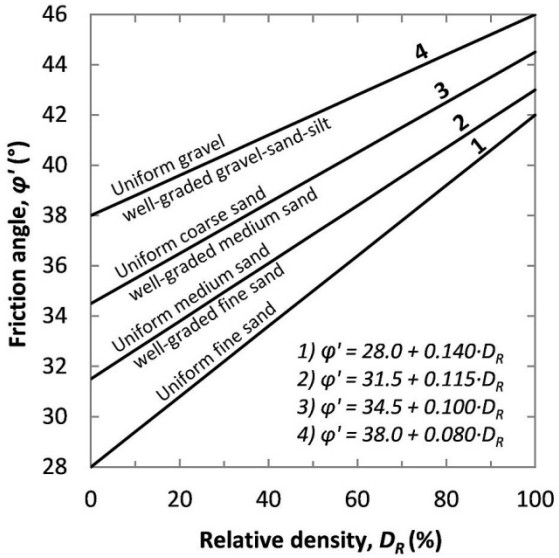

Fig. 2.5. Empirical equations for estimating φ' according to D_R and grain-size (Schmertmann, 1978).

On the other hand, while the possible Over Consolidation Ratio (OCR) of shallow layers is not influent on the penetration resistance and the angle of shear resistance of granular soils, the partial saturation or dry condition can lead to an overestimate of the φ' values (Lo Presti et

al., 2009), but unfortunately it is not possible to overcome this problem in a simple way and without additional in situ measurements.

2.4 Results

2.4.1 Laboratory analysis

Sampling depth, grain-size distribution parameters and Atterberg limits of the soil samples are summarized in Table 2.4. 19 samples were taken on the scarp of some shallow landslides (sites A, B, E, F), while 14 samples, collected in technical reports, were taken in boreholes at depth ranging between 1.0 m to 12.5 m (sites C, D, G).

Figure 2.6 shows the grain-size distribution of all soil samples. The grain-size distribution of the 15 soil samples collected during this work on sites A and B (Tramonte area) is showed in Fig. 2.6a. In general, the soil samples coming from site A have a higher fine content (between 21.8% and 33.2%) than those coming from site B (between 7.0% and 25.3%, Table 2.4).

Figure 2.7 shows the grain-size composition of 15 soil samples (sites A and B) collected and analysed during this work and of 18 samples coming from technical reports (sites C–G). Three different soil types are highlighted by the coloured ovals: (i) sandy soils (21 samples), (ii) gravelly soils (5), and (iii) fine-grained soils (7). High variability of grain-size is recognizable for the considered samples (Fig. 2.7; Table 2.4). Inspection of Fig. 2.7 and Table 2.4 indicates that the analysed soils have a sandy component ranging from 19.4% to 80.6% (average 49.8%), a gravelly component ranging from 0.1% to 67.0% (average 19.1%), and a fine content ranging between 7.0% and 64.0% (average 31.2%).

On the basis of laboratory test and according to the USCS classification, 21 soil samples were classified as sandy soils, including: silty sand SM, silty sand with gravel (SM)g, silty clayey sand SC-SM, silty clayey sand w/gravel (SC-SM)g, clayey sand SC, clayey sand w/gravel (SC)g, poorly graded sand w/silt SP-SM, well-graded sand w/silt SW-SM and well-graded sand w/silt and gravel (SW-SM)g. 5 soil samples were classified as gravelly soil: silty gravel w/sand (GM)s, clayey gravel w/sand (GC)s, well-graded gravel w/sand (GW-GM)s and silty clayey gravel w/sand (GC-GM)s. 7 soil samples were classified as fine grained soil: sandy silt s(ML), sandy lean clay s(CL), sandy lean clay w/gravel s(CL), sandy silty clay s(CL-ML).

Table 2.4. Grain-size distribution parameters, Atterberg limits and USCS classification of the soil samples. The second column indicates the sampling depth. The first 15 samples were taken during this research in the sites A and B, while the other 19 samples were analysed in technical reports and come from the sites C–G.

Sample	Depth (m)	Gravel (%)	Sand (%)	Fines, *Fc* (%)	D_{50}	C_U	C_C	*LL* (%)	*PL* (%)	*PI* (%)	USCS class
A-1	0.5	33.6	44.6	21.8	0.37	41.8	0.4	22	20	2	(SM)g
A-2	0.5	23.6	50.6	25.8	0.24	101.0	5.6	21	17	4	(SC-SM)g
A-3	0.5	12.5	56.5	31.0	0.16	40.2	4.0	21	18	3	SM
A-4	0.5	8.6	58.2	33.2	0.14	35.4	4.9	22	19	3	SM
A-5	0.5	4.2	70.4	25.4	0.19	20.9	2.8	20	16	4	SC-SM
A-6	0.5	16.6	58.5	24.9	0.25	53.8	2.3	22	16	6	(SC-SM)g
B-1	0.5	12.4	80.6	7.0	0.36	5.0	1.0	-	-	-	SP-SM
B-2	0.5	21.3	69.3	9.4	0.54	10.2	1.2	-	-	-	(SW-SM)g
B-3	0.5	12.5	76.8	10.6	0.37	8.0	1.3	21	18	3	SW-SM
B-4	0.5	23.8	55.5	20.7	0.42	31.0	0.7	19	17	2	(SM)g
B-5	0.5	25.5	56.0	18.5	0.48	26.5	0.7	19	16	3	(SM)g
B-6	0.5	12.1	70.4	17.4	0.33	10.2	0.8	20	19	1	SM
B-7	0.5	25.0	61.9	13.1	0.58	18.8	0.6	-	-	-	(SM)g
B-8	0.5	19.9	63.7	16.4	0.41	23.7	1.1	-	-	-	(SM)g
B-9	0.5	3.5	71.2	25.3	0.19	13.9	1.8	19	16	3	SM
C-1	1.5	13.4	34.2	52.4	0.07	126.7	2.4	34	21	13	s(CL)
C-2	4.5	45.5	26.0	28.5	2.50	1174.8	0.1	28	21	7	(GC-GM)s
C-3	3.0	15.7	30.0	54.3	0.06	-	-	38	22	16	s(CL)g
D-1	1.0	28.6	45.3	26.1	0.46	-	-	35	22	13	(SC)g
D-2	1.7	67.0	22.6	10.4	10.05	196.6	7.1	-	-	-	(GW-GM)s
E-1	0.3	11.2	59.3	29.5	0.14	153.9	21.6	-	-	-	SM
E-2	0.3	12.8	60.9	26.3	0.30	200.0	15.3	-	-	-	SM
F-1	0.5	9.4	53.0	37.6	0.16	-	-	25	21	4	SM
F-2	0.5	1.5	60.5	38.0	0.16	-	-	28	24	4	SM
G-1	4.9	1.4	35.8	62.8	0.03	-	-	37	25	12	s(ML)
G-2	3.0	15.0	28.0	57.0	0.05	-	-	28	20	8	s(CL)g
G-3	9.0	55.0	24.0	21.0	6.00	450.0	0.6	39	29	10	(GM)s
G-4	3.5	2.0	34.0	64.0	0.04	-	-	24	17	7	s(CL-ML)
G-5	3.0	47.5	19.4	33.1	3.90	800.0	0.0	43	29	14	(GM)s
G-6	7.2	0.3	39.3	60.4	0.05	28.0	3.6	31	21	10	s(CL)
G-7	12.5	30.9	28.0	41.1	0.21	266.7	0.7	30	20	10	(GC)s
G-8	5.0	16.7	33.1	53.2	0.065	75.0	2.1	29	19	10	s(CL)g
G-9	10.5	0.1	66.0	33.9	0.14	100.0	6.3	30	22	8	SC

The letter in the first column indicates the site where the sample was collected, which and is showed in Fig. 2.2.

D_{50}: particle size for which 50% of particles are finer; C_U: coefficient of uniformity; C_C: coefficient of curvature; *LL*: liquid limit; *PL*: plastic limit; *PI*: Plastic Index; -: undetermined data.

Gravel: D ≥ 4.75 mm, according to the USCS; Fines: D < 0.075 mm, according to the USCS.

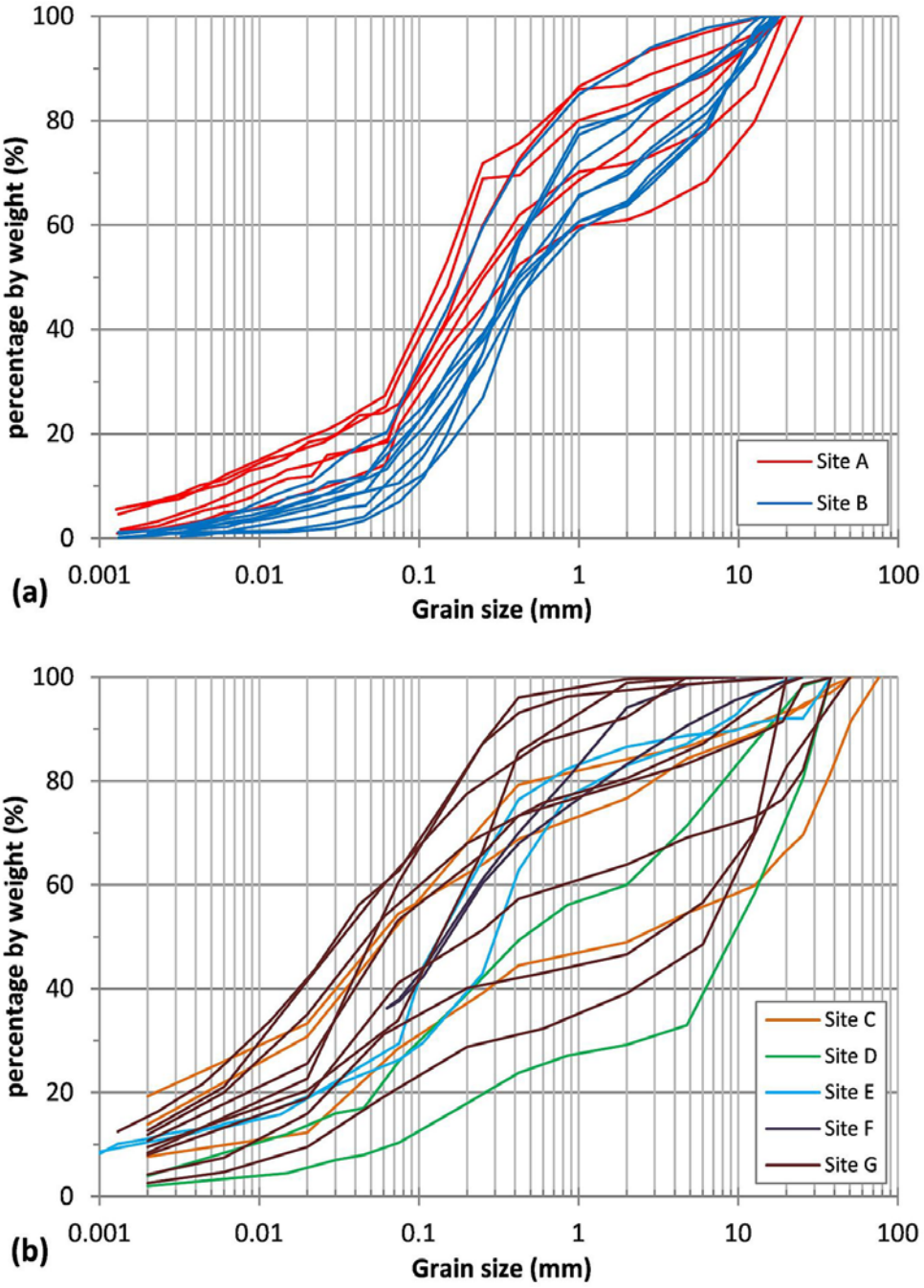

Fig. 2.6. Grain-size distribution of the soil samples collected in the sites A and B **(a)** and in the sites C-G **(b)** on the slopes involved in shallow landslides.

The plot of the Atterberg limits (Table 2.4) on the Casagrande Plasticity Chart (Fig. 2.8) shows that the fine-grained fraction of the soil samples may be classified as silt (ML, 13 samples), silt-clay (ML-CL, 5 samples) and clay (CL, 8 soil samples) of low plasticity (*PI* generally less than 10%). In general the silty fraction prevails (Fig. 2.8).

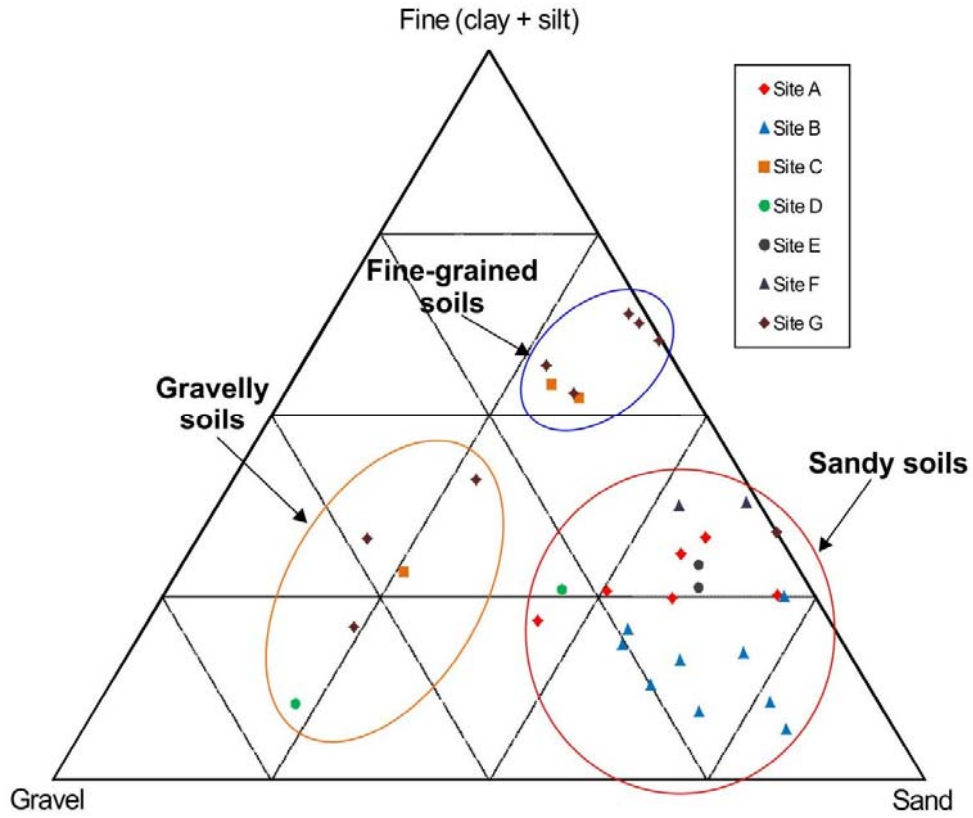

Fig. 2.7. Grain-size composition of the soil samples. Sandy soils, gravelly soils and fine-grained soils are included in the red, orange and blue ovals, respectively.

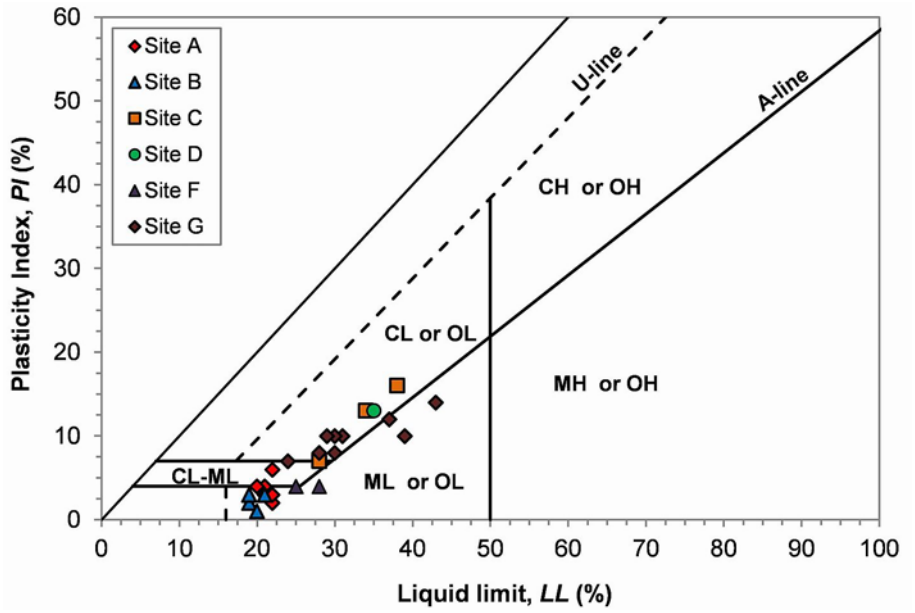

Fig. 2.8. Casagrande Plasticity Chart (ASTM standards) plotting the fine-grained portion of soil samples collected in the shallow landslide source areas. CL, CH: clays with low and high plasticity, respectively; ML, MH: silts with low and high plasticity, respectively; OL, OH: organic soils with low and high plasticity, respectively.

As noted by Robertson (2009), if the fine portion is non-plastic, the soil behaviour will be controlled more by the sand component. As mentioned above, the analysed soils have a sand content ranging from 19.4% to 80.6%, and the 50 percent of these soils have a sand content ranging from 34.0% to 61.9%. Moreover it should be considered that it is easier to collect samples from the most fine part of the deposit. Therefore, the considered soils have mainly a "drained" soil behaviour type. Thus, the use of the equations showed in paragraph 2.3.3 (valid for coarse-grained materials) seems appropriate to estimate relative density and friction angle of the considered soils.

Finally, the shear strength parameters (cohesion c' and friction angle φ') obtained by 12 DS tests on undisturbed samples, collected on sites C and G (Fig. 2.2) and available in the technical reports, are listed in Table 2.5. These samples come from the boreholes performed close to the DP sites. The depth of sampling ranges from 1.5 m (C-1) to 12.5 m (G-7).

Table 2.5. Shear strength parameters determined by DS tests performed on soil samples collected in the sites C (Vinchiana area) and G (Villa Basilica area). The letter in the first column indicates the site where the sample was collected, which and is showed in Fig. 2.2.

Sample	Depth (m)	USCS class	Friction angle, φ' (°)	Cohesion, c' (kPa)
C-1	1.5	s(CL)	33.8	1.3
C-2	4.5	(GC-GM)s	36.3	0.3
C-3	3.0	s(CL)g	29.3	22.9
G-1	4.9	s(ML)	32.0	18.6
G-2	3.0	s(CL)g	33.0	13.1
G-3	9.0	(GM)s	33.0	20.9
G-4	3.5	s(CL-ML)	32.0	27.7
G-5	3.0	(GM)s	35.0	0.4
G-6	7.2	s(CL)	37.2	2.3
G-7	12.5	(GC)s	35.2	2.9
G-8	5.0	s(CL)g	37.0	0.3
G-9	10.5	SC	37.9	1.6

The φ' value for the fine-grained soil ranges from 29.3° (C-3 in Table 2.5) to 37.2° (G-6), while φ' ranges from 33.0° (G-3) to 37.9° (G-9) for the coarse-grained soils (Table 2.5). Cohesion ranges from 0.3 kPa to 27.7 kPa for fine-grained soils and from 0.3 kPa to 20.9 kPa for gravelly soils (Table 2.5). The high variability of φ' and c' may be due to different grain-size distribution and different sampling depth of the soil analyzed (Table 2.5).

Unfortunately, the data obtained by DS tests are less numerous than those obtained by DP tests. Difficulties of probing and high costs make hard to obtain undisturbed samples from the considered soils, especially at superficial level, where the soil is more loose. Nevertheless, the results of DS tests (Table 2.5) were compared with the φ' values estimated by DP tests in the sites C and G.

Anyway, it is evident that undisturbed samples have been retrieved from the most fine part of the soil deposit and only in very few cases a cohesion in between 13 and 30 kPa has been observed. Therefore it seems reasonable to assume for the majority of the study area a nil value of c'.

2.4.2 Dynamic Probing tests

Estimation of the geotechnical parameters requires the subdivision and classification of soil into homogeneous layers, according to their $(N_1)_{60}$ values. A soil type (A - sand-silt mixtures, B - sands, C - sand-gravel mixtures) is attributed to each layer by comparing the trend of $(N_1)_{60}$ values with site observations and borehole logs, if available, close to the DP test. For example, a significant increase of $(N_1)_{60}$ value may be due to gravelly levels, while a jagged trend of the $(N_1)_{60}$ values may be due to alternation between sand and gravel (Fig. 2.9).

As previously observed, the attribution of soil type is essential to estimate the relative density D_R and the friction angle φ' by means of the Skempton's (1986) and Schmertmann's (1978) empirical equations, respectively.

For each soil type the average values of D_R and φ' were calculated, together with their statistical indicators of dispersion and central tendency. These parameters were obtained for all layers probed by DPSH and DPM tests (Tables 2.6 and 2.7).

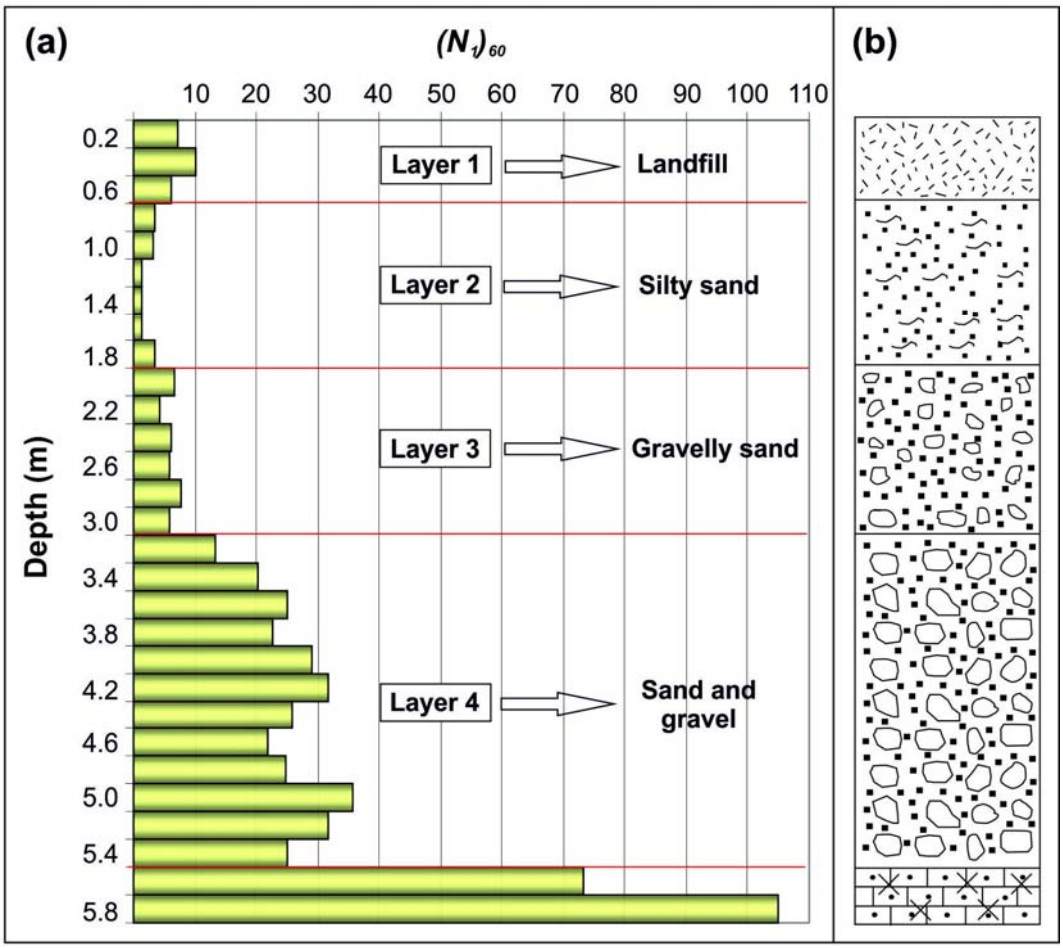

Fig. 2.9. DP profile **(a)** and soil profile **(b)** coming from the site C. The soil is subdivided in homogeneous layers according to the $(N_1)_{60}$ trend. Each layer is associated to a grain-size category. The red lines indicate the transition between different layers.

Table 2.6. Average values of D_R and related statistical indicators of dispersion for the three considered soil types. No. of data: number of layers of each soil type investigated by DPSH and DPM tests.

Soil type	DP type	Average (%)	St. Error (%)	St. Deviation (%)	Range (%)	Max (%)	Min (%)	No. of data
Soil type A	DPSH	31.5	0.965	5.459	20.3	39.6	19.3	33
	DPM	32.8	0.766	9.030	44.7	59.8	15.2	139
Soil type B	DPSH	44.1	1.338	8.358	39.8	69.0	29.3	39
	DPM	48.5	0.944	10.889	58.6	84.8	26.2	133
Soil type C	DPSH	58.5	2.224	13.711	64.5	82.3	17.8	38
	DPM	67.9	1.943	15.178	65.3	97.4	32.2	61

Table 2.7. Average values of φ' and related statistical indicators of dispersion for the three considered soil types. No. of data: number of layers of each soil type investigated by DPSH and DPM tests.

Soil type	DP type	Average (°)	St. Error (°)	St. Deviation (°)	Range (°)	Max (°)	Min (°)	No. of data
Soil type A	DPSH	32.4	0.138	0.793	3.0	33.8	30.7	33
	DPM	32.6	0.107	1.264	6.3	36.4	30.1	139
Soil type B	DPSH	36.6	0.153	0.957	4.5	39.4	34.8	39
	DPM	37.1	0.109	1.252	6.7	41.3	34.5	133
Soil type C	DPSH	40.8	0.289	1.780	7.1	43.4	36.3	38
	DPM	41.5	0.223	1.739	7.6	44.9	37.3	61

Dispersion and variability of D_R and φ' are also shown by box plots of Figs. 2.10, 2.11 for each soil type. The box plots show the D_R (Fig. 2.10) and φ' (Fig. 2.11) data in term of: (i) minimum value (min), (ii) lower quartile (Q1), (iii) median (Q2), (iv) upper quartile (Q3), and (v) maximum value (max). Moreover, the boxes in the diagrams (Figs. 2.10, 2.11) represent the interquartile range (IQR), i.e. the difference between Q3 and Q1. IQR is 50% of the range (range = max-min, Tables 2.6, 2.7).

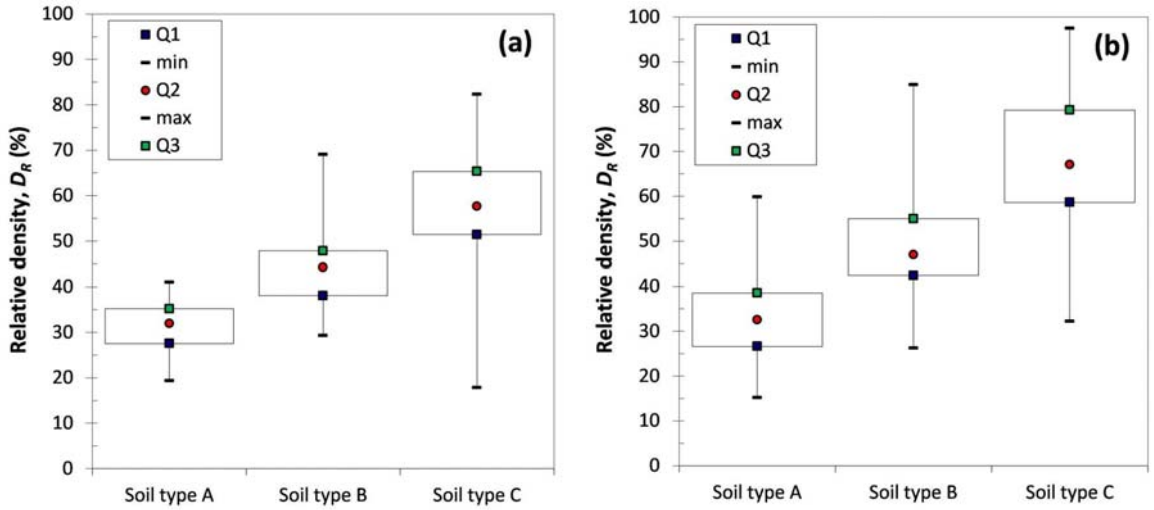

Fig. 2.10. Dispersion and variability of D_R values obtained by DPSHs **(a)** and DPMs **(b)**. Q1: first quartile; Q2: median ; Q3: third quartile.

IQR rises with the increase in gran-size for D_R (Fig. 2.10a) and φ' (Fig. 2.11a) obtained by DPSHs. Relating to friction angle, IQR is 1.1%, 1.1% and 2.5% for A, B and C soil types,

respectively (Fig. 2.10a). For friction angle obtained by DPMs (Fig. 2.11b), IQR is 1.7%, 1.4% and 2.3% for A, B and C soil types, respectively.

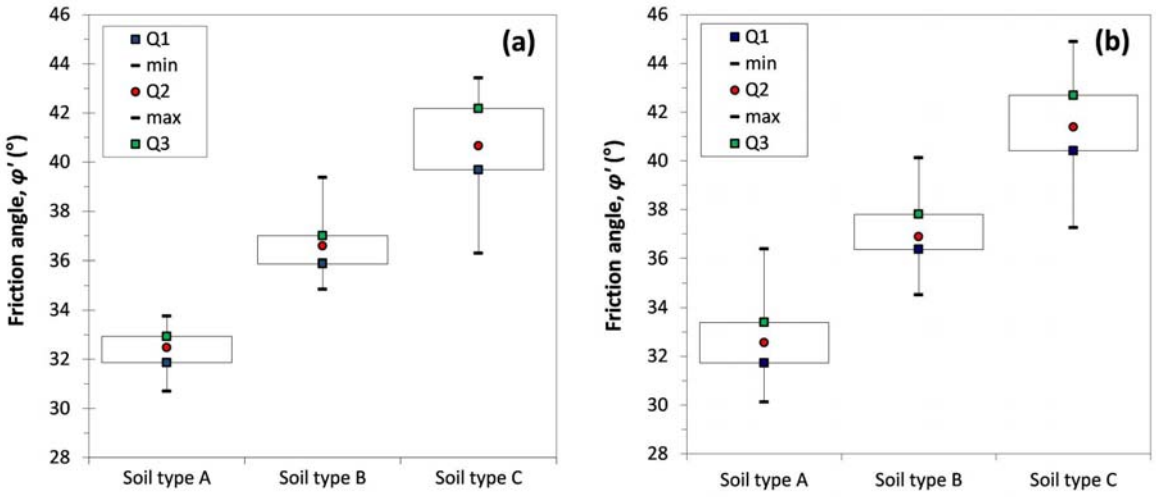

Fig. 2.11. Dispersion and variability of φ' values obtained by DPSHs **(a)** and DPMs **(b)**. Q1: first quartile; Q2: median ; Q3: third quartile.

Moreover, Figs. 2.12 and 2.13 show the distribution of D_R (Fig. 2.12) and φ' (Fig. 2.13) values for each soil type, according to the probing depth. The number of layers probed by means of DPM (Figs. 2.12b and 2.13b) is greater than that investigated by DPSH (Figs. 2.12a and 2.13a), especially for superficial levels (< 2 m). Really, DPM is more suitable to get data on soils in difficult access slopes, as in the source areas of shallow landslides.

The data plotted show a considerable but reasonable dispersion (Figs. 2.12 and 2.13), probably due to grain-size heterogeneity and mineralogical variation within the soil. The φ' values for the soil type A, obtained by DPSHs, are included in a range of 3.0° (between 30.7° and 33.8°, Table 2.7, Fig. 2.13a), while the φ' values obtained by DPMs range from 30.1° to 36.4° (range of 6.3°, Table 2.7, Fig. 2.13b). The D_R and φ' ranges for other soil type are listed in Tables 2.6 and 2.7.

Dispersion is greater in the superficial levels (< 2 m), where influences of root system of the plants on the soil resistance can be major (Roering et al., 2003; Schwarz et al., 2010). It is rather typical of data coming from indirect investigations, such as DP tests. Nevertheless, the D_R mean values coming from DPM and DPSH tests for the three soil types remain comparable; major differences are associated to increasing in grain-size (Table 2.6).

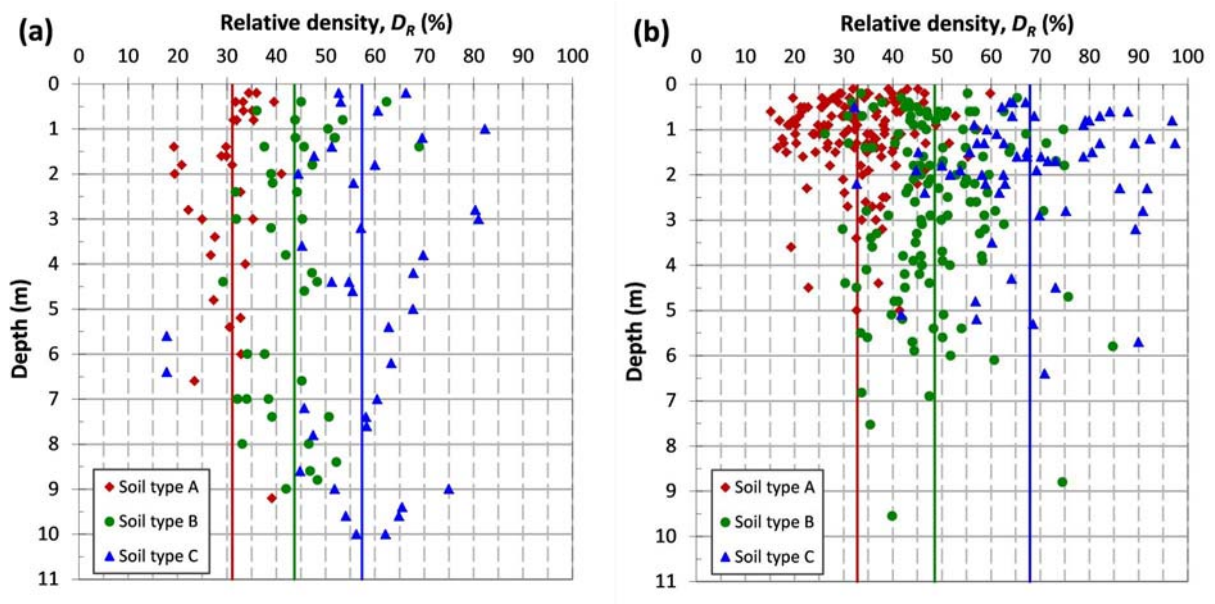

Fig. 2.12. Distribution of D_R obtained by DPSH **(a)** and DPM tests **(b)** for each soil type, according to the probing depth. Red line: average D_R for soil type A; green line: average D_R for soil type B; blue line: average D_R for soil type B.

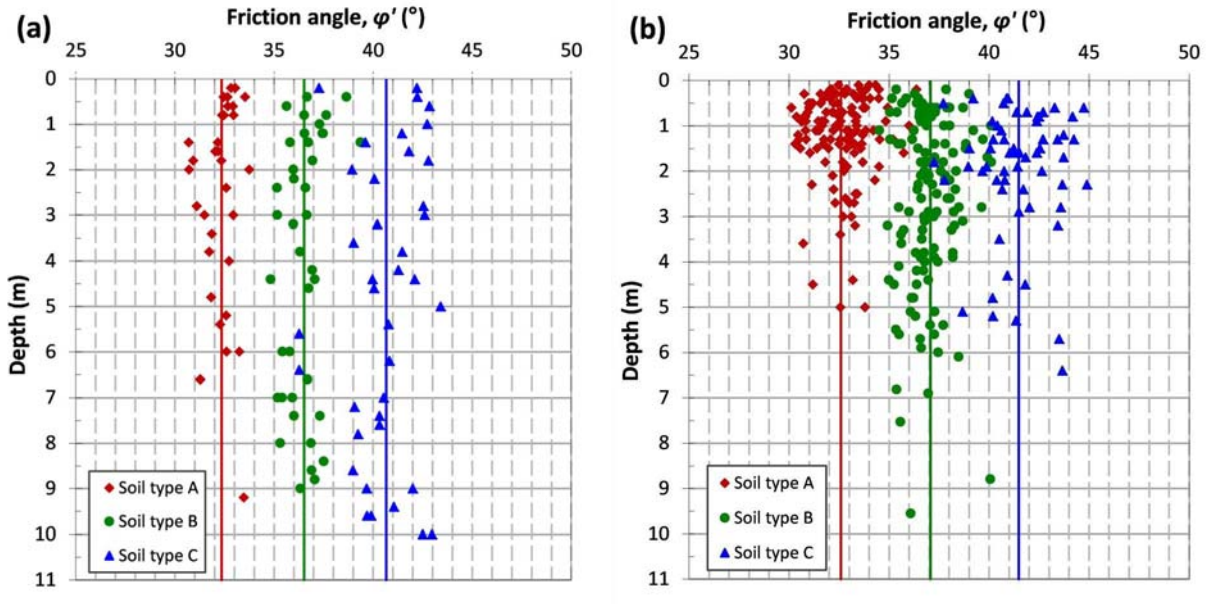

Fig. 2.13. Distribution of φ' obtained by DPSH **(a)** and DPM tests **(b)** for each soil type, according to the probing depth. Red line: average φ' for soil type A; green line: average φ' for soil type B; blue line: average φ' for soil type B.

D_R and φ' show an increase in scattering around the mean values (coloured lines in Figs. 2.12 and 2.13) with the increase in grain-size and sorting. DPM tests show this trend more

clearly than DPSH tests. The presence of pebbles in a silty-sand mixture or in the sands, even if in low percentage, can probably cause significant increase in N_{DP} (number of blows of DP test), and consequently in the D_R and φ' values.

Furthermore, at shallow depth commonly investigated by DPs (usually less than 5-6 m in order to investigate the soil involved in shallow landslides), D_R and φ' of each soil type do not show significant increase with depth (Figs. 2.12 and 2.13).

2.4.3 Comparison of results

In order to validate the results of the research, D_R and φ' obtained by DPSH and DPM tests were compared with those obtained in similar soils by SPT tests and DS tests.

Firstly, the average values of D_R and φ' were compared with those obtained by 46 SPTs (8 on soil type A, 11 on soil type B and 27 on soil type C), available in the technical reports. This comparison is useful, because the empirical equations used in this work are based on SPT.

The average φ' values obtained by SPTs are: 35.4° for the soil type A, 37.4° for the soil type B and 42.5° for the soil type C (Table 2.8). Their standard deviation ranges from 1.3° for the soil type C to 2.6° for the soil type B (Table 2.8). In general, as noted by Squeglia et al. (2006) for alluvial deposits of the Arno River in Tuscany, dispersion of SPT data is higher than that of DP ones. In this research, the φ' values, obtained by SPT tests for the soil types A and B, have standard deviations higher than those obtained by DP tests for the same soil types. The comparison between SPT, DPSH and DPM data shows small differences (Fig. 2.14). In general, SPTs provided slightly higher D_R and φ' values than DPs, especially for the soil type A (Fig. 2.14). Therefore DPs seem more conservative than SPTs.

Table 2.8. Average values of φ' and related statistical indicators of dispersion for the three considered soil types probed by means of SPT. No. of data: number of layers of each soil type investigated by SPTs.

Soil type	Average (°)	St. Error (°)	St. Deviation (°)	Range (°)	Max (°)	Min (°)	No. of data
Soil type A	35.4	0.698	2.225	6.9	38.8	31.9	8
Soil type B	37.4	0.779	2.603	8.7	42.7	34.0	11
Soil type C	42.5	0.245	1.319	5.4	45.4	40.0	27

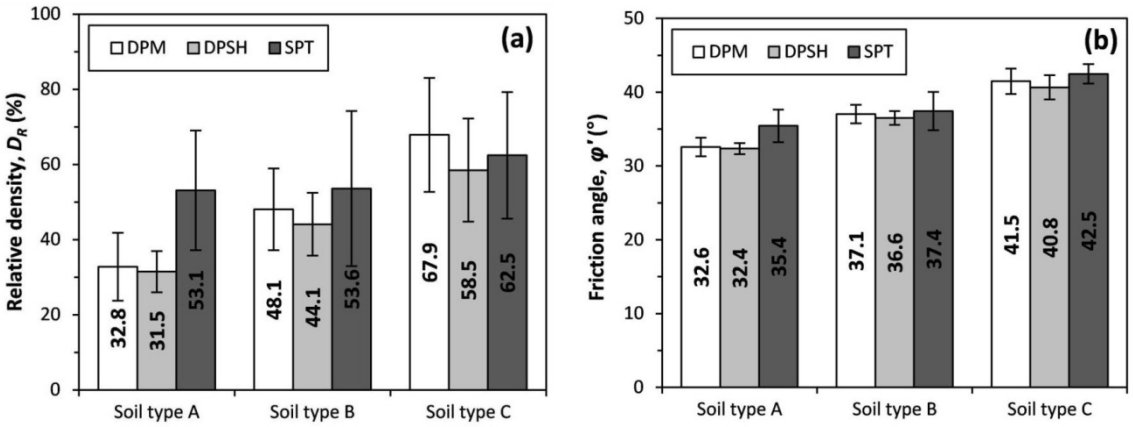

Fig. 2.14. Comparison between the D_R **(a)** and φ' **(b)** values obtained for each soil type by DPM, DPSH and SPT tests. The little bars show the standard deviation.

Moreover, the φ' values obtained by Dynamic Probing tests were compared with those resulting from DS tests (when available) (Table 2.9). The DS tests were performed on undisturbed samples taken in boreholes in the same soil type close to the DP sites, at the same depth and stress conditions, as described above.

Table 2.9. Comparison between the φ' values estimated by DS tests (φ'_{DS}) and by DP tests (φ'_{DP}). The tests were performed on the same site and soil class. The location of the boreholes and the DP tests is show in Fig. 2.15.

Site	Borehole		Soil sample				Dynamic Probing test			
	n°	Depth (m)	n°	Depth (m)	USCS class	φ'_{DS} (°)	n°	DP distance from borehole (m)	φ'_{DP} (°)	Average φ'_{DP} (°)
C	C-BH1	11.0	C-1	1.5	s(CL)g	33.8	C-DP4	60.0	33.5	33.5
	C-BH3	15.0	C-3	3.00	s(CL)	29.3	C-DP1	38.0	32.6	32.0
							C-DP2	53.0	31.6	
							C-DP3	62.0	31.8	
G	G-BH6	30.0	G-6	7.2	s(CL)	37.2	G-DP3	44.0	36.3	36.3
	G-BH8	20.0	G-8	5.0	s(CL)g	37.0	G-DP1	13.5	37.1	37.0
							G-DP2	11.5	36.8	

Table 2.9 lists the φ' values obtained by DS and DP tests in the sites C and G (Fig. 2.15) and used for the comparisons. The φ' determined by DS tests was compared with the φ' obtained by DP tests close to the sampling site (Table 2.9; Fig. 2.15). In two cases was used the φ' value obtained by a single DP test (soil samples C-1 and G-6), while in other two cases (soil samples C-3 and G-8) was used the average value of φ' obtained by few DP tests.

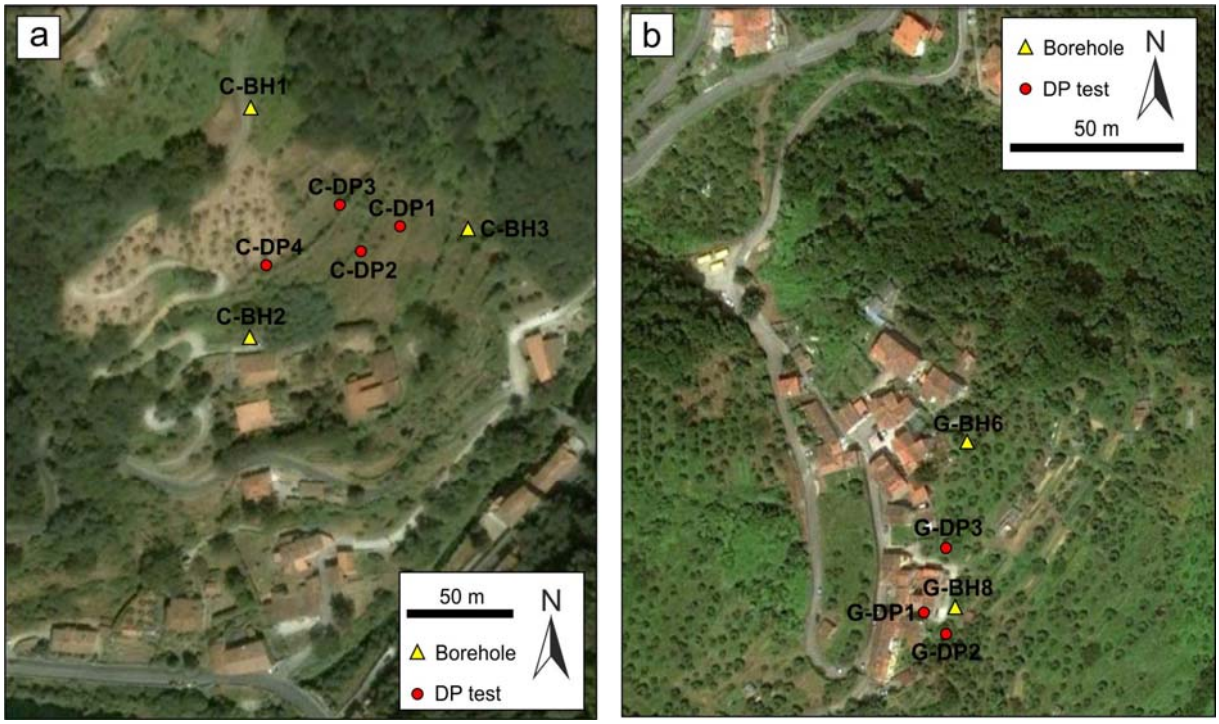

Fig. 2.15. Satellite view of the sites C (**a**) and G (**b**) where soil samples were collected (base map by Google Earth, 2012). Location of boreholes and DP tests is highlighted.

Figure 2.16 underlines that in 2 cases the φ' obtained by DP tests is underestimated in respect to that obtained by DS tests (samples: C-1 and G-6), while in one case it is overestimated (sample C-3). The friction angle resulting from DS and DP tests show good linear correlation ($R^2 = 0.92$, Fig. 2.16), confirming the satisfactory and repeatable results of DP tests.

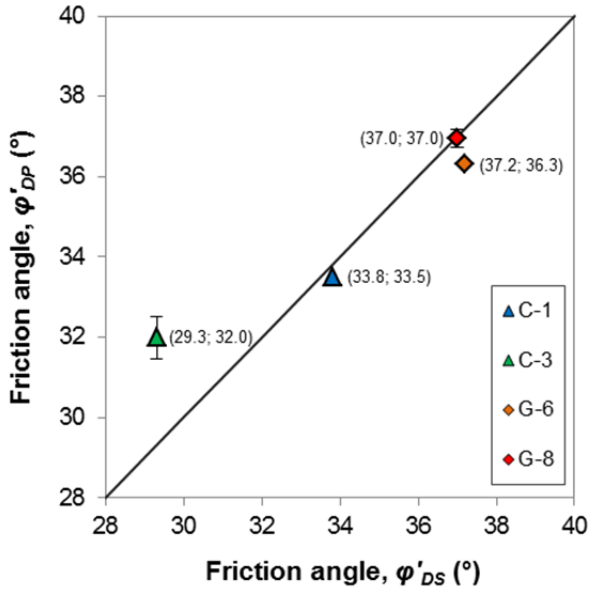

Fig. 2.16. Comparison between the φ' values resulting from DS tests and DP tests, performed on the same site and soil type. The little bars show the standard deviation of the φ' values estimated by DP tests close to the sampling point.

2.5 Final remarks and perspectives

Utility and suitability of the DP tests in characterizing the soil slope cover emerged in this research. The study mainly focused on the soil formed on the most typical arenaceous formations, such as the Macigno Fm., vastly cropping out in Northern Tuscany. It was based on DP tests (DPM and DPSH), commonly used because of their numerous advantages. Even though literature does not offer many data on the mechanical properties of these granular materials, DPs supplied useful data, allowing a reliable characterization of soil.

In detail, 91 DPMs, 40 DPSHs, 46 SPTs and 12 DS tests were analysed. The data discussed above show good consistency. By means of DP tests a lot of data can be easily and quickly acquired, so characterizing wide areas and parameter variability instead of having at our disposal just few spotty data from boring, undisturbed sampling and laboratory tests. Some direct and indirect situ tests (drilling, seismic survey, etc.) can calibrate and improve the empirical equations for obtaining the required geotechnical properties. Difficulties or impossibility of undisturbed sampling in coarse-grained soils might be surmounted by in situ direct shear tests. They can represent a possible and significant improvement in the

knowledge of the soil behaviour and can also give data on the residual strength. Undisturbed sampling by in situ freezing may be another effective approach to obtain undisturbed materials for laboratory testing.

In this way actual and reliable parameters may be achieved, on which landslide susceptibility and hazard maps can be based. However, DP apparatus should be standardized in Italy and worldwide, in order to get more comparable results, which is actually one of the main difficulties in using DP tests. Another general limit of the DP method includes the use of empirical relationships, often obtained considering only homogeneous sandy materials. From this point of view, a complete analysis of numerous DP tests in different soil materials could allow calculations using more suitable, specifically calibrated equations.

Despite such limits, the use of DPs in difficult areas can give interesting results. Examples in applying the DPs results come from slope stability analyses and particularly from the shallow landslide hazard assessment (Giannecchini et al., 2007; D'Amato Avanzi et al., 2009).

The methodological approach here presented may be improved in several aspects, which will be considered in developing this research:

- soil profile survey and description in selected, representative source areas of shallow landslides;
- in situ mechanical and hydrogeological tests and direct shear stress tests, in order to get peak and residual friction angles, cohesion, permeability, effective infiltration, etc.;
- undisturbed sampling for laboratory tests (mass weight, mechanical and hydrogeological parameters);
- calibration of DP results and performing of empirical relations specifically calibrated on the considered soils;
- performing of geotechnical and susceptibility maps and comparison with rainfall thresholds for triggering shallow landslides;
- preparation of landslide hazard maps and scenarios for different rainfall amounts.

References

American Society for Testing and Materials: Annual Book of ASTM Standards, Soil and Rock Construction, Section 4, American Society for Testing and Materials, Philadelphia, Pennsylvania, 1182 pp., 1996.

Bellotti, R., Ghionna, V., Jamiolkowski, M., Lancellotta, R., and Manfredini G.: Deformation Characteristics of Cohesionless Soils from in Situ Tests, in: Use of In Situ Tests in Geotechnical Engineering, Geotechnical Special Publication, No. 6, S.P., Clemence, S. P. (Eds.), ASCE, 47–73, 1986.

Bieniawski, Z. T.: Engineering Rock Mass Classification, Wiley, New York, 1989.

Blijenberg, H. R.: In-situ strength tests of coarse, cohesionless debris on scree slopes, Eng. Geol., 39, 137–146, 1995.

Bolton, M. D.: The strength and dilatancy of sands, Geotechnique, 36(1), 65–78, 1986.

Campbell, R.H.: Soil slip, debris flows, and rainstorms in the Santa Monica mountains and vicinity, southern California, U. S. Geological Survey Professional Paper 851, 51 pp., 1975.

Carmignani, L. and Lazzarotto, A.: Geological Map of Tuscany (Italy), Regione Toscana, Special Edition for the IGC 32 Florence-2004, 2004.

Carmignani, L., Conti, P., Cornamusini, G., and Meccheri, M.: The internal Northern Apennines, the northern Tyrrhenian sea and the Sardinia-Corsica block, in: Crescenti, V., D'Offizi, S., Merlino, S. and Sacchi, L. (Eds.), Geology of Italy, Special Volume of the Italian Geological Society for the IGC 32 Florence-2004, 59–77, 2004.

Casagli, N., Dapporto, S., Ibsen, M. L., Tofani, V. and Vannocci, P.: Analysis of the landslide triggering mechanism during the storm of 20th-21st November 2000, in Northern Tuscany, Landslides, 3, 13–21, 2006.

Cestari, F.: Prove geotecniche in sito, third ed. Geo-Graph, Segrate, Italy, 2005.

Clayton, C. R. I.: The Standard Penetration Test (SPT): methods and use, Construction Industry Research and Information Association, Report 143, CIRIA, London, 143 pp., 1995.

Conti, P. and Lazzarotto, A.: Geology of Tuscany: evolution of the state-of-knowledge presented by geological maps and the new geological map of Tuscany, 1:250,000 scale, in: Morini, D. and Bruni, P. (Eds.), The Regione Toscana Project of Geological Mapping: Case Histories and Data Acquisition, Regione Toscana - Servizio Geologico Regionale, Firenze, 33–50, 2004.

Corominas, J., Remond, J., Farias, P., Estevao, M., Zézere, J., Díaz de Terán, R., Dikau, R., Schrott, L., Moya, J. and González, A.: Debris flow, in: Dikau, R., Brunsden, D., Schrott, L. and Ibsen, M. L. (Eds.), Landslide Recognition, Identification, Movement and Causes, Chichester, Wiley, 161–180.

Cruden, D. M. and Varnes, D. J.: Landslide types and processes, in: Turner, A. K. and Schuster, R. L. (Eds.), Landslides: Investigation and Mitigation, Special Report 247, Transportation Research Board National Academy of Sciences, Washington, 36–75, 1996.

Cubrinovski, M. and Ishihara, K.: Empirical correlation between SPT *N*-value and relative density for sandy soils, Soils and Foundations, 39(5), 61–71, 1999.

D'Amato Avanzi, G., Falaschi F., Giannecchini, R. and Puccinelli, A.: Soil slip susceptibility assessment using mechanical-hydrological approach and GIS techniques: an application in the Apuan Alps (Italy), Nat. Hazards, 50(3), 591–603, 2009.

D'Amato Avanzi, G., Giannecchini, R. and Puccinelli, A.: The influence of the geological and geomorphological settings on shallow landslides. An example in a temperate climate environment: the June 19, 1996 event in the north western Tuscany (Italy), Eng. Geol., 73, 215–228, 2004.

Delmonaco, G., Leoni, G., Margottini, C., Puglisi, C. and Spizzichino, D.: Large scale debris-flow hazard assessment: a geotechnical approach and GIS modelling, Nat. Hazards Earth Syst. Sci., 3, 443–455, 2003.

Del Prete, M., Guadagno, F. M. and Hawkins, A. B.: Preliminary report on the landslides of 5 May 1998, Campania, southern Italy. B. Eng. Geol. Environ., 57(2), 113–129, 1998.

De Mello V. F. B.: The Standard Penetration Test, Proc. 4th American Conf. On Soil Mech. and Found. Engineering 1, 1971.

De Vita, P., Di Clemente, E., Rolandi, M. and Celico, P.: Engineering geological models of the initial landslides occurred on April 30th, 2006, at the mount di Vezzi (Ischia Island, Italy), Italian Journal of Engineering Geology and Environment, 2, 119–141, 2007.

Dunham, J. W.: Pile foundations for buildings, Proc. ASCE, Soil and Foundation Division, 1954.

Ekanayake, J. C. and Philipps, C. J.: Slope stability thresholds for vegetated hillslopes: a composite model, Can. Geotech. J., 39(4), 849–862, 2002.

Ellen, S. D. and Wieczorek, G. F.: Landslides, floods, and marine effects of the storm of January 3-5, 1982, in the San Francisco Bay region, California, U.S. Geological Survey Professional paper 1434, 310 pp., 1988.

Eurocode 7: Geotechnical Design – Part 3, 1997-3. Design Assisted by Fieltesting; Chapt 6, Dynamic Probing (DP), 2004.

Federici, P.R., Puccinelli, A., D'Amato Avanzi, G., Falaschi, F., Giannecchini, R., Marchetti, D., Pochini, A., Rapetti, F. and Ribolini, A.: Zoning and mapping landslide hazard in the Castelnuovo di Garfagnana region (Tuscany, Italy), in: Catani, F., Margottini, C. and Iadanza, C. (Eds.), The Second World Landslide Forum – Abstract Book, 3-9 October 2011, FAO, Rome, Italy, ISPRA, 90, 2011.

Giannecchini, R.: Rainfall triggering soil slips in the southern Apuan Alps (Tuscany, Italy), 6th Plinius Conf. on Mediterranean Storms (European Geosciences Union), Mediterranean Sea, 17-24 October 2004, Advances in Geosciences, 2, 21–24, 2005.

Giannecchini, R.: Relationship between rainfall and shallow landslides in the southern Apuan Alps, Nat. Hazards Earth Syst. Sci., 6, 375–364, 2006.

Giannecchini, R., Naldini, D., D'Amato Avanzi, G. and Puccinelli, A.: Modelling of the initiation of rainfall-induced debris flows in the Cardoso basin (Apuan Alps, Italy), Quatern. Int., 171–172, 108–117, 2007.

Giannecchini, R. and Pochini, A.: Geotechnical influence on soil slips in the Apuan Alps (Tuscany): first results in the Cardoso area, Proc. Int. Conf. on fast slope movements-prediction and prevention for risk mitigation (IC-FSM 2003), Naples, Italy, 11-13 May 2003, 241–245, 2003.

Giannecchini, R. and D'Amato Avanzi, G.: Historical research as a tool in estimating hydrogeological hazard in a typical small alpine-like area: The example of the Versilia River basin (Apuan Alps, Italy), J. Phys. Chem. Earth, doi:10.1016/j.pce.2011.12.005, 2012.

Guadagno, F. M. and Revellino, P.: Debris avalanches and debris flows of the Campania Region (southern Italy), in: Jakob, M., Hungr, O. (Eds.), Debris-flow Hazard and Related Phenomena. Springer, Berlin, 489–518, 2005.

Hatanaka, M. and Uchida, A.: Empirical correlation between penetration resistance and internal friction angle of sandy soils, Soils and Foundations, 36(4), 1–9, 1996.

Hettiarachchi, H. and Brown, T.: Use of SPY blow counts to estimate shear strength properties of soils: energy balance approach, J. Geotech. Geoenviron., 135(6), 830–834, 2009.

Hungr, O., Evans, S. G., Bovis, M. J., Hutchinson J. N.: A review of the classification of landslides of the flow type, Environ. Eng. Geosci., 7(3), 221–238, 2001.

Il Rischio sismico in Toscana: http://www.rete.toscana.it/sett/pta/sismica/, last access: 24 February 2012.

ISRM: International society for rock mechanics commission on standardization of laboratory and field tests: Suggested methods for the quantitative description of discontinuities in rock masses. International Journal of Rock Mechanics and Mining Sciences & Geomechanics Abstracts, 15(6), 319–368, 1978.

ISRM: Rock Characterization, Testing and Monitoring: ISRM Suggested Methods, Pergamon Press, New York, 1981.

Japan Road Association: Specifications for highway bridges, Part IV, 1990.

Jibson, R. W.: Debris flows in southern Puerto Rico, in: Schultz, A. P. and Jibson, R. W., (Eds.), Landslide Processes in Eastern North America and Puerto Rico, Geol. Soc. Am. S. 236, 29–55, 1989.

Kokusho, T., Tanaka, Y., Tadashi, K., Kouji, K., Kouichi, S., Shinji, T. and Shintaro, A.: Case study of rock debris avalanche gravel liquefied during 1993 Hokkaido-Nansei-Oki earthquake, Soil and Foundations, 35, 83–95, 1995.

Liao, S. S. C. and Whitman, R. V.: Overburden correction factors for SPT in sand, Journal of Geotechnical Engineering, 112(3), 373–377, 1986.

Lo Presti, D., Meisina, C., and Squeglia, N.: Use of cone penetration tests for soil profiling, Italian Geotechnical Journal, 2, 29–51, 2009.

Lo Presti, D. and Squeglia, N.: Prove Penetrometriche Dinamiche, Hevelius Edizioni, Benevento, Italy, 2008.

Lo Presti, D., Squeglia, N., Pallara, O., Mensi, E. and Ferrini, M.: Soil testing: a critical analysis in the framework of EC8 and OPCM 3274, Italian Journal of Engineering Geology and Environment, 1, 49–68, 2007.

Mohammadi, S. D., Nikoudel, M. R., Rahimi, H. and Khamehchiyan, M.: Aplication of the Dynamic Cone Penetrometer (DCP) for determination of the engineering parameters of sandy soils, Eng. Geol., 101, 195–203, 2008.

Odebrecht, E., Schnaid, F., Rocha, M. M. and Bernardes, G. P.: Energy efficiency for standard penetration test, J. Geotech. Geoenviron., 131(10), 1252–1263, 2005.

Pagani Geotechnical Equipment: http://www.pagani-geotechnical.com/index.php?id=67, last access: 24 February 2012.

Pandeli, E., Ferrini, G. and Lazzari, D.: Lithofacies and petrography of the Macigno formation from the Abetone to the Monti del Chianti areas (Northern Apennines), Memorie della Società Geologica Italiana, 48, 321–329, 1994.

Parker, E. R. and Jenny, H.: Water infiltration and related soil properties as affected by cultivation and organic fertilization, Soil Science, 60, 353–376, 1945.

Peck, R. B., Hanson, W. E. and Thornburn, T. H. E.: Foundation Engineering, John Wiley & Sons, Inc., 222 pp., 1953.

Pierson, T. C., Costa, J. E.: A rheologic classification of subaerial sediment-water flows, in: Costa, J. E. and Wieczorek, G.F. (Eds.), Debris flows/avalanches: process, recognition, and mitigation, Reviews in Engineering Geology 7, Geological Society of America, Boulder, CO, 1–12, 1987

Robertson, P. K.: Interpretation of cone penetration tests – a unified approach, Can. Geotech. J., 46, 1337–1355, 2009.

Robertson, P. K. and Wride C. E.: Cyclic liquefaction and its evaluation based on the SPT and CPT, in: Proceedings of the NCEER Workshop on evaluation of liquefaction Resistance of soils, Salt Lake City, Technical Report NCEER-97-0022, National Centre of Earthquake Engineering Research, Buffalo, NY, 41–87, 1997.

Roering, J. J., Schimdt, K. M., Stock, J. D., Dietrich, W. E. and Montgomery, D. R.: Shallow landsliding, root reinforcement, and the spatial distribution of trees in the Oregon Coast Range, Can. Geotech. J., 40, 237–253, 2003.

Rogers, D. J.: Subsurface exploration using the Standard Penetration Test and the Cone Penetration Test, Environ. Eng. Geosci., 12(2), 161–179, 2006.

Schmertmann, J. H.: Use of SPT to measure dynamic soil properties? Yes, but…! Dynamic Geotechnical Testing, ASTM SPT 654, 341–355, 1978.

Schnaid, F.: In Situ Testing in Geomechanics: The main tests, Taylor & Francis (Eds.), 2 Park Square, Milton Park, Abingdon, Oxon OX14 4RN, 2009.

Schnaid, F., Odebrecht, E., Rocha, M. M. and Bernardes, G. P.: Prediction of soil properties from the concepts of energy transfer in dynamic penetration tests, J. Geotech. Geoenviron., 135(8), 1092–1100, 2009.

Schwarz, M., Preti, F., Giadrossich, F., Lehmann, P. and Or, D.: Quantifying the role of vegetation in slope stability: A case study in Tuscany (Italy), Ecol. Eng., 36, 285–291, 2010.

Sivrikaya, O. and Toğrol, E.: Determination of undrained strength of fine-grained soils by means of SPT and its application in Turkey, Eng. Geol., 86, 52–69, 2006.

Skempton, A. W.: Standard penetration test procedures and the effects in sands of overburden pressure, relative density, particle size, ageing and overconsolidation, Geotecnique, 36(3), 425–447, 1986.

Squeglia, N., Pallara, O. and Mensi, E.: Caratterizzazione meccanica dei depositi di terreni mediante prove penetrometriche dinamiche, in: Proceeding of Incontro Annuale dei Ricercatori di Geotecnica 2006 – IARG 2006, 26-28 June 2006, 2006.

Stefanoff, G., Sanglerat, G., Bergdahl, U. and Melzer, K. J.: Dynamic probing (DP): International reference test procedure, in: De Ruiter (Eds.), Proc. ISOPT-I, 1, Balkema, 53–70, 1988.

Wang, F. W., Sassa, K. and Wang, G.: Mechanism of a long-runout landslide triggered by the August 1998 heavy rainfall in Fukushima Prefecture, Japan, Eng. Geol., 63(1–2), 169–185, 2002.

Wieczorek, G. F.: Landslide triggering mechanisms, in: Turner, A. K. and Schuster, R. L. (Eds.), Landslides: Investigation and Mitigation, Special Report 247, Transportation Research Board National Academy of Sciences, Washington, 76–90, 1996.

Youd, T. L. and Idriss, I. M.: Liquefaction resistance of soils: summary report from the 1996 NCEER and 1998 NCEER/NSF Workshops on Evaluation of Liquefaction Resistance of Soils, Journal of Geotechnical and Geoenvironmental Engineering, 127(4), 297–313, 2001.

3 Critical rainfall thresholds for triggering shallow landslides in the Serchio River Valley (Tuscany, Italy)

Abstract

The Serchio River Valley, in north-western Tuscany, is a well-known tourism area between the Apuan Alps and the Apennines. This area is frequently hit by heavy rainfall, which often triggers shallow landslides, debris flows and debris torrents, sometimes causing damage and death. The assessment of the rainfall thresholds for the initiation of shallow landslides is very important in order to improve forecasting and to arrange efficient alarm systems.

With the aim of defining the critical rainfall thresholds for the Middle Serchio River Valley, a detailed analysis of the main rainstorm events was carried out. The hourly rainfall recorded by three rain gauges in the 1935-2010 interval was analysed and compared with the occurrence of shallow landslides. The rainfall thresholds were defined in terms of mean intensity I, rainfall duration D and normalized using the mean annual precipitation. Some attempts were also carried out to analyse the role of rainfall prior to the damaging events. Finally, the rainfall threshold curves obtained for the study area were compared with the local, regional and global curves proposed by various authors. The results of these analysis suggest that in the study area landslide activity initiation requires a higher amount of rainfall and greater intensity than elsewhere.

Keywords: Shallow landslides, critical rainfall threshold, antecedent rainfall, Serchio River Valley, Tuscany.

3.1 Introduction

Intense or prolonged rainfall events often cause considerable landslides, floods, damage and casualties, as frequently happens in Northern Tuscany. The Serchio River Valley is situated between the Apuan Alps to the W-SW and the Tuscan-Emilian Apennines to the E-NE (Fig. 3.1). The main peaks reach almost 2,000 m a.s.l., while the valley bottom is about 30-100 m a.s.l. (Fig. 3.2).

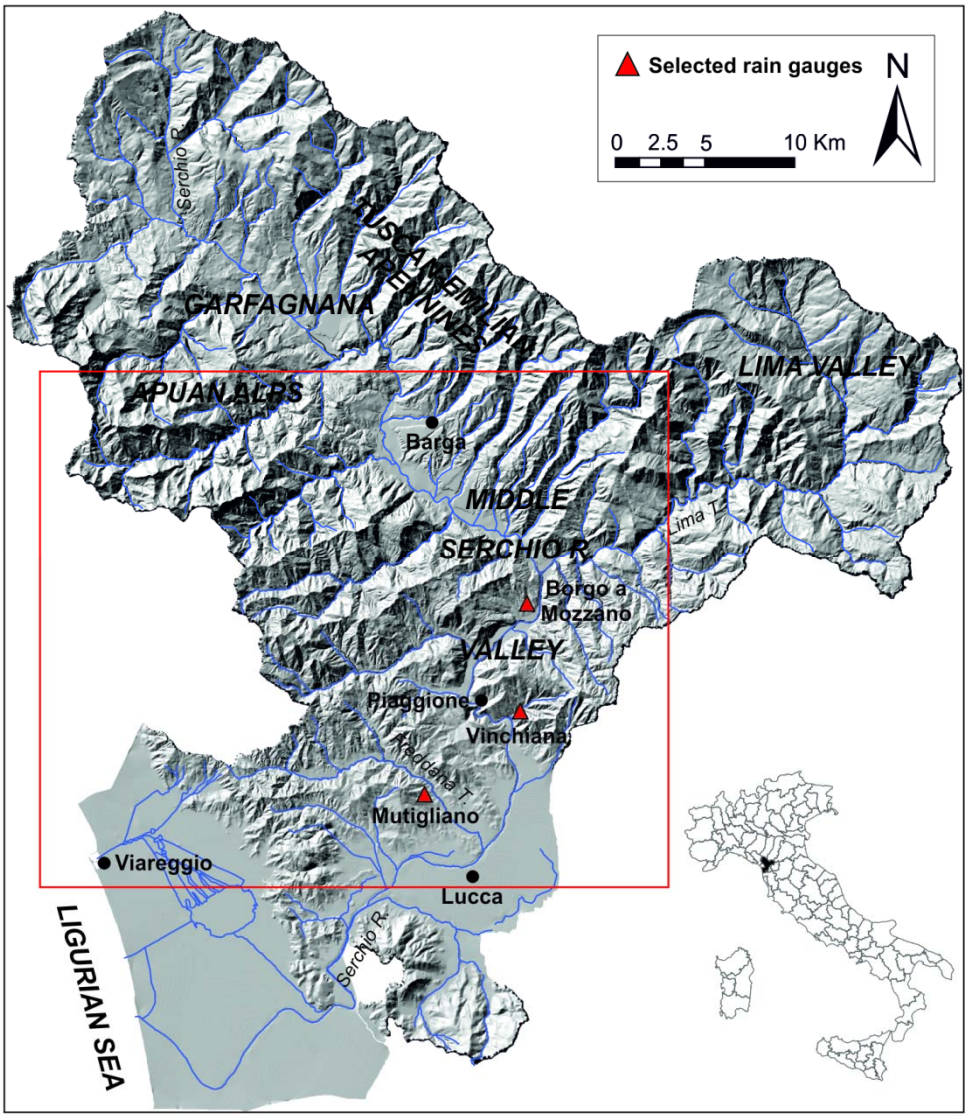

Fig. 3.1. Map of the Serchio River Valley and location of the three selected rain gauges. Red rectangle shows the Middle Serchio R. Valley. Base map: courtesy of the Authority of the Serchio River Basin.

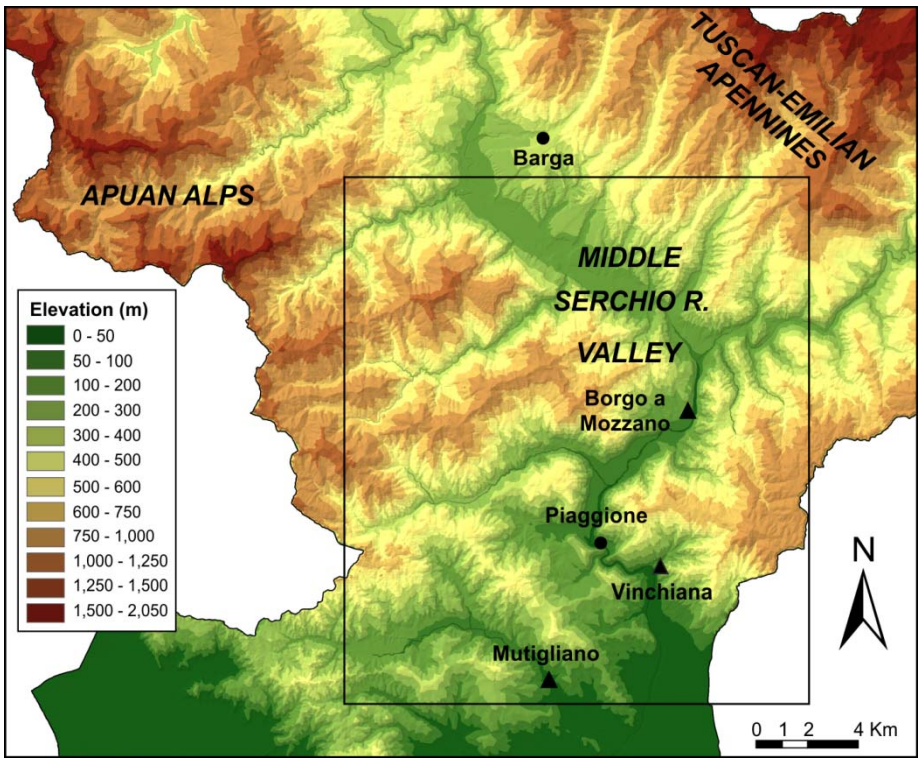

Fig. 3.2. Map of MSRV. Shades of colour show elevation, from 5×5m DEM. Black triangles show location of the 3 considered rain gauges. The black frame shows the study area. DEM: courtesy of the Authority of the Serchio River Basin.

Heavy rainfall events characterize the Middle Serchio River Valley (MSRV), where the mean annual precipitation (MAP) is between 1,300 and 1,700 mm and can exceed 3,000 mm in the Apuan Alps (Fig. 3.3). In several cases, intense rainstorms striking the study area have triggered many shallow landslides (mainly soil slips, debris flows), which have exposed the local population to risk.

Shallow landslides typically involve a small volume of earth and/or debris, but are characterized by high velocity and high impact energy. Furthermore, during intense rainstorms many shallow landslides initiate almost simultaneously. Some shallow landslides often direct towards the streams, increasing the torrent load. As an example, on 20 November 2000 heavy rainfall hit the MSRV, inducing around 150 failures (Fig. 3.4) and killing 5 people. Other rainstorms occurred on 20 January 2009, 24 December 2009 and 19 June 2010, triggering many shallow landslides that caused severe damage to buildings and infrastructures. The shallow landslides often affect the road network, generally due to a lack or deficiency of surface water draining systems, which is a recurrent case in many regions of

the world (Anderson, 1983; Haigh et al., 1993; Larsen and Parks, 1997; D'Amato Avanzi et al., in press). For example, during the 24 December 2009 rainstorm 132 landslides affected the roads: 22 occurred along the main roads, the other 110 along local ones. This generally blocks the traffic, often isolating villages and stopping productive activities (D'Amato Avanzi et al., 2012).

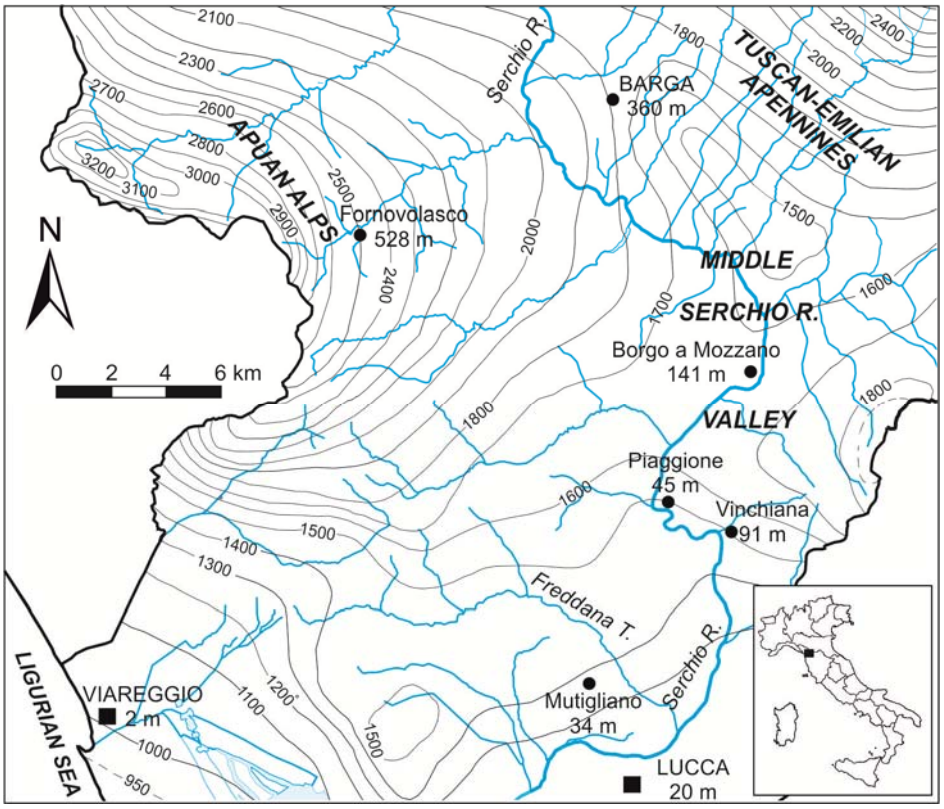

Fig. 3.3. Isohyet map of the MSRV for the 1951-1981 interval (after Baldacci et al., 1993, modified).

The definition of rainfall thresholds for the initiation of shallow landslides can provide a crucial decision-making tool in risk management. In the relevant literature, two approaches have been proposed for evaluating the relationship between rainfall and landslide occurrence. The first approach is based on physical, process-based models (Montgomery and Dietrich, 1994; Wilson and Wieckzorek, 1995; Wu and Sidle, 1995; Iverson, 2000; Crosta and Frattini, 2003), whereas the second approach relies on the definition of empirical thresholds (Caine, 1980; Reichenbach et al., 1998; Corominas, 2000; Aleotti, 2004; Wieczorek and Glade, 2005; Giannecchini, 2006; Guzzetti et al., 2007, 2008; Cannon et al., 2008; Dahal and Hasegawa, 2008, Brunetti et al., 2010; Saito et al., 2010).

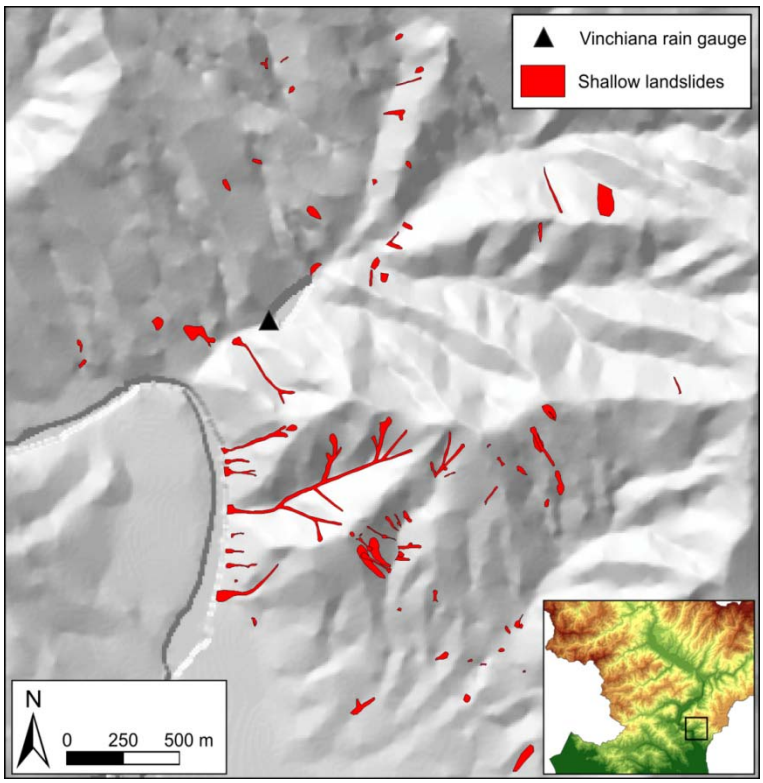

Fig. 3.4. Sketch map of the main shallow landslides triggered during the 20 November 2000 rainstorm in the Vinchiana area.

The physical models generally require numerous and expensive geotechnical characterization of the materials involved in landsliding, and therefore may be applied only in restricted areas.

The empirical approach can be classified according to the geographical extent over which the critical thresholds are defined (i.e. global, national, regional or local), and by the type of rainfall information used to determine the threshold (Guzzetti et al., 2007, 2008).

Rainfall duration D, rainfall intensity I, cumulative event rainfall E, and antecedent rainfall $A(D)$ are the most commonly investigated variables. In particular, landslide initiation is frequently related to rainfall intensity and duration (Caine, 1980; Aleotti, 2004; Giannecchini, 2006; Guzzetti et al., 2007, 2008; Cannon et al., 2008; Coe et al., 2008; Dahal and Hasegawa, 2008). Antecedent rainfall, geological and climatic context play important roles in triggering landslides, but the rate of water infiltration and its movement below the surface are the key aspects of landslide initiation and are considered in physically based, process driven methods (Caine, 1980; Reichenbach et al., 1998; Iverson, 2000; Crosta and Frattini, 2003; Giannecchini et al., 2007; D'Amato Avanzi et al., 2009). The empirical approach avoids

quantifying the numerous parameters needed by the physically-based models. It could be used in applying physically-based approaches.

The mathematical or statistical criteria used in defining critical rainfall thresholds are not usually specified in the literature, except in rare cases, as in Guzzetti et al.'s reviews (2007, 2008). A rainfall threshold is generally obtained on a linear or logarithmic-scale graph by drawing the differentiation line between the rainfall features (e.g., rainfall duration and intensity) that cause landslides and those that do not, or by drawing the lower boundary of the rainfall features resulting in failures. Recently, some authors (Guzzetti et al., 2007, 2008; Brunetti et al., 2010; Saito et al., 2010), criticizing the above-mentioned approaches due to their lack of objectivity and repeatability, have introduced some statistical methods for the definition of more objective rainfall intensity-duration (ID) thresholds. A first method is based on a probabilistic approach ("Bayesian inference method") and can be used to determine the minimum-ID threshold for the initiation of landslides (Guzzetti et al., 2007, 2008; Brunetti et al., 2010). Brunetti et al. (2010) also adopts a "Frequentist" approach in order to determine the intercept α and the slope β of the power law curve selected to represent the rainfall threshold. Other statistical criteria use quantile regression to determine the ID thresholds objectively (Saito et al., 2010). In order to define the minimum-ID rainfall thresholds, a quantile regression may be performed for some percentiles, for example in the 2nd and 5th percentiles of the rainfall events dataset.

In this work the hourly rainfalls recorded by three rain gauges (Borgo a Mozzano from 1942 to 2010, Mutigliano from 1937 to 2010 and Vinchiana from 1964 to 2010) of the MSRV were analyzed and compared with the occurrence of shallow landslides involving homogeneous areas in terms of geological, geomorphologic and climatic features.

In accordance with more traditional methods (Giannecchini, 2006 and reference therein), the rainfall thresholds and the normalized rainfall thresholds were obtained using manual fitting methods by determining a differentiation line of the dataset including rainfall conditions that did or did not result in landslides. Considering the fragility of the study area, the possibility of obtaining and managing more cautionary rainfall thresholds prompted the use of manual fitting.

3.2 Study area

The MSRV is situated between the Apuan Alps to W-SW and the Apennine chain to E-NE (Fig. 3.2). It falls within the Northern Apennines, a fold-and-thrust belt formed during the Upper Cretaceous-Upper Miocene. From the Upper Miocene, the tensional tectonics gave origin to tectonic depressions bounded by NW-SE trending normal faults, in which either marine or continental successions were deposited. From top to bottom, the Ottone unit, the Canetolo unit and the Tuscan Nappe crop out. These originated in different paleogeographic domains: the Ligurian, the Sub-Ligurian and Tuscan domains, respectively (Elter et al., 1975; Carmignani and Kligfield, 1990; Carmignani et al., 2000; Puccinelli et al., 2012). Pliocene and Quaternary continental deposits extensively cover the slopes.

The morphology is highly influenced by the geological and structural features. NW-SE trending normal faults delineate the fundamental configuration of the Serchio River Valley, which can be considered as a consequent valley, adapted to the tectonic structure. The uplift movements of the late orogenic stages determined relevant height differences, while the fluvial and slope processes shaped the landscape. Glacial processes involved the higher areas close to the main watershed (Castaldini et al., 2004).

The climatic conditions of the MSRV are directly related to the geographical and morphological features. The mountains intercept Atlantic and Mediterranean humid air masses, forcing adiabatic ascent and subsequent condensation, which results in heavy precipitation events. The rainfall regime of the MSRV can be ascribed to the Apennine-Mediterranean type with transition to the sub-coastal type. It is characterised by dry summers and cold winters, with a primary peak of rainfall in autumn and a secondary maximum in spring. The mean annual rainfall depends on the altitude. It ranges from 1,300 mm of the valley floor to about 1,800 mm at higher altitudes (Fig. 3.3, Baldacci et al., 1993).

Intense rainstorms are quite frequent and can trigger a lot of shallow landslides, mostly involving the colluvium and debris deposits of the Macigno Fm. (Tuscan *Nappe*). This formation underlies about 35% of the study area. It consists of siliciclastic turbidites made of grey-brown sandstone and normally shows a high sandstone/shale ratio and thick to very thick, coarse-grained strata. Based on Bieniawski's (1989) Rock Mass Rating, the Macigno Fm. can be typically described as a stratified medium strong rock, intersected by orthogonal, NW and SE trending joint sets. The joint sets are closely spaced, very persistent, open, smooth or slightly rough, from moderately to highly weathered and dry to damp. Infilling is

not very significant. The basic Rock Mass Rating is of about 35 (poor rock). Intense deformation and fracturing of the rock, together with chemical alteration, lead to a considerable production of debris and colluvium. These deposits consist of sand and gravel with a minor part of finer materials (silt and clay) and can mantle vast slopes, with a thickness commonly between 0.5 m and 2-3 m.

The shallow landslides considered here can be classified as complex, rapid to extremely rapid debris slide-debris flows (Cruden and Varnes, 1996) and are also known as soil slip-debris flows, or simply debris flows (Campbell, 1975). They commonly involve the entire thickness of the slope deposit, up to an impermeable or less permeable bedrock (mostly consisting of the Macigno Fm.). A thin portion (0.5-1 m) of highly weathered bedrock may also be involved. Afterwards, the material usually flows into the riverbeds and quickly reaches the main valley bottom, where the reduced slope gradient induces deposition and stops the flowing mass.

3.3 Methodology

The main rainfall events recorded by three rain gauges in the MSRV (Figs. 3.1 and 3.2) were analysed with the goal of defining the rainfall thresholds for the initiation of shallow landslides.

The analysis of rainfall events shorter than 24 hours requires hourly rainfall data. Therefore it considered different operating periods for the three rain gauges: from 1935 to 2010 for the Mutigliano rain gauge (34 m a.s.l.), from 1942 to 2010 for the Borgo a Mozzano rain gauge (141 m a.s.l.), and from 1964 to 2010 for the Vinchiana rain gauge (91 m a.s.l.). Despite different operating periods of the rain gauges analyzed, these stations are believed the most effective for the analysis. They are quite close together, since 12 km separate the Mutigliano and Borgo a Mozzano rain gauges, while the Vinchiana one is exactly halfway between them (Figs. 3.1 and 3.2).

The rain gauges were equipped with pluviographs until 2000. In 2000 the Borgo a Mozzano and Mutigliano rain gauges were equipped with electronic rain gauges, while the Vinchiana rain gauge was replaced by an electronic one about 2 km away (near the village of Piaggione, 45 m a.s.l.).

The mean annual precipitation (MAP) was calculated for the whole recording time of the stations, including the period of both daily and hourly recording. The MAP for each instrument increases with altitude: 1,331 mm at Mutigliano, 1,376 mm at Vinchiana and 1,565 mm at Borgo a Mozzano.

During the period considered in this research, 335 rainfall events were analysed on the basis of the combination of rainfall duration *D* and cumulative rainfall *E*. From 1942 onwards, 97 events were recorded by at least two rain gauges. Since 1964, 29 events have been recorded in all the rain gauges. Altogether 490 rainfall records were analyzed (195 at Borgo a Mozzano, 155 at Mutigliano, and 140 at Vinchiana).

Each event was evaluated on the basis of the pluviograph data (Fig. 3.5). For example, events with low duration (1-2 hours) and high intensity (20-45 mm h^{-1}), or high duration (80-100 hours) and low intensity (1.5-3 mm h^{-1}) and intermediate events were considered. For each event the following rainfall variables were collected: (i) cumulative rainfall *E* (mm), (ii) rainfall duration *D* (hours), (iii) mean intensity *I* (mm h^{-1}), and (iv) antecedent rainfall $A_{(D)}$ (mm) related to 3, 7, 15 and 30 days.

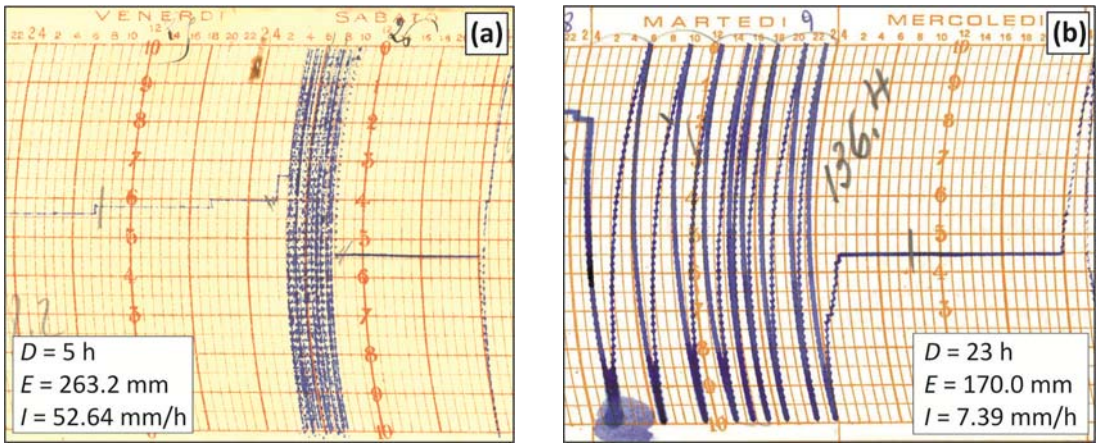

Fig. 3.5. Examples of pluviograph charts (*D*: rainfall duration; *E*: cumulative event rainfall; *I*: rainfall intensity): record of the 26 September 1942 rainstorm in the Borgo a Mozzano area **(a)**; record of the 9 January 1979 rainstorm in the Mutigliano area **(b)**.

For each rainfall event a thorough research on its consequences in the study area (number of shallow landslides, damage, deaths) was carried out. Areas of about 10-15 km around each rain gauge were considered in order to find possible consequences of the rainfall events. Different sources of information were analysed, including: (i) archives of the local municipal

councils, (ii) scientific papers, (iii) technical reports, (iv) regional and local newspapers, and (v) information provided by local inhabitants. However, most of the information came from local newspapers (Fig. 3.6).

cronaca di lucca

Il Tirreno
Giovedì 11 Novembre 1982 18

Viabilità completamente sconvolta nella Media Valle

Franate molte strade

Divorata dalla piena la SS 12 per 300 metri

Pericolante il ponte di Borgo a Mozzano

LA STRADA statale 12 dell'Abetone e del Brennero è stata divorata dalla piena del Serchio per circa 300 metri a Socciglia di Borgo a Mozzano. Inghiottita dalle acque tumultuose del fiume, della vecchia arteria non resta più traccia. C'è solo la montagna a strapiombo sul Serchio che dieci metri più in basso scorre limaccioso e rapidissimo.

Il crollo delle cui dimensioni non era stata capita in un primo momento la grandezza (era stato giudicato dalla Polizia stradale di circa 50 metri) è apparso in tutta la sua gravità ieri mattina alle prime luci dell'alba. La strada già

A Socciglia la via del Brennero non esiste più

L'alluvione a Ponte del Diavolo

La SS 12 vicino al Piaggione (Foto by Vip)

Fig. 3.6. Example of information coming from a local newspaper. The main title reads: "Many roads affected by landslides" (source: *Il Tirreno*, 11 November 1982).

The rainfall events investigated were subdivided into three groups on the basis of the consequences induced on the territory and gathered by the archive research. Since the 1980s the rainfall events can be discriminated on a quantitative basis: (i) events that induced ten or more shallow landslides (A events, in the following tables and graphs), (ii) events that induced less than ten shallow landslides (B events); and (iii) events that did not trigger any landslides, including those events for which no information on consequences was found in archives and newspapers (C events). Before the 1980s information about the number and consequences of landslides are often confused and incomplete. Therefore, on the basis of qualitative descriptions reported by newspapers and documents, events that induced several landslides have been included in the A-type, while events that only locally induced few landslides have been considered as B-type. For the A events information on the effects is very clear. For example, during the 20 November 2000 heavy rainstorm approximately 150 shallow landslides occurred, causing 5 fatalities. Table 3.1 shows number and frequency of A, B and C-type events for each rain gauge.

Table 3.1. Frequency of the A, B and C events at the three rain gauges of the study area (A: events that induced ten or more shallow landslides; B: events that induced less than ten shallow landslides; C: events that did not trigger any landslides). %: percentage of events that fall in A, B and C group for each considered rain gauge.

Rain gauge	A events		B events		C events		Total
	no.	%	no.	%	no.	%	no.
Borgo a Mozzano	5	3	35	18	155	79	195
Mutigliano	5	3	25	16	125	81	155
Vinchiana	6	4	26	19	108	77	140

3.4 Critical threshold analysis

3.4.1 Intensity-Duration thresholds

In the 1935-2010 period the rain gauges recorded many rainfall events: 195 at Borgo a Mozzano, 155 at Mutigliano, and 140 at Vinchiana. Most of them were recorded by all three rain gauges.

The research highlighted that very heavy rainstorms occurred: on 25 November 1990, 20 November 2000, and 19 June 2010 in the Vinchiana area, on 26 September 1942, 21 September 1994, and 20 January 2009 in the Borgo a Mozzano area, and on 9 January 1979, 9 June 1992, and 5 October 1998 in the Mutigliano area. With reference to the seasonal distribution, the analyzed rainstorm events preferentially occurred in autumn (almost 50% in the September-November period, Fig. 3.7), the rainiest season in the study area. Giannecchini (2006) found a comparable seasonal distribution for the adjacent Southern Apuan Alps, while Guzzetti (2000) and Guzzetti et al. (2005) obtained similar results on a national scale for rainfall events that caused deaths or missing people. Figure 3.7 shows the seasonal distribution of all the analysed rainstorms (Fig. 3.7a) and of those inducing shallow landslides and damage (Fig. 3.7b). The most severe rainstorms usually occurred between September and November, and in the June-August period.

In order to construct the rainfall intensity-duration (ID) thresholds, all the duration D and intensity I data were plotted together on a bi-logarithmic scale (D on the x-axis, I on the y-axis), where the A, B and C events were also plotted. Then, manual fitting was used to draw the critical threshold curve, i.e. the curves better differentiating the A, B and C events.

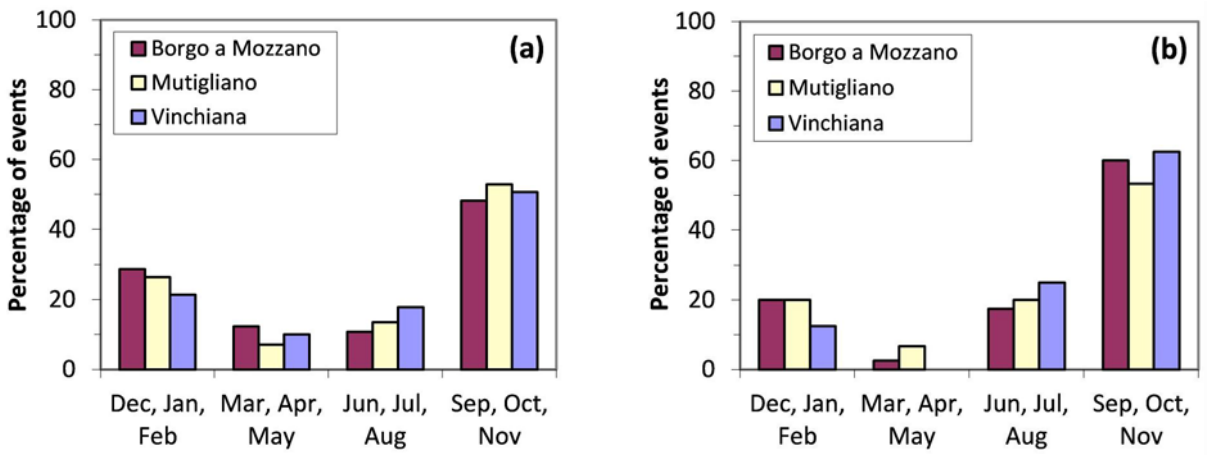

Fig. 3.7. Seasonal distribution of the main rainstorms occurring in the MSRV from 1935 to 2010, recorded at the Borgo a Mozzano, Mutigliano and Vinchiana rain gauges: **(a)** distribution of all the rainstorms analysed; **(b)** distribution of the rainstorms inducing shallow landslides.

Upper and lower threshold curves can be traced. They subdivide the ID field into three parts, including the rainfall conditions of rainstorms which induce different stability conditions (Fig. 3.8). The rainfall events falling between the two curves should trigger only a few landslides, while those falling above the upper curve should trigger more than ten landslides. Below the lower curves no consequences are expected.

The threshold curves are expressed in the form (Caine, 1980):

$$I = \alpha \times D^{-\beta} \tag{3.1}$$

where I is the rainfall intensity (mm h^{-1}), D is the duration of the rainfall event (hours), α is the intercept, and β defines the slope of the power law curve.

The rainfall thresholds are defined for the range of duration $2<D<70$ h, $1.5<D<80$ h and $1<D<80$ h for the Borgo a Mozzano, Mutigliano and Vinchiana rain gauges, respectively (Fig. 3.8; Table 3.2). Generally the upper thresholds are defined in the range of mean intensity $4<I<60$ mm h^{-1}, while the lower thresholds are defined in the range of $2<I<40$ mm h^{-1} (Fig. 3.8). Inspection of Fig. 3.8 indicates that both the upper and lower threshold curves are similar for the three rain gauges.

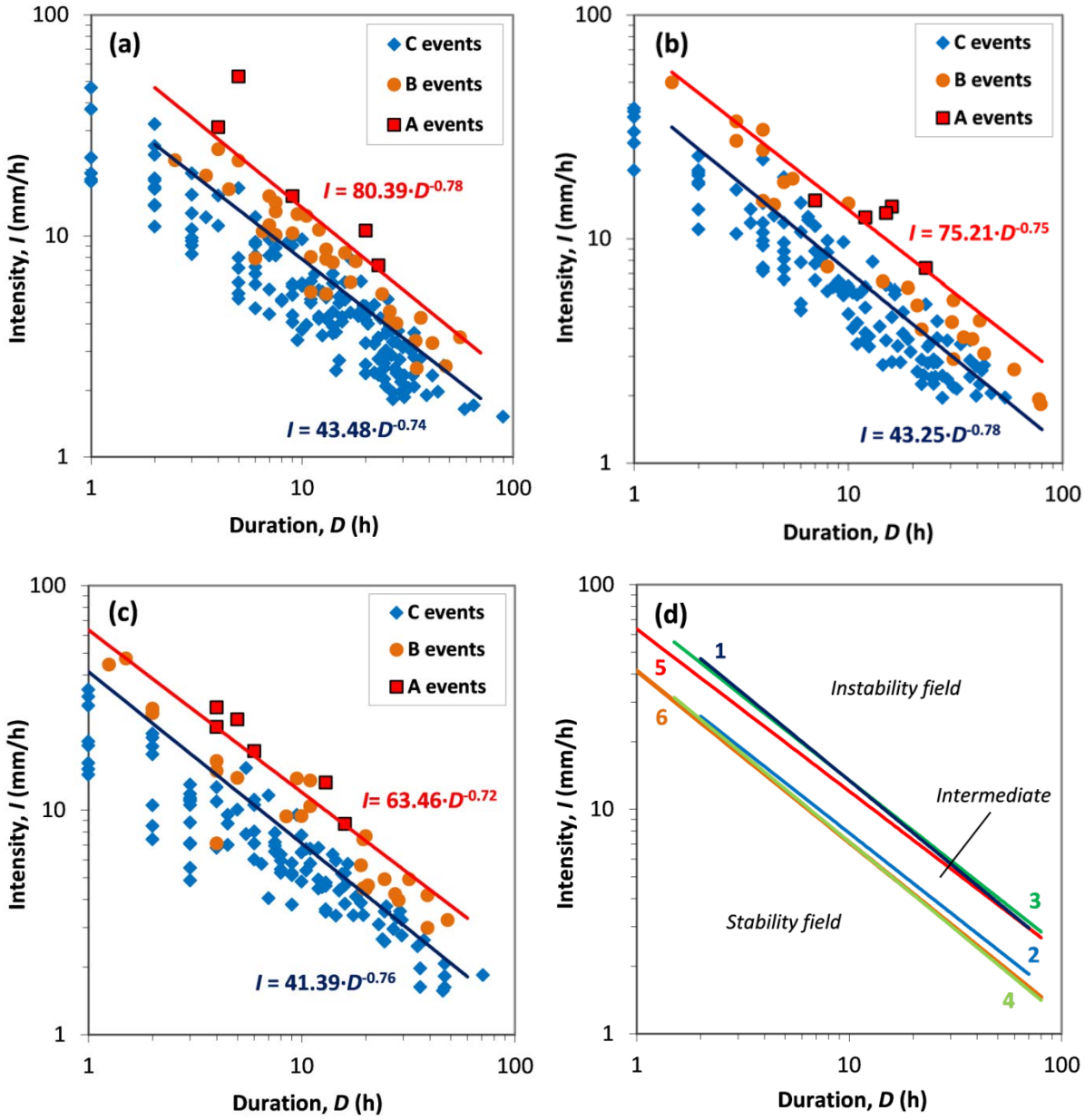

Fig. 3.8. Intensity-duration correlation for the Borgo a Mozzano **(a)**, Mutigliano **(b)** and Vinchiana **(c)** rain gauges. The lower (blue) and upper (red) threshold curves are shown. **(d)** Comparison between the ID thresholds obtained for the study area. The three stability fields are highlighted; 1) Borgo a Mozzano upper curve; 2) Borgo a Mozzano lower curve; 3) Mutigliano upper curve; 4) Mutigliano lower curve; 5) Vinchiana upper curve; 6) Vinchiana lower curve.

Rainfall events lasting approximately 10 hours are quite frequent in the study area. Therefore, rainfall durations of both 10 and 24 h were considered. For a rainfall duration D of 10 h rainfall intensities are 13.4, 13.5 and 12.0 mm h^{-1} for the Borgo a Mozzano, Mutigliano and Vinchiana upper thresholds (1, 3 and 5 in Fig. 3.8d, respectively).

For a duration of 24 h, intensities are 6.7, 6.9 and 6.4 mm h^{-1} for the Borgo a Mozzano, Mutigliano and Vinchiana upper thresholds (1, 3 and 5 in Fig. 3.8d, respectively). The Vinchiana upper threshold is the lowest, i.e. the most conservative for a duration less than 30 h, and especially for short events ($D \leq 10$ h).

Table 3.2. Rainfall ID thresholds for initiation of shallow landslides for the Borgo a Mozzano, Mutigliano and Vinchiana rain gauges. Equation: D, rainfall duration in hours; I, rainfall intensity in mm h^{-1}. Range: range of validity for the threshold.

Rain gauge	Type	Equation	Range
Borgo a Mozzano	upper curve	$I=80.39 \cdot D^{-0.78}$	$2<D<70$
	lower curve	$I=43.48 \cdot D^{-0.74}$	$2<D<70$
Mutigliano	upper curve	$I=75.21 \cdot D^{-0.75}$	$1.5<D<80$
	lower curve	$I=43.25 \cdot D^{-0.78}$	$1.5<D<80$
Vinchiana	upper curve	$I=63.46 \cdot D^{-0.72}$	$1<D<80$
	lower curve	$I=41.39 \cdot D^{-0.76}$	$1<D<80$

As regards the lower thresholds (Fig. 3.8), for a duration of 10 h the rainfall intensity is 7.8 mm h^{-1}, 7.2 mm h^{-1}, and 7.1 mm h^{-1} at Borgo a Mozzano (2 in Fig. 3.8d), Mutigliano (4 in Fig. 3.8d) and Vinchiana (6 in Fig. 3.8d) rain gauges, respectively. For $D \geq 24$ h, the Borgo a Mozzano lower threshold is less conservative.

Figure 3.8 also shows some misclassifications of the type of events. Some A events fall in the B events field and vice versa. Such exceptions are probably due to uncertainty in the areal extent of the damage, which can often be based only on historical description or information by newspapers. Other misclassifications occur between B and C events. For example, in the Borgo a Mozzano case (Fig. 3.8a) there are 12.9% missing events. These missing events are not linkable to definite causes. Occasional and extemporary causes probably add to the triggering rainfall and induce unexpected landslides. Otherwise, bad functioning of the rain gauge could be an alternative cause.

In Fig. 3.8 the upper and lower threshold curves identify three fields with differing degrees of stability. Below the lower threshold (blue line) stability generally prevails. Above the upper curve (red line) instability prevails, while the field between the two curves includes

intermediate or uncertain stability (Fig. 3.8d). The probability of each A, B or C event to fall within a defined stability field can be estimated. The results are shown in Table 3.3.

Table 3.3. Frequency of the A, B and C events in each stability field for the three rain gauges The percentage of the events falling in the proper field is in bold (theoretically it should be 100%).

Rain gauge	Event type	No. events	Stability field (%)	Intermediate (%)	Instability field (%)
Borgo a Mozzano	A	5	0	0	**100**
	B	35	12.9	**87.1**	0
	C	155	**86.5**	13.5	0
Mutigliano	A	5	0	10	**80**
	B	25	8	**80**	12
	C	125	**81.6**	18.4	0
Vinchiana	A	6	0	0	**100**
	B	26	3.8	**84.7**	11.5
	C	108	**85.2**	14.8	0

3.4.2 Normalization

Various authors assert that each area is in equilibrium with its rainfall conditions (Guidicini and Iwasa, 1977; Govi and Sorzana, 1980; Cannon, 1988; Bacchini and Zannoni, 2003; Aleotti, 2004; Giannecchini, 2006). Therefore, in order to normalize the rainfall data, they are commonly compared to the mean annual precipitation (MAP).

The MAP was calculated all through the investigated period for each rain gauge. The MAP was 1,565 mm at Borgo a Mozzano (from 1921 to 2010), 1,376 mm at Vinchiana (from 1930 to 2010) and 1,331 mm at Mutigliano (from 1934 to 2010). The MAP is different for each rain gauge, since it rises with altitude. Guidicini and Iwasa, (1977) introduced the normalized event rainfall (E_{MAP}), i.e. the cumulative event rainfall divided by MAP. Based on this parameter, the relationships $E_{MAP}I$ and $E_{MAP}D$ were analysed for each rain gauge (Figs. 3.9 and 3.10; Tables 3.4 and 3.5).

On the basis of the same empirical approach and manual fitting used for the identification of the ID thresholds, two threshold curves were drawn (Figs. 3.9 and 3.10). For each rain gauge the bi-logarithmic functions E_{MAP} (I) and E_{MAP} (D) describe the thresholds (Tables 3.4 and 3.5).

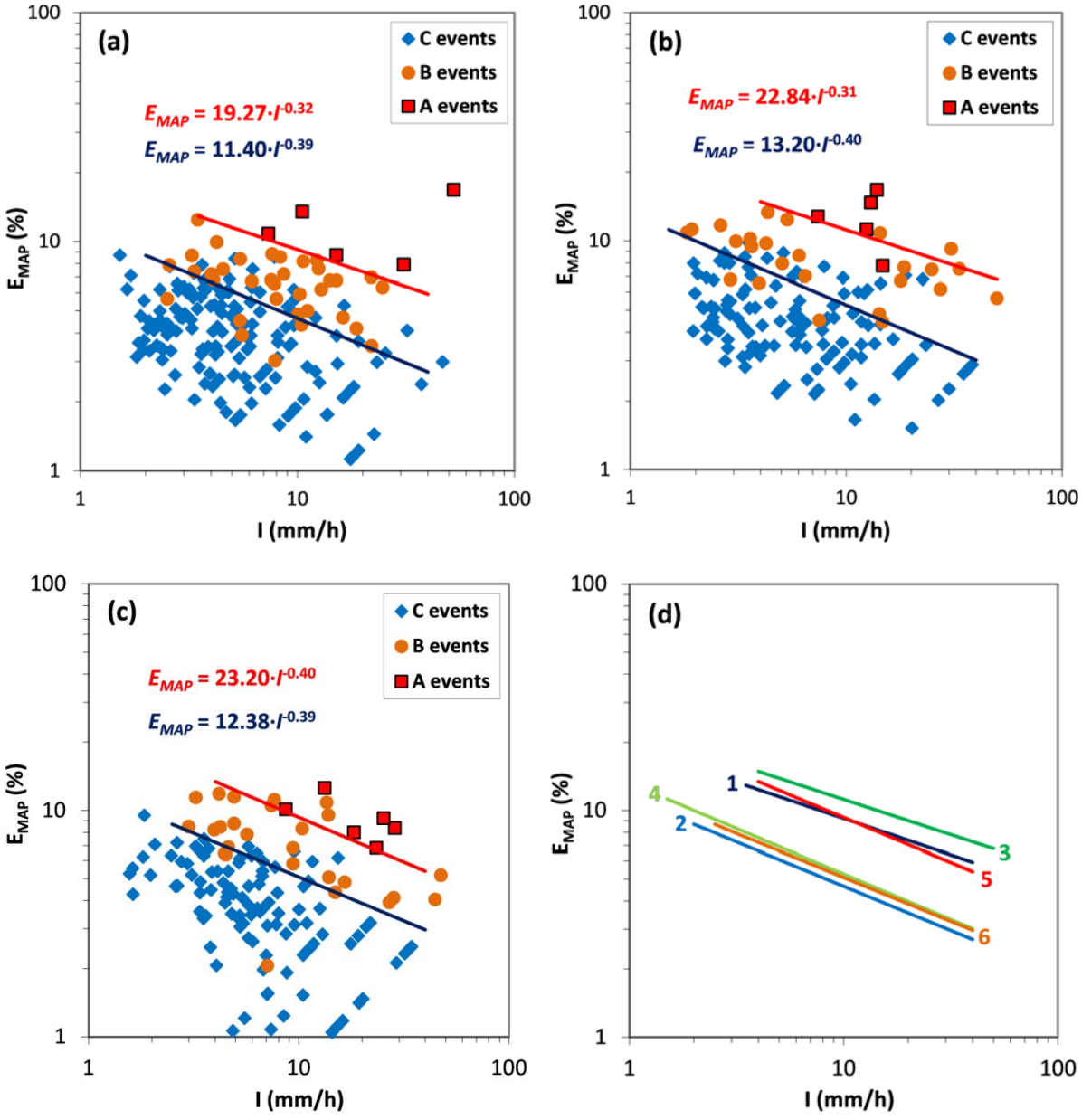

Fig. 3.9. Bi-logarithmic E_{MAP}I correlation for the Borgo a Mozzano **(a)**, Mutigliano **(b)** and Vinchiana **(c)** rain gauges. Upper (red) and lower (blue) critical threshold curves are shown. **(d)** Comparison between the different thresholds; 1) Borgo a Mozzano upper curve; 2) Borgo a Mozzano lower curve; 3) Mutigliano upper curve; 4) Mutigliano lower curve; 5) Vinchiana upper curve; 6) Vinchiana lower curve.

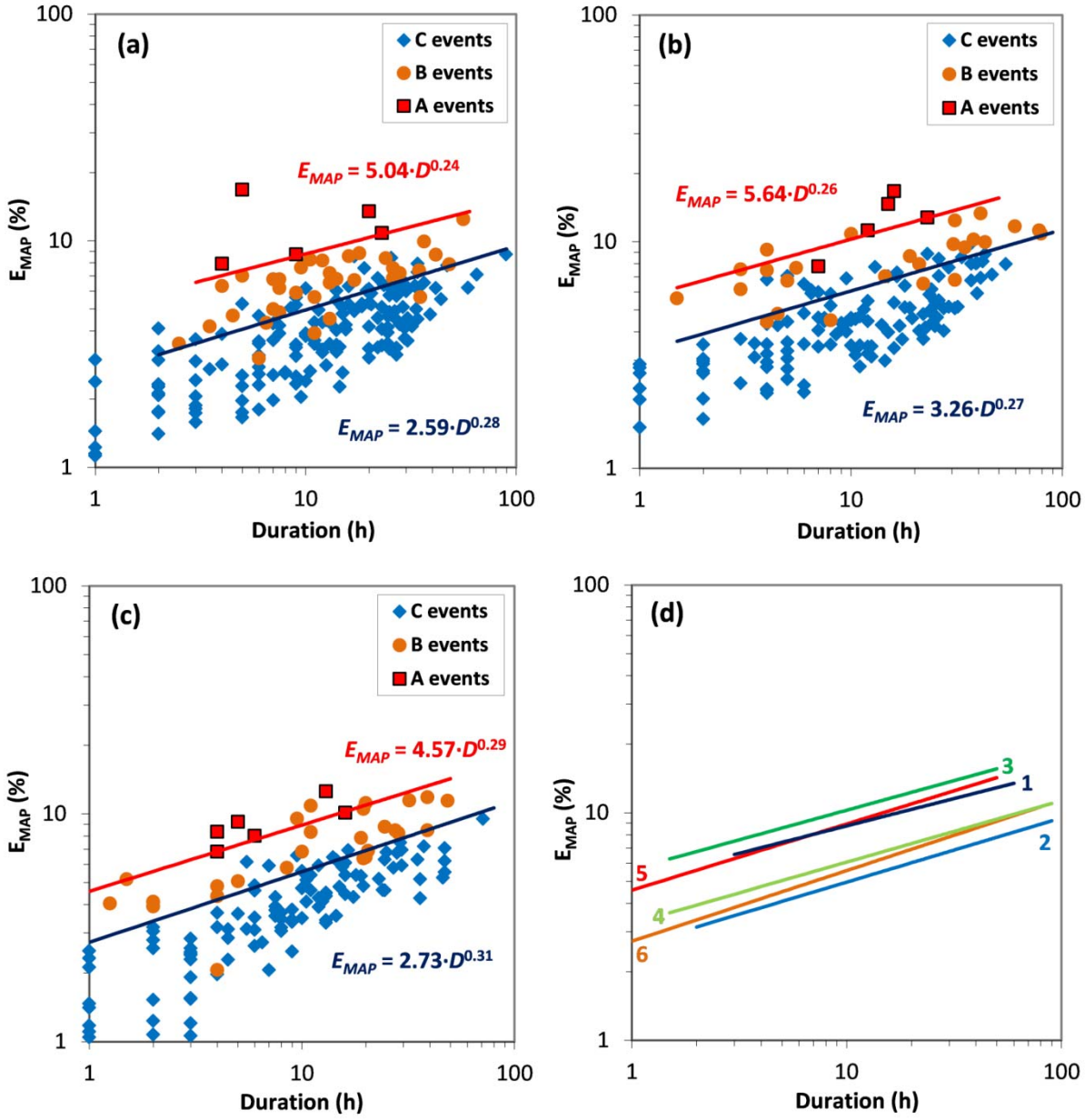

Fig. 3.10. Bi-logarithmic $E_{MAP}D$ correlation for Borgo a Mozzano **(a)**, Mutigliano **(b)** and Vinchiana **(c)** rain gauges. Upper (red) and lower (blue) critical threshold curves are shown. **(d)** Comparison between the thresholds; 1) Borgo a Mozzano upper curve; 2) Borgo a Mozzano lower curve; 3) Mutigliano upper curve; 4) Mutigliano lower curve; 5) Vinchiana upper curve; 6) Vinchiana lower curve.

The $E_{MAP}I$ and the $E_{MAP}D$ thresholds are expressed by the equations (3.2) and (3.3), respectively:

$$E_{MAP} = \alpha \times I^{-\beta} \tag{3.2}$$

$$E_{MAP} = \alpha \times D^{\beta} \tag{3.3}$$

where E_{MAP} is the normalized event rainfall, I is the rainfall intensity (in mm h^{-1}), D is the duration of the rainfall event (in hours), α is the intercept, and β defines the slope of the power law curve.

Two threshold curves delimit three fields of stability (Figs. 3.9 and 3.10): stability generally prevails (below the lower curve), uncertain stability (between the two curves), instability (above the upper curve). Figures 3.9 and 3.10 show that some B events (triggering less than ten shallow landslides) fall below the lower threshold curves. These missing events can be due to occasional and extemporary causes or to bad functioning of the rain gauge.

Inspection of Fig. 3.9 and Table 3.4 indicates that the E_{MAP}, the critical amount for triggering shallow landslides, decreases with increasing I. The lower thresholds obtained for the three rain gauges are similar. The Borgo a Mozzano lower threshold (2 in Fig. 3.9d) is the most conservative, while the Mutigliano upper threshold (3 in Fig. 3.9d) is higher than those of Borgo a Mozzano (1 in Fig. 3.9d) and Vinchiana (5 in Fig. 3.9d). This result depends on the MAP value. In fact, the MAP obtained for Mutigliano (1,331 mm) is lower than those for Vinchiana (1,376 mm) and Borgo a Mozzano (1,565 mm). The Vinchiana upper threshold is steeper (β=0.40) than those for Borgo a Mozzano (β=0.32) and Mutigliano (β=0.31). This indicates that, for the Vinchiana upper threshold, the rainfall intensity is more important than the cumulative rainfall in discriminating rainfall conditions triggering several or few shallow landslides.

Table 3.4. $E_{MAP}I$ thresholds for initiation of shallow landslides for the Borgo a Mozzano, Mutigliano and Vinchiana rain gauges. Equation: I, rainfall intensity in mm h^{-1}; E_{MAP}, cumulative event rainfall normalized by MAP. Range: range of validity for the threshold.

Rain gauge	Type	Equation	Range
Borgo a Mozzano	upper curve	$E_{MAP}=19.27 \cdot I^{0.32}$	$3.5<I<40$
	lower curve	$E_{MAP}=11.40 \cdot I^{0.39}$	$2<I<40$
Mutigliano	upper curve	$E_{MAP}=22.84 \cdot I^{0.31}$	$4<I<50$
	lower curve	$E_{MAP}=13.20 \cdot I^{0.40}$	$1.5<I<40$
Vinchiana	upper curve	$E_{MAP}=23.20 \cdot I^{0.40}$	$4<I<40$
	lower curve	$E_{MAP}=12.38 \cdot I^{0.39}$	$2.5<I<40$

Table 3.5. $E_{MAP}D$ thresholds for the initiation of shallow landslides for the Borgo a Mozzano, Mutigliano and Vinchiana rain gauges. Equation: D, rainfall duration in hours; E_{MAP}, cumulative event rainfall normalized by MAP. Range: range of validity for the threshold.

Rain gauge	Type	Equation	Range
Borgo a Mozzano	upper curve	$E_{MAP}=5.04 \cdot D^{0.24}$	$3<D<60$
	lower curve	$E_{MAP}=2.59 \cdot D^{0.31}$	$2<D<90$
Mutigliano	upper curve	$E_{MAP}=5.64 \cdot D^{0.26}$	$1.5<D<50$
	lower curve	$E_{MAP}=3.26 \cdot D^{0.27}$	$1.5<D<90$
Vinchiana	upper curve	$E_{MAP}=4.57 \cdot D^{0.29}$	$1<D<50$
	lower curve	$E_{MAP}=2.73 \cdot D^{0.31}$	$1<D<80$

3.5 Effect of antecedent rainfall

The antecedent rainfall plays an important role in the initiation of landslides (Wieczorek, 1987), but its influence is difficult to quantify. It depends on several factors, including: local climatic conditions, slope angle, and heterogeneity of soils in terms of physical-mechanical properties and permeability (Aleotti, 2004). For example, coarse soils with large interparticle voids are very permeable. So, the antecedent rainfall is not generally a significant factor for triggering debris flows (Corominas and Moya, 1999). On the contrary, in low-permeability soils the antecedent rainfall can be important in reducing soil suction and increasing the pore-water pressure (Aleotti, 2004; D'Amato Avanzi et al., 2004).

Several rainfall variables take antecedent rainfall into consideration, for example the normalized critical rainfall (C_{MAP}, Aleotti, 2004) or the daily rainfall (R, Dahal and Hasegawa, 2008). For shallow landslide events, various authors analyse different time intervals to quantify the rainfall prior to a rainstorm: 3 days (Dahal and Hasegawa, 2008), 5 days (Wieczorek et al., 2000), 10 days (Crozier, 1999; Glade at al., 2000), 15 days (Aleotti, 2004), or 25 days (Terlien, 1998). In order to correlate the rainstorms triggering shallow landslides with antecedent rainfall in the study area, the cumulative rainfall at time intervals of 3, 7, 15, and 30 days was analysed and compared with the rainstorm features.

The cumulative event rainfall E as well as the antecedent rainfall $A_{(D)}$ were normalized by MAP. The relationship between normalized rainfall event E_{MAP} and normalized antecedent rainfall $A_{(D)MAP}$ ($A_{(D)}/MAP$) of 3, 7, 15, and 30 days for the A, B and C events were plotted

together (Figs. 3.11, 3.12 and 3.13). For antecedent rainfall of 3 and 7 days the graphs show a pronounced discrimination between events that triggered shallow landslides (A and B events) and those that did not (C events). For 15 and 30 days discrimination is not so evident. In general, the $E_{MAP}A(_D)_{MAP}$ relationship suggests that the E_{MAP} amount needed for triggering shallow landslides decreases with increasing $A(_D)_{MAP}$.

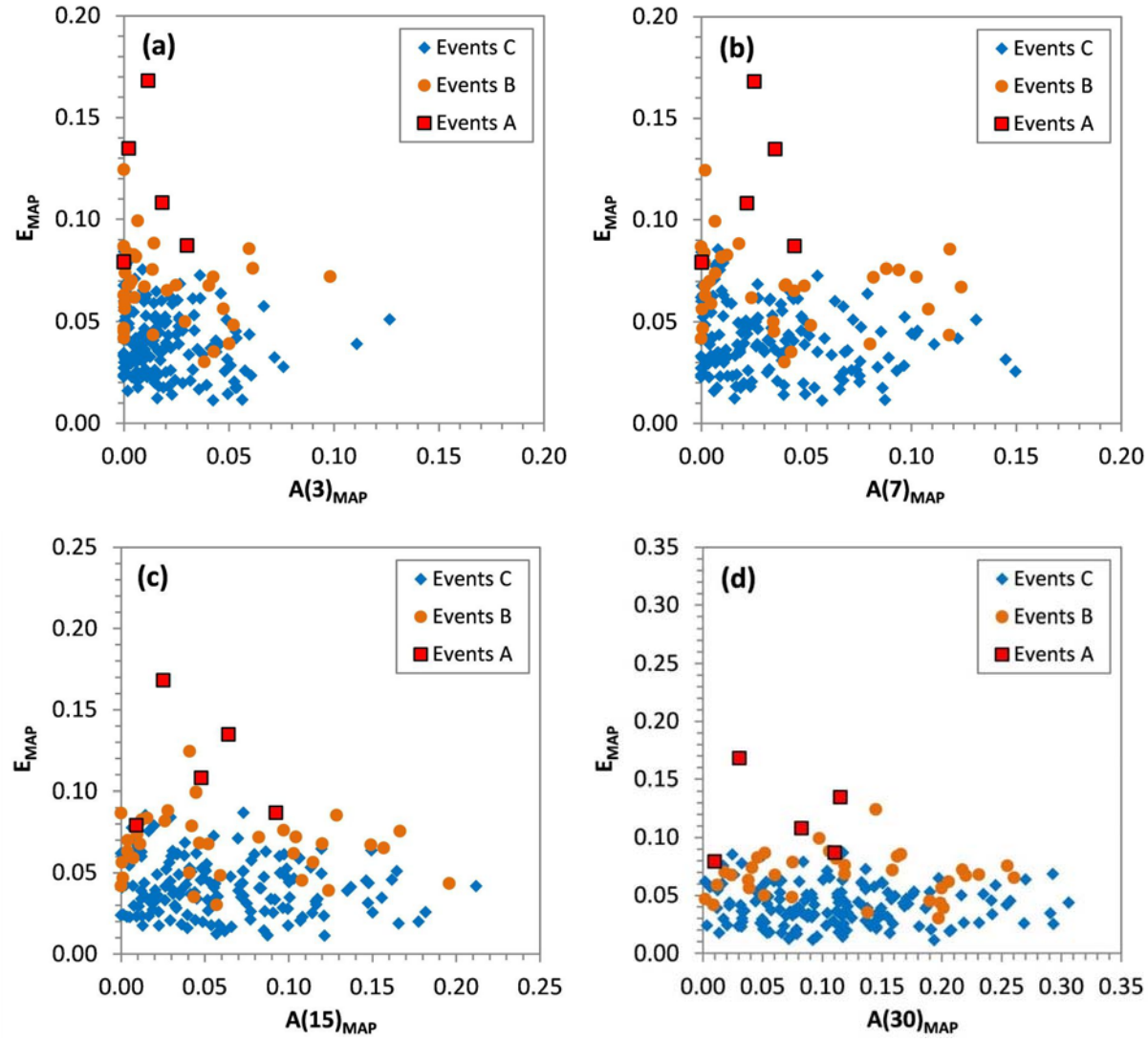

Fig. 3.11. Relationship between normalized antecedent rainfall $A(_D)_{MAP}$ and normalized event rainfall E_{MAP} for the Borgo a Mozzano rain gauge. The time intervals considered are of 3 **(a)**, 7 **(b)**, 15 **(c)** and 30 **(d)** days.

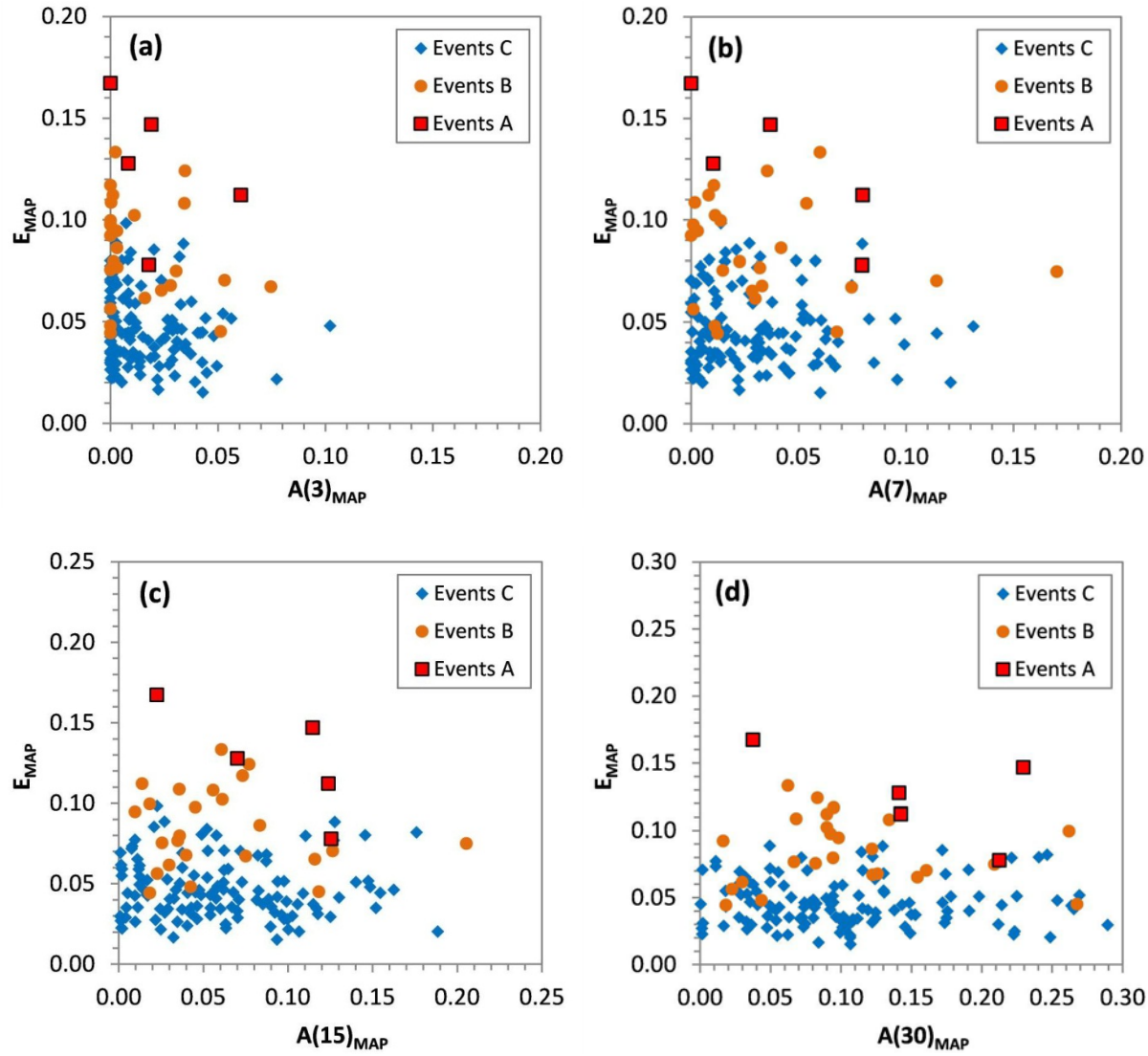

Fig. 3.12. Relationship between normalized antecedent rainfall $A(_D)_{MAP}$ and normalized event rainfall E_{MAP} for the Mutigliano rain gauge. The time intervals considered are of 3 **(a)**, 7 **(b)**, 15 **(c)** and 30 **(d)** days.

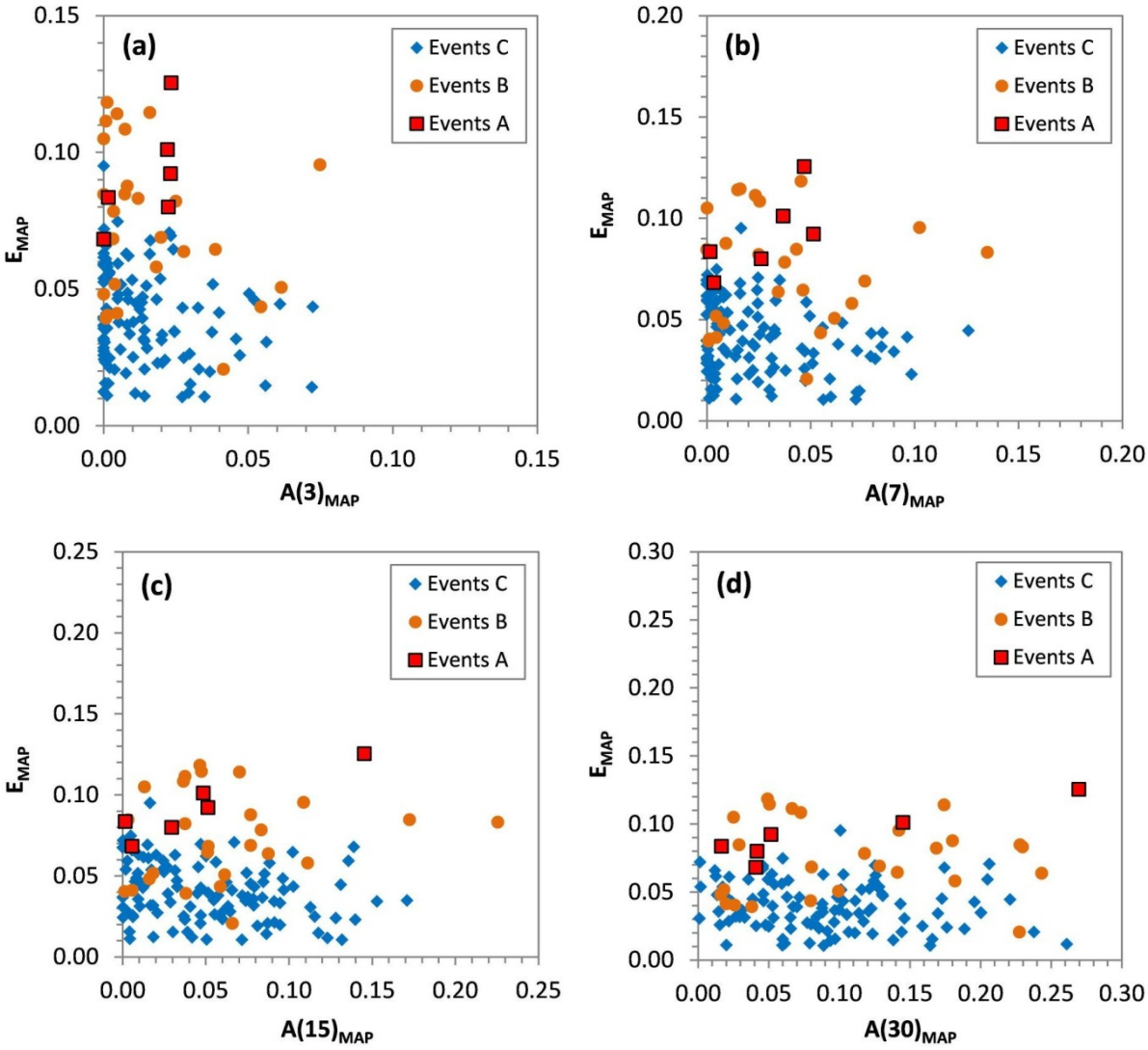

Fig. 3.13. Relationship between normalized antecedent rainfall $A(D)_{MAP}$ and normalized event rainfall E_{MAP} for the Vinchiana rain gauge. The time intervals considered are of 3 **(a)**, 7 **(b)**, 15 **(c)** and 30 **(d)** days.

3.6 Discussion

3.6.1 Comparison of rainfall thresholds

The rainfall ID thresholds obtained for the MSRV (Fig. 3.8; Table 3.2) can be compared with regional and local thresholds proposed for Italy (Figs. 3.15) and with the global thresholds (Fig. 3.16).

Firstly, the thresholds were compared with those proposed by different authors for some areas of north-western Tuscany and Eastern Liguria (Figs. 3.14 and 3.15). The thresholds obtained in this work (1-6 in Fig. 3.15) fall in the range of rainfall intensity and duration

defined by other thresholds for surrounding areas (7-16 in Fig. 3.15). Furthermore, the slope of the threshold curves of the areas of north-western Tuscany (1-12) is similar (Fig. 3.15), probably because their climatic, geological, and geomorphologic features are similar.

Fig. 3.14. Area between Liguria and Tuscany where different authors have identified rainfall thresholds (base map by Google Maps, 2010).

In general, as noted by Govi and Sorzana (1980) and for the Apuan Alps area by Giannecchini (2006), the critical rainfall amount needed to trigger shallow landslides rises with the mean annual precipitation (MAP). For example, the upper curves obtained for the Southern Apuan Alps (MAP = 1,870 mm) and for the Lower Garfagnana (MAP = 2,498 mm) are higher than those obtained in this research (Fig. 3.15). An exception is represented by the Carrara Marble Basin (Northern Apuan Alps), where shallow landslides and debris flows usually involve the quarry waste. It often shows low permeable or impermeable intervals and lies in valley bottoms and on steep slopes, where landslide susceptibility is higher.

The thresholds obtained in this research were also compared with the ID thresholds proposed for different areas of Italy, including six regional and three local thresholds (Fig. 3.15). A high position, namely a larger mean intensity is highlighted for the MSRV thresholds (1-6 in Fig. 3.15). It is an expected outcome of the climatic conditions of the MSRV, which is characterized by high MAP and high frequency of heavy rainfall. This confirms that each area

is in equilibrium with its ordinary climatic conditions, as noted by Govi at al. (1985) for the Piedmont Region.

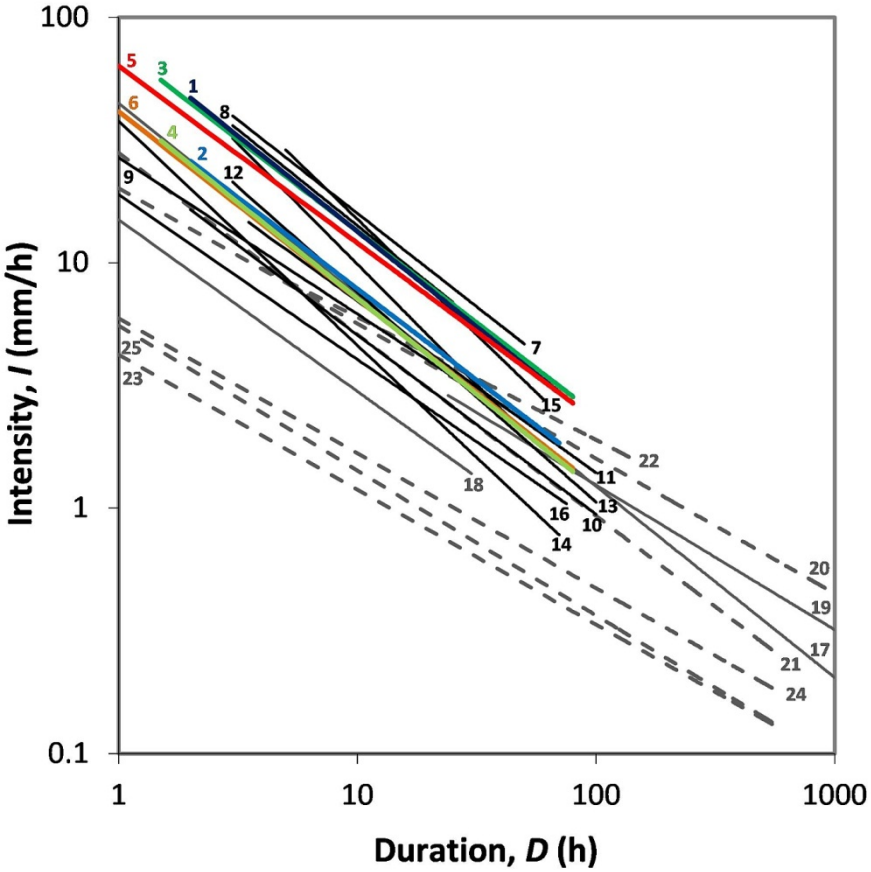

Fig. 3.15. Comparison between the ID thresholds obtained in this study with some local and regional thresholds. The thresholds for the MSRV are coloured: dark blue, Borgo a Mozzano upper curve; blue, Borgo a Mozzano lower curve; green, Mutigliano upper curve; light green, Mutigliano lower curve; red, Vinchiana upper curve; orange, Vinchiana lower curve. Thresholds for MSRV (colour) and surrounding areas (black), local (gray) and regional (gray dashed) thresholds; source: (1-6), this work; (7), Lower Garfagnana (Governi, 2005); (8-9), Southern Apuan Alps (Giannecchini, 2006); (10-12), Carrara, Fossacava and Rifugio Belvedere (Carrara Marble Basin, unpublished data); (13-14), Portovenere (Cinque Terre area, Giannecchini et al., 2010); (15-16), Levanto (Cinque Terre area, Giannecchini et al., 2010); (17), Valtellina, Lombardy (Cancelli and Nova, 1985); (18), Moscardo Torrent, NE Alps (Marchi et al., 2002); (19), Valzangona, Northern Apennines (Floris et al., 2004); (20), Lombardy (Ceriani et al., 1994 in Bacchini and Zannoni, 2003); (21), Campania (Calcaterra et al., 2000); (22), Piedmont (Aleotti, 2004); (23-25), Abruzzo (Brunetti et al., 2010).

The thresholds were also compared with the national thresholds for Italy obtained by Brunetti et al. (2010) and some global ID thresholds for shallow landslide occurrence

proposed by several authors (Fig. 3.16), including Caine (1980), Innes (1983), Jibson (1989), Clarizia et al. (1996), Crosta and Frattini (2001), Cannon and Gartner (2005), and Guzzetti et al. (2008). The comparison shows that the ID thresholds obtained by this study are (1-6 in Fig. 3.16) higher than the global thresholds, for the reasons cited above.

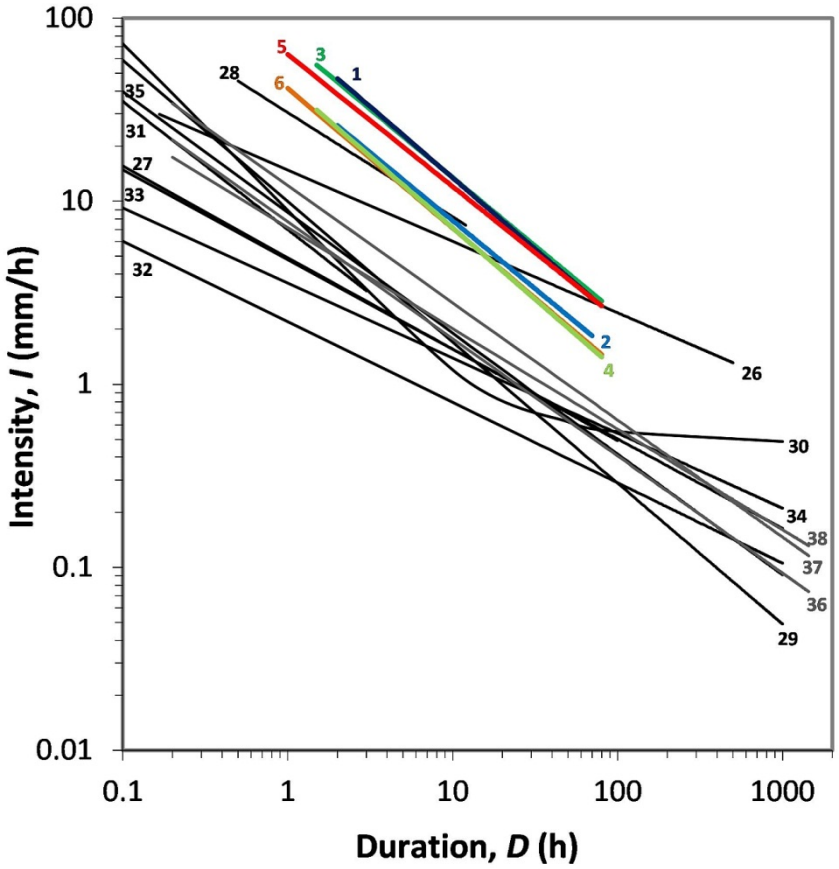

Fig. 3.16. Comparison between the ID thresholds obtained in this study with some global thresholds. The thresholds for the MSRV are coloured: dark blue, Borgo a Mozzano upper curve; blue, Borgo a Mozzano lower curve; green, Mutigliano upper curve; light green, Mutigliano lower curve; red, Vinchiana upper curve; orange, Vinchiana lower curve. Global (black) and national (gray) thresholds compared with MSRV (colour) thresholds; source: (1-6), this work; (26), Caine (1980); (27), Innes (1983); (28), Jibson (1989); (29), Clarinza et al. (1996); (30), Crosta and Frattini (2001); (31), Cannon and Gartner (2005); (32-35), Guzzetti et al. (2008); (36-38), National thresholds for Italy (Brunetti et al., 2010).

Also the $E_{MAP}I$ thresholds obtained for the MSRV were compared with those proposed for some other areas of Italy (Fig. 3.17). The upper thresholds for the Borgo a Mozzano (1 in Fig. 3.17), Mutigliano (3) and Vinchiana (5) rain gauges fall in the range of the normalized event rainfall E_{MAP} for the Piedmont Region (9-10, Govi et al., 1985) and for the Southern Apuan Alps (7, Giannecchini, 2006). The lower thresholds for Borgo a Mozzano (2), Mutigliano (4)

and Vinchiana (6) are less conservative than the lower threshold (8) proposed by Giannecchini (2006) for the Southern Apuan Alps (Fig. 3.17).

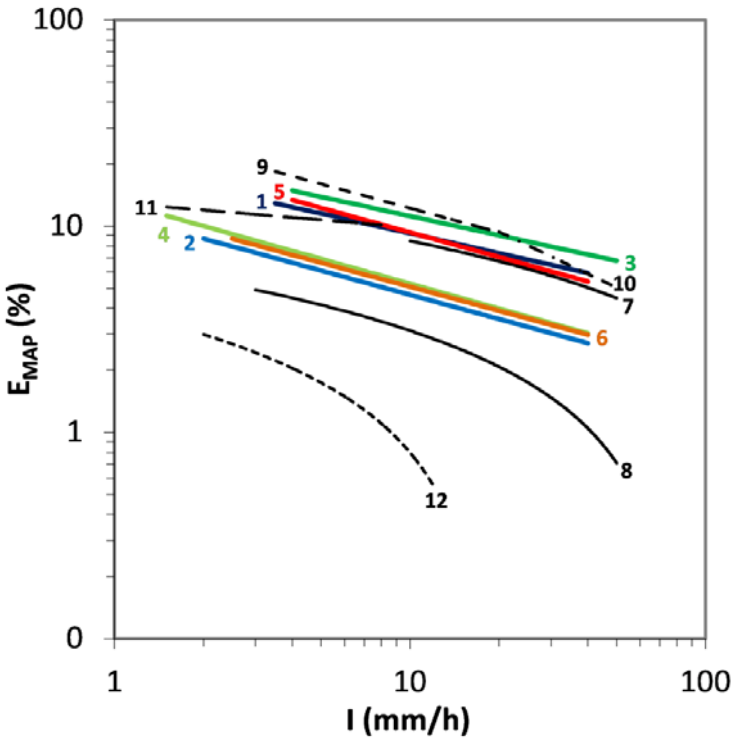

Fig. 3.17. Comparison between the $E_{MAP}I$ thresholds obtained in this research with the thresholds proposed for other areas of Italy. 1) Borgo a Mozzano upper curve; 2) Borgo a Mozzano lower curve; 3) Mutigliano upper curve; 4) Mutigliano lower curve; 5) Vinchiana upper curve; 6) Vinchiana lower curve; 7) Southern Apuan Alps upper curve (Giannecchini, 2006); 8) Southern Apuan Alps lower curve (Giannecchini, 2006); 9-11) Piedmont Region (Govi et al., 1985); 12) Cancia, Dolomites, North-Eastern Italy (Bacchini and Zannoni, 2003).

3.6.2 Threshold validation

The data used in the elaboration include the whole 1935-2010 period. Therefore, in order to validate the ID thresholds obtained for the MSRV, the main recent rainfall events from 1 January 2011 to 20 November 2011 were considered. In this period of 2011 shallow landslides did not occur in the study area. Therefore, C-type rainfall events were analysed. Figure 18 compares the rainfall ID thresholds of Borgo a Mozzano (Fig. 3.18a), Mutigliano (Fig. 3.18b) and Vinchiana (Fig. 3.18c) with the ID values of the main 2011 rainfall events.

The main rainfall events recorded at Borgo a Mozzano in 2011 correctly fall below the lower threshold (Fig. 3.18a), whereas the 4 September 2011 event falls between the lower and the upper threshold curves (intermediate stability field) in the Mutigliano (Fig. 3.18b) and

Vinchiana (Fig. 3.18c) graphs. Nevertheless, this event did not cause landslides in the study area, but damage to the road network, mainly caused by a lot of fallen trees. This highlights equilibrium limit conditions on slopes, which can be represented by uncertainty in the graphs. Therefore, the results of this validation seem encouraging, even if they are based on a small number of rainfall events.

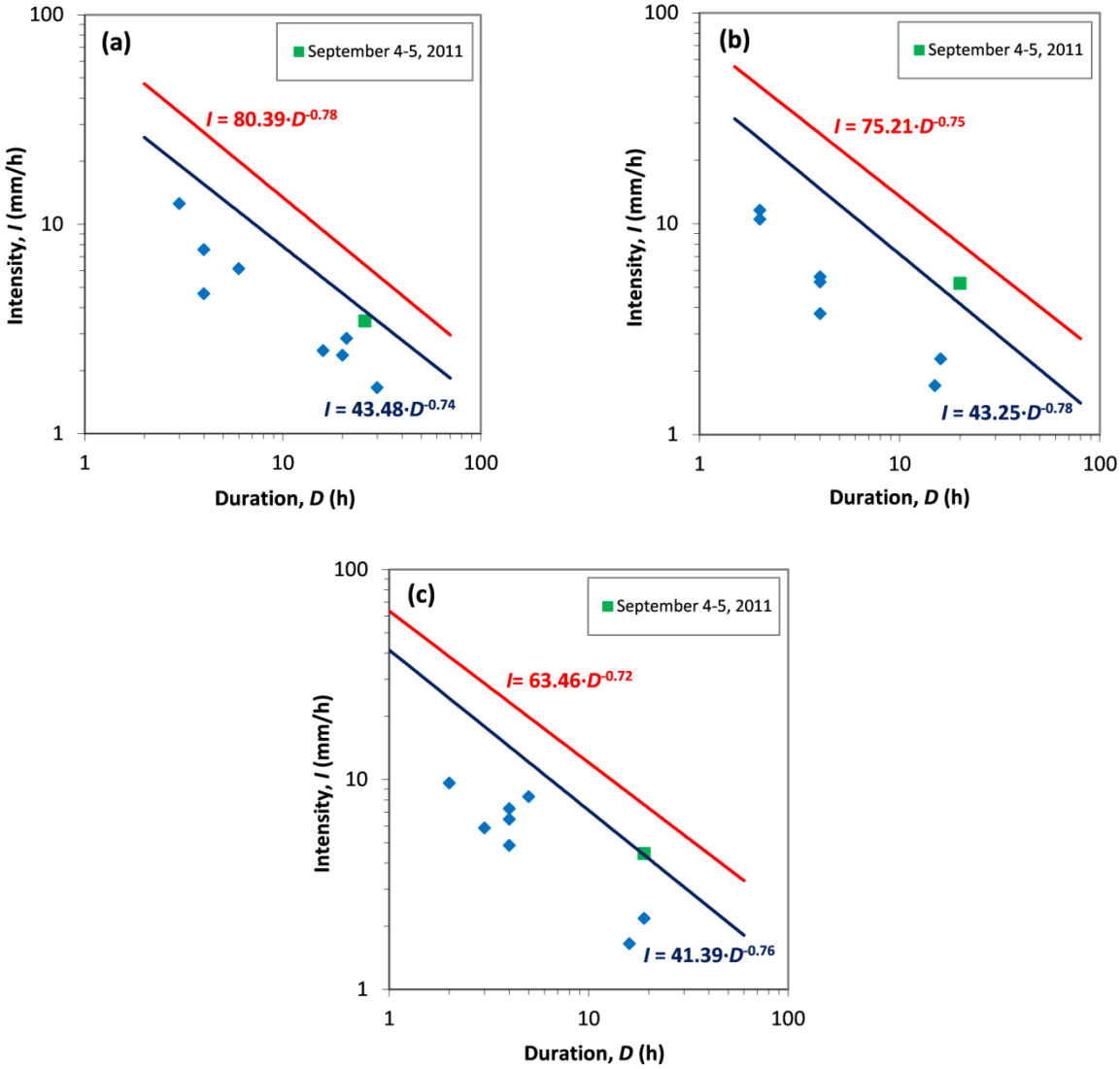

Fig. 3.18. Comparison between the ID thresholds and the main rainfall events occurring during the January 1, 2011-November 20, 2011 period in the MSRV, for the Borgo a Mozzano **(a)**, Mutigliano **(b)** and Vinchiana **(c)** rain gauges. The lower (blue) and upper (red) threshold curves are recognizable.

3.6.3 Use of rainfall thresholds

The thresholds obtained for the MSRV in this work can provide guidance for setting up warning systems and planning emergency actions in the event of heavy rainstorms. Decisions on warning and emergency response can be made on the basis of the comparison of the rainfall forecasts and real-time measurements with the threshold curves. Thus, the threshold curves can help in preparing hazard scenarios, provided that a reliable weather forecast is available.

When the combination of duration and rainfall intensity exceeds the upper threshold curve, tens of shallow landslides can be anticipated (Fig. 3.8d). If the rainfall events fall between the upper and the lower thresholds (field of intermediate stability), a few shallow landslides are expected (Fig. 3.8d). On the basis of a reliable weather forecast, an appropriate scenario can be adopted and an emergency system activated. If a real-time rainfall monitoring system is available the rainfall evolution can be followed and analyzed step by step.

The threshold curves obtained for the Borgo a Mozzano, Mutigliano and Vinchiana rain gauges are similar (Fig. 3.8d). Among them, the Vinchiana ones are more conservative. They could be used for testing early warning systems for the entire MSRV, considering its relatively small size and uniformity.

3.7 Conclusion

The intensity-duration (ID) approach allows us to obtain the rainfall threshold curves for shallow landslide initiation in the MSRV.

The comparison with other ID thresholds for north-western Tuscany highlighted the high rainfall thresholds for triggering shallow landslides in the study area. This is linked to the high mean annual precipitation (MAP) and the high frequency of rainstorms hitting the study area, which induce a natural, dynamic equilibrium between climatic features and slopes.

The analysis of the role of the antecedent rainfall in triggering shallow landslides shows that the antecedent period in which the cumulative rainfall should be considered ranges from 3 to 7 days.

Some misclassifications of the rainfall events are highlighted in the threshold plots, probably due to imprecise information about landslides and damage up until the 1980s. The

threshold validation was performed using rainfall events occurring in 2011, which did not induce shallow landslides and proved that the threshold curves function.

The manual fitting used to construct the threshold curves led to cautionary results. However, mathematical and statistical approaches will be tested and compared with the present results in the next stages of this research.

The threshold curves found by this work can be the basis to set up warning systems, and face hydrogeological emergencies and assess risk. This requires reliable weather forecast systems to be in operation.

The evolution of this research is towards defining risk scenarios for different rainfall amounts, directly linked to the rainfall thresholds. This can be crucial for reliable planning of civil protection strategies.

References

Aleotti, P.: A warning system for rainfall-induced shallow failures, Eng. Geol., 73, 247–265, 2004.

Anderson, M. G.: Road-cut slope topography and stability relationships in St. Lucia, West Indies, Applied Geography., 3, 104–114, 1983.

Bacchini, M. and Zannoni, A.: Relations between rainfall and triggering of debris-flow: case study of Cancia (Dolomites, Northeastern Italy), Nat. Hazards Earth Syst. Sci., 3, 71–79, 2003.

Baldacci, F., Cecchini, S., Lopane, G., and Raggi, G.: Le risorse idriche del Fiume Serchio ed il loro contributo all'alimentazione dei bacini idrografici adiacenti, Memorie della Società geologica Italiana, 49, 365–391, 1993.

Bieniawski, Z. T.: Engineering Rock Mass Classification, Wiley, New York, 1989.

Brunetti, M. T., Peruccacci, S., Rossi, M., Luciani, S., Vaglini, D., and Guzzetti, F.: Rainfall thresholds for the possible occurrence of landslides in Italy, Nat. Hazards Earth Syst. Sci., 10, 447–458, 2010.

Caine, N.: The rainfall intensity-duration control of shallow landslides and debris flows, Geogr. Ann. A, 62, 23–27, 1980.

Calcaterra, D., Parise, M., Palma, B., and Pelella, L.: The influence of meteoric events in triggering shallow landslides in pyroclastic deposits of Campania, Italy, in: Proceedings of the 8th International Symposium on Landslides, edited by: Bromhead, E., Dixon, N., and Ibsen, M. L., A. A. Balkema, Cardiff, 1, 209–214, 2000.

Campbell, R. H.: Soil slips, debris flows and rainstorms in the Santa Monica Mountains and vicinity, Southern California, U.S. Geological Survey Professional Paper, 851, 51 pp., 1975.

Cancelli, A. and Nova, R.: Landslides in soil debris cover triggered by rainstorms in Valtellina (central Alps – Italy), in: Proceedings of the 4th International Conference and Field Workshop on Landslides, The Japan Geological Society, Tokyo, 267–272, 1985.

Cannon, S. H.: Regional rainfall-threshold conditions for abundant debris-flow activity, in: Landslides, floods, and marine effects of the storm of January 3–5, 1982, in the San

Francisco Bay Region, California, edited by: Ellen S.D. and Wieczorek G.F., US Geological Survey Professional Paper, 1434, 35–42, 1988.

Cannon, S. H. and Gartner, J. E.: Wildfire-related debris flow from a hazards perspective, in: Debris flow hazards and related phenomena, edited by: Jakob, M. and Hungr. O., Springer, Berlin, 363–385, 2005.

Cannon, S. H., Gartner, J. E., Wilson R. C., Bowers J. C., and Laber J. L.: Storm rainfall conditions for floods and debris flows from recently burned areas in southwestern Colorado and southern California, Geomorphology, 96, 250–269, 2008.

Carmignani, L., Conti, P., Disperati, L., Fantozzi, P.L., Giglia, G., and Meccheri, M.: Carta Geologica del Parco delle Alpi Apuane, Apuan Regional Park, S.El.Ca Ed., Florence, 2000.

Carmignani, L. and Kligfield, R.: Crustal extension in the Northern Apennines: the transition from compression to extension in the Alpi Apuane Core Complex, Tectonics, 9(6), 1275–1303, 1990.

Castaldini, D., Caredio, F., D'Amato Avanzi, G., Perilli, N., and Puccinelli, A.: Glacial features in the Tuscan-Emilian Apennines (Italy): evidences from the Abetone area, in: The Regione Toscana Project of Geological Mapping. Case Histories and Data Acquisition, edited by: Morini, D. and Bruni, P., Regione Toscana, Firenze, 67–76, 2004.

Ceriani, M., Lauzi, S., and Padovan, N.: Rainfall thresholds triggering debris-flows in the alpine area of Lombardia Region, central Alps – Italy, Proc. Man and Mountain, I Conv. Intern. per la Protezione e lo Sviluppo dell'ambiente montano, Ponte di Legno (BS), 123–139, 1994.

Clarizia, M., Gullà, G., and Sorbino, G.: Sui meccanismi di innesco dei soil slip, in: Proceedings of International Conference on Prevention of Hydro-geological Hazards: The Role of Scientific Research, Alba, Italy, 5–7 November 1996, 1, 585–597.

Coe, J. A., Kinner, D. A., and Godt, J. W.: Initiation conditions for debris flows generated by runoff at Chalk Cliffs, central Colorado, Geomorphology, 96, 270–297, 2008.

Corominas, J.: Landslides and climate. Keynote lecture, in: Proceedings of the 8th International Symposium on Landslides, edited by: Bromhead, E., Dixon, N., and Ibsen, M. L., A. A. Balkema, Cardiff, 4, 1–33, 2000.

Corominas, J. and Moya, J.: Reconstructing recent landslide activity in relation to rainfall in the Llobregat river basin, Eastern Pyrenees, Spain, Geomorphology, 30, 79–93, 1999.

Crosta, G. B. and Frattini, P.: Distributed modelling of shallow landslides triggered by intense rainfall, Nat. Hazards Earth Syst. Sci., 3, 81–93, 2003.

Crosta, G. B. and Frattini, P.: Rainfall thresholds for triggering soil slips and debris flow, in: Proceedings of the 2nd EGS Plinius Conference on Mediterranean Storms, edited by: Mugnai, A., Guzzetti, F., and Roth, G., Siena, Italy, 16-18 October 2001, 463–487.

Crozier, M. J.: Prediction of rainfall-triggered landslides: a test of the antecedent water status model, Earth Surf. Proc. Land., 24, 825–833,1999.

Cruden, D. M. and Varnes, D. J.: Landslide type and processes, In Turner, A K and Schuster R L (eds) "Landslides investigation and mitigation". Transportation Research Board Special Report 247, National Research Council, National Academy Press, Washington D., 36–75, 1996.

D'Amato Avanzi, G., Falaschi, F., Giannecchini, R. and Puccinelli, A.: Soil slip susceptibility assessment using mechanical-hydrological approach and GIS techniques: an application in the Apuan Alps (Italy). Nat. Hazards, 50, 591–603, 2009.

D'Amato Avanzi, G., Giannecchini, R., and Puccinelli, A.: The influence of the geological and geomorphological settings on shallow landslides. An example in a temperate climate environment: the June 19, 1996 event in northwestern Tuscany (Italy), Eng. Geol., 73(3–4), 215–228, 2004.

D'Amato Avanzi, G., Galanti, Y., Giannecchini, R., and Puccinelli, A.: Fragility of territory and infrastructures resulting from rainstorms in Northern Tuscany (Italy), in: Proceedings of The 2nd World Landslide Forum, Roma, 3–9 October 2011, Springer-Verlag, in press, 2012.

Dahal, R. K. and Hasegawa, S.: Representative rainfall thresholds for landslides in the Nepal Himalaya, Geomorphology, 100, 429–443, 2008.

Floris, M., Mari, M., Romeo, R. W., and Gori, U.: Modelling of landslide-triggering factors - A case study in the northern Apennines, Italy, Lect. Notes Earth Sci. 104, 745–753, 2004.

Giannecchini, R.: Relationship between rainfall and shallow landslides in the southern Apuan Alps, Nat. Hazards Earth Syst. Sci., 6, 375–364, 2006.

Giannecchini, R., Damilano, D., and Puccinelli, A.: Critical rainfall thresholds for triggering rapid shallow landslides in the Eastern Ligurian Riviera (Italy), in: Proceedings of 85° Italian Geological Society National Congress, Pisa, Italy, 6–8 September 2010, 2, 596–597, 2010.

Giannecchini, R., Naldini, D., D'Amato Avanzi, G., and Puccinelli, A.: Modelling of the initiation of rainfall-induced debris flows in the Cardoso basin (Apuan Alps, Italy), Quatern. Int., 171–172, 108–117, 2007.

Glade, T., Crozier, M. J., and Smith, P.: Applying probability determination to refine landslide-triggering rainfall thresholds using empirical ''antecedent daily rainfall model'', Pure Appl. Geophys., 157, 1059–1079, 2000.

Governi, S.: Valutazione delle soglie pluviometriche critiche per l'innesco di frane rapide nella Media Val di Serchio (LU), Degree thesis, University of Pisa, Italy, 206 pp., 2005.

Govi, M. and Sorzana, P. F.: Landslide susceptibility as function of critical rainfall amount in Piedmont basin (North-Western Italy), Studia Geomorphologica Carpatho-Balcanica, 14, 43–60, 1980.

Govi, M., Mortara, G., and Sorzana P. F.: Eventi idrologici e frane, Geologia Applicata e Idrogeologia, 20(2), 359–375, 1985.

Guidicini, G. and Iwasa, O. Y.: Tentative correlation between rainfall and landslides in a humid tropical environment, Bull. Int. Assoc. Eng. Geol., 16, 13–20, 1977.

Guzzetti, F.: Landslide fatalities and the evaluation of landslide risk in Italy, Eng. Geol., 58, 89–107, 2000.

Guzzetti, F., Peruccacci, S., Rossi, M., and Stark, C. P.: Rainfall thresholds for the initiation of landslides in central and southern Europe, Meteorol. Atmos. Phys., 98, 239–267, 2007.

Guzzetti, F., Peruccacci, S., Rossi, M., and Stark, C. P.: The rainfall intensity-duration control of shallow landslides and debris flows: an update, Landslides, 5(1), 3–17, 2008.

Guzzetti, F., Stark, C. P., and Salvati, P.: Evaluation of flood and landslide risk to the population of Italy, Environ. Manage., 36(1), 15–36, 2005.

Haigh, M. J., Rawat, J. S., and Bartarya, S. K.: Environmental correlations of landslide frequency along new highways in the Hymalaya - preliminary results, Catena, 15, 539–553, 1988.

Innes, J. L.: Debris flows, Prog. Phys. Geogr., 7, 469–501, 1983.

Iverson, R. M.: Landslide triggering by rain infiltration, Water Resour. Res., 36(7), 1897–1910, 2000.

Jibson, R. W.: Debris flow in southern Porto Rico, Geological Society of America, 236, 29–55, 1989.

Larsen, M. C. and Parks, J. E.: How wide is a road? The association of roads and mass-wasting in a forested montane environment, Earth Surf. Proc. Land., 22, 835–848, 1997.

Marchi, L., Arattano, M., and Deganutti, A. M.: Ten years of debris-flow monitoring in the Moscardo Torrent (Italian Alps), Geomorphology, 46, 1–17, 2002.

Montgomery, D. R. and Dietrich, W. E.: A physically based model for the topographic control on shallow landsliding, Water Resour. Res., 30(4), 1153–1171, 1994.

Puccinelli, A., D'Amato Avanzi, G., and Perilli, N.: Carta Geologica d'Italia alla scala 1:50.000. Foglio 250 Castelnuovo di Garfagnana, http://www.isprambiente.gov.it/media/carg/250_Castelnuovo/Foglio.html, in press, 2012.

Reichenbach, P., Cardinali, M., De Vita, P., and Guzzetti, F.: Regional hydrological thresholds for landslides and floods in the Tiber River Basin (central Italy), Environm. Geol., 35(2–3), 146–159, 1998.

Saito, H., Nakayama, D., and Matsuyama, H.: Relationship between the initiation of a shallow landslide and rainfall intensity-duration thresholds in Japan, Geomorphology, 118, 167–175, 2010.

Terlien, M. T. J.: The determination of statistical and deterministic hydrological landslide-triggering thresholds, Environm. Geol., 35(2–3), 124–130, 1998.

Wieczorek, G. F.: Effect of rainfall intensity and duration on debris flows in central Santa Cruz Mountains, California, in: Debris Flows/Avalanches: Processes, Recognition and Mitigation, edited by: Costa, J.E., Wieczorek, G.F., Reviews in Engineering Geology, Geological Society of America, 7, 23–104, 1987.

Wieczorek, G. F., Morgan, B. A., and Campbell, R. H.: Debris flow hazards in the Blue Ridge of Central Virginia, Environ. Eng. Geosci., 6(1), 3–23, 2000.

Wieczorek, G. F. and Glade, T.: Climatic factors influencing occurrence of debris flows, in: Debris flow hazards and related phenomena, edited by: Jakob, M. and Hungr, O., Berlin Heidelberg, Springer, 325–362, 2005.

Wilson, R. C. and Wieczorek, G. F.: Rainfall thresholds for the initiation of debris flow at La Honda, California, Environ. Eng. Geosci., 1(1), 11–27, 1995.

Wu, W. and Sidle, R. C.: A distributed slope stability model for steep forested basins, Water Resour. Res., 31, 2097–2110, 1995.

Acknowledgements

It would not have been possible to write this PhD thesis without the help and support of the kind people around me, to only some of whom it is possible to give particular mention here.

I am sincerely and heartily grateful to my Tutor Prof. Alberto Puccinelli for his valuable suggestions, guidance, and encouragement.

Deepest gratitude are also due to my co-tutors, Dott. Giacomo D'Amato Avanzi and Dott. Roberto Giannecchini, without whose knowledge and assistance this study would not have been successful.

I would like to thank Prof. Diego Lo Presti whose suggestions significantly improved the second paper of this Thesis.

I wish to thank two referees Prof. Carlo Alberto Garzonio and Dott. Leonardo Disperati, whose suggestions significantly improved the manuscript.

I wish to thank the Tuscany Region Hydrologic Service (especially to Luca Pisani) for providing the rainfall data.

I wish to thank the Authority of the Serchio River Basin and the Seismic Risk Division of Tuscany region for providing the geotechnical data.

Finally, I would like to thank my girlfriend Azzurra for her personal support and great patience at all times. My parents have given me their unequivocal support throughout, as always, for which my mere expression of thanks likewise does not suffice.